PhD thesis

Institute of Physical Chemistry
Polish Academy of Sciences
Kasprzaka 44/52
01-224 Warszawa, Poland

Aqueous-Phase Kinetics of Complex Reactions of Isoprene for Air Quality Modeling

Inna Kuznietsova

Ph.D. Thesis

This dissertation was prepared within the International Ph.D. in Chemistry Studies

at the Institute of Physical Chemistry of the Polish Academy of Sciences,

the Group of Environmental Chemistry, Department of Catalysis on Metals

Supervisor: Lech Gmachowski, D.Sc.

Professor at Technical University of Warsaw

Warsaw, September 2012

Acknowledgements

I would like to thank dissertation supervisor Lech Gmachowski D.Sc. for giving me the opportunity to work on an interesting topic during my Ph.D. study.

I would like to thank Dr. Rafał Szmigielski for his direct advisory during my work related to this Ph.D. and also for his help and scientific discussions. I am grateful to him for teaching me mass spectrometry basics that I did not have before.

I would like to express my gratitude to Dr. Krzysztof Jan Rudziński for his substantial support (even when he had no time), guidance, friendliness, and relentless patience throughout my Ph.D. study, in teaching me things related to the kinetic studies.

I would like thank to Prof. Witold Danikiewcz from the Institute of Organic Chemistry for collaboration and opportunity to perform mass spectrometry analysis. I am grateful Mr. Grzegorz Spólnik, for recording mass spectra and tentative interpretation of mass spectra.

I would like to thank for all my friends from Warsaw and Dolina for support and interesting versatile discussion.

I want to thank my mother for her never-ending encouragement and motivation, my father for never-asking support and acceptance, and my sister Natasha for her inexhaustible patience, encouragement, support, and trusting in my abilities. I am grateful to my family for their persistent love.

I would like to thank Jacek for his support and understanding.

To my parents and sister

Abstract

Results of laboratory study of aqueous-phase chemical kinetics, mechanisms and products of complex isoprene transformations in the presence of selected inorganic compounds present in the atmosphere – dissolved forms of SO_2 ($SO_2 \times H_2O$, HSO_3^-, SO_3^{2-}), nitrite ions/nitrous acid, oxygen and manganese(II) sulfate – is reported. Isoprene reacted with sulfoxy radical-anions, which were produced by the autoxidation of dissolved forms of SO_2 catalyzed by $MnSO_4$, also in the presence of nitrite ions and nitrous acid.

Isoprene, nitrite ions and nitrous acid, individually, exhibited the significant influence on the kinetics of S(IV) autoxidation in the way depending on the initial acidity of the reaction solutions ($pH_o = 2.2 \div 8.7$). Nitrous acid altered the rates of the transformation of isoprene during the autoxidation of S(IV) in the acidic solution.

Molecular structures of newly formed products from the reaction of isoprene with sulfoxy radical-anions were elucidated using a triple-quadruple negative electrospray mass spectrometry (–)ESI-MS/MS, nuclear magnetic resonance and UV spectroscopy, and confirmed by the comparison of their mass spectrometric behavior with that of the synthesized model compounds. Namely, the following compounds were firmly identified:

1-*O*-sulfonyl-4- hydrox-2-methylbut-2-ene

4-*O*-sulfonyl-3-methylbut-2-enal

4-*O*-sulfinyl-3-methylbut-2-enal

1-*O*-sulfinyl-4-hydrox-2-methylbut-2-ene
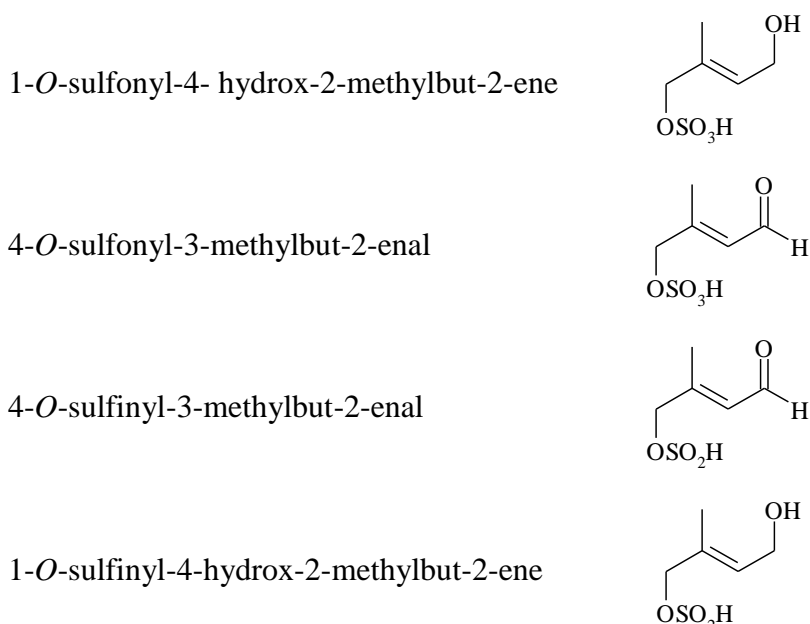
Quantum chemical calculations were used to assess the thermodynamic stability of novel products formed.

Mechanism of the aqueous-phase transformation of isoprene was proposed and supported, partly, with chemical-kinetic simulations.

Streszczenie

W pracy niniejszej zaprezentowano wyniki badań laboratoryjnych nad mechanizmami i kinetyką chemiczną złożonych reakcji 2-metylobuta-1,3-dienu (izoprenu) w roztworach wodnych, w obecności wybranych związków nieorganicznych obecnych w atmosferze – chemicznych form tlenku siarki(IV) rozpuszczonego w wodzie ($SO_2 \times H_2O$, HSO_3^-, SO_3^{2-}), azotanu(III) jonów/kwasu azotowego(III), tlenu oraz siarczanu(VI) manganu. Izopren reaguje z anionorodnikami siarkotlenowymi, które powstają w katalizowanej siarczanem(VI) manganu(II) reakcji autooksydacji (utleniania z udziałem tlenu cząsteczkowego) chemicznych form tlenku siarki(IV) rozpuszczonego w wodzie. Zbadano również wpływ obecności jonów azotanowych(III) oraz kwasu azotowego (III) na przebieg procesów w mieszaninie reakcyjnej.

Stwierdzono, że obecność zarówno izoprenu, anionów azotanowych(III) oraz kwasu azotowego(III) ma znaczący wpływ na kinetykę autooksydacji związków siarki(IV). Kinetyka tej reakcji zależna jest również od początkowego odczynu mieszaniny reakcyjnej w zakresie (pH = 2,2 ÷ 8,7). Obecność kwasu azotowego(III) ma również wpływ na szybkość przemian chemicznych izoprenu podczas autooksydacji związków siarki w środowisku kwaśnym.

Struktury chemiczne związków powstałych w reakcji izoprenu z anionorodnikami siarkotlenowymi zostały określone na podstawie wyników badań metodami spektrometrii mas w układzie potrójny kwadrupol z jonizacją w trybie ujemnym, magnetycznego rezonansu jądrowego i spektroskopii UV oraz potwierdzone poprzez porównanie ich widm masowych z widmami masowymi zsyntetyzowanych związków modelowych.
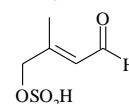
1-*O*-sulfonylo-4- hydroxy-2-metyolbuta-2-en
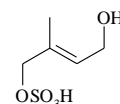
4-*O*-sulfonylo-3-metylobuta-2-enal
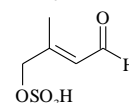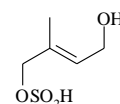
4-*O*-sulfinylo-3-metylobuta-2-enal

1-*O*-sulfinylo-4-hydroxy-2-metylbuta-2-en

Oszacowano trwałość termodynamiczną zidentyfikowanych produktów za pomocą obliczeń kwantowo-mechanicznych.

Zaproponowano mechanizm chemiczny przemian izoprenu w roztworach wodnych i poparto go w części wynikami komputerowych symulacji kinetyki tych przemian zgodnymi z obserwacjami doświadczalnymi.

Abbreviations

Abbreviation	Meaning
AA	Atmospheric aerosols
CCN	Cloud condensation nuclei
CE	collision energy
CID	Collision induced dissociation experiments
ESI	Electrospray ionization
(−)ESI	Electrospray ionization in negative mode
HPLC	High-Performance Liquid Chromatography
MOS	Experiments with *manganese, oxygen and sulfite*
MON	Experiments with *manganese, oxygen, and nitrite*
MOSN	Experiments with *manganese, oxygen, sulfite, and nitrite*
MOSC	Experiments with *manganese, oxygen, sulfite, and isoprene*
MOCN	Experiments with *manganese, oxygen, isoprene, and nitrite*
MOSCN	Experiments with *manganese, oxygen, sulfite, isoprene, and nitrite*
MS spectrum	First order mass spectrum
MS/MS spectrum	Second order mass spectrum
MS	Mass spectrometry
m/z	Mass per charge
MW	Molecular weight
N(III)	Inorganic compounds of trivalent nitrogen
NMR	Nuclear Magnetic Resonance
OA	Organic aerosols
POA	Primary organic aerosols
$ppmO_2$	Parts per million O_2
S(IV)	Inorganic compounds of tetravalent sulfur
SOA	Secondary organic aerosols
TMI	Transition metal ions
UV spectrum	Ultraviolet spectrum
UV-VIS spectrophotometry	Ultraviolet-visible spectrophotometry
VOC	Volatile organic compounds

Table of content

Introduction

The Earth atmosphere is a mixture of various gases. The main constituents are nitrogen (78%), oxygen (21%), and argon (1%) while numerous trace compounds add up to the remaining 1%. The latter originate from various emissions (from biogenic and anthropogenic sources). In addition, the atmosphere contains solid particles (aerosol) and liquid droplets (wet aerosol) that form *in situ* or are uplift from the Earth surface.

Conceptually, the atmosphere is a huge chemical reactor driven by the solar radiation providing space for gas-phase, heterogeneous (surfaces of solid particles and liquid droplets) and aqueous-phase (cloud water, rain, fog etc.) reactions. Atmospheric aerosols are colloids or suspensions of fine particles or liquid droplets dispersed in the air. Examples of liquid droplets suspended in the air are mist, fog, and haze. On the other hand, smoke, fume, fly ash, dust, smoke, soot, and smog represent solid particles in the air.

The atmospheric components combine in complex chemical reactions which lead to the formation of myriads of new trace components (secondary pollutants) in the gas phase, in new or modified solid particles (secondary aerosol) and in aqueous phases. Specially, during the gas-particle conversion processes and from heterogeneous and multiphase chemical reactions of volatile organic compounds, Secondary Organic Aerosols (SOA) are formed. All these processes are called "atmospheric chemistry".

The emission of primary trace compounds and the production of secondary trace compounds change the composition of ambient air and, consequently, influence everything the air surrounds and is vital for – humans, animals, plants, and non-living matter, including human-made objects. In this context we talk about air quality and its impact on health and condition of the biosphere and anthroposphere. Our ultimate goal is to understand the air quality and to control it for better standard of living.

For this purpose it is necessary to understand the rates and mechanisms of chemical processes behind the transformation of atmospheric trace compounds, so that we can use modeling to predict the changes in air quality and the effectiveness of measures of the air quality control and management.

The presented thesis aims to provide insight into aqueous-phase reactions which can significantly influence the production of new components of the atmospheric air, secondary aerosols, and precipitation that affect the air quality. Specifically, the thesis aims to evaluate

the kinetics and the formation mechanisms for the aqueous-phase reactions of isoprene, C_5H_8, in the presence of oxygen, O_2, and dissolved forms of sulfur dioxide, SO_2, nitrous acid, HONO, and manganese(II) sulfate, $MnSO_4$.

Isoprene is the most abundant non-methane hydrocarbon emitted into the troposphere by 410 TgC annually (Müller *et al.*, 2008). In the previous studies, isoprene has not been shown to contribute to formation of Secondary Organic Aerosols (SOA) through aqueous-phase mechanism. This was largely due to the limited physical solubility of isoprene in water, and high volatility of isoprene and its first-generation products of gas-phase oxidation in the presence of nitrogen oxides ($NO_x = NO\cdot + \cdot NO_2^*$), such as methacrolein (MACR), methyl-vinyl ketone (MVK), and formaldehyde. Moreover, early-stage smog chamber studies showed that isoprene oxidation did not lead to the formation of SOA. However, field observations and sophisticated smog chamber experiments proved the reverse.

Sulfur dioxide (SO_2) is a major sulfur-bearing pollutant of the atmosphere. The in-cloud SO_2 oxidation accounts for 60% of sulfate aerosols formed which play an important role in the chemistry of the atmosphere. Recent studies have revealed organosulfate esters in SOA collected in the field campaigns and confirmed SOA formation by heterogeneous reaction of isoprene with sulfuric acid (Surratt *et al.*, 2007a; 2007b).

Nitrous acid (HONO) is a crucial trace compound of the air – a major precursor of the atmospheric hydroxyl radicals ($OH^\bullet$). Recent studies showed that SOA contains esters derived from organic compounds and nitrous acid or nitrite ions.

Manganese(II) sulfate ($MnSO_4$) represent salts of transition metals. Trace amount of transition metals are abundant in the atmospheric liquids phase (wet aerosol, cloud, fog, rain). Iron (Fe), manganese (Mn), and copper (Cu) are the major metals that participate in the processes occurring in the atmospheric water, often working as catalysts of chemical reactions involved. In this thesis, manganese(II) sulfate was selected for the simplicity of its hydrolytic speciation in aqueous solutions considered (mild alkaline to mild acidic) to simplify further analysis of experimental results.

The aims of the thesis are justified by a large gap between field measurement and model predictions of the composition and concentration of secondary organic aerosols as well as its properties. The aqueous-phase reactions in clouds, fogs, and deliquescent aerosols provide an additional important pathway of SOA formation. Studies of aqueous-phase

---

* The radical notation "$\cdot NO_2$" and "$NO\cdot$" is used throughout this thesis to indicate unpaired electrons in NO_2 and NO, and their radical character.

transformations of atmospheric trace compound can provide missing formation routes of several components of SOA and rainwater, and therewith, help to evaluate the regional and global impact of atmospheric aerosols on visibility, climate, and human health and life, and solve some problems connected with it.

1 Literature review

1.1 Isoprene

1.1.1 Sources of isoprene

Isoprene (2-methylbuta-1,3-diene, C_5H_8) is the most abundant non-methane hydrocarbon released to the atmosphere. Its emission is estimated at ~ 600 Tg yr^{-1} (Günther *et al.*, 2006), and lately ~ 410 Tg yr^{-1} (Müller *et al.*, 2008) that roughly equal to global emission of methane. Terrestrial vegetation is the main source of isoprene. The most of the hydrocarbon is produced by tropical rain forests, the lowest – by agricultural areas and boreal forests (Kesselmeier and Staudt, 1999). Among species that release isoprene are 1) broad-leaved trees: the aspen, the sedge, the oak, the eucalypt, and the willow; 2) needle-leaved trees: the spruce, the fir, palms, shrubs, vines, and mosses; 3) some crops, plants used to produce biofuel and commercial forestry species (Hellén *et al.*, 2006; Haapanala *et al.*, 2006; Tiiva *et al.*, 2007; Pacifico *et al.*, 2009; Ekberg *et al.*, 2009). Interestingly, even the same genus has species that make isoprene and others which are not.

Isoprene, in small amounts, is synthesized in plastids (chloroplasts) from pyruvate and glyceraldehydes-3-phosphate (Kesselmeier and Staudt, 1999). There are suggestions about a close relationship between isoprene production and photosynthesis (Delwiche and Sharkey, 1993), and non-photosynthetic, without this connection (Affek and Yakir, 2002).

The isoprene flux to the atmosphere was observed also from the open ocean (Baker *et al.*, 2000; Matsunaga *et al.*, 2002) by marine phytoplankton (Shaw *et al.*, 2003) and seaweeds (several macroalgal species: red, green and brown (Gist and Lewis, 2006). Global ocean isoprene emission is from < 1 to > 10 Tg C yr^{-1}(Carlton *et al.*, 2009).

Isoprene emission was observed from molds (Berenguer *et al.*, 1991) and bacteria (Fall and Copley, 2000; Kuzma *et al.*, 1995; Wagner *et al.*, 1999) with emission at levels of 0.15 to 0.71 pmoles cm^{-2} hr^{-1} (Acuna-Alvarez *et al.*, 2009).

Moreover, mammals (Deneris *et al.*, 1985) and humans (Diskin *et al.*, 2003; Fenske and Paulson, 1999) release isoprene. There is theory that isoprene emission from human body is connected with the mevalonate pathway of cholesterol biosynthesis (Deneris *et al.*, 1984). Investigation of breath isoprene becomes popular because isoprene may serve as a sensitive, non-invasive indicator for analyzing some metabolic effects in the human body. Being a by-

product of cholesterol biosynthesis, isoprene form breath was suggested as an additional diagnostic parameter for patients suffering from lipid metabolism disorders such as hypercholesterolemia. However, significant analytic problems in breath isoprene analysis and variability in isoprene levels with age, exercise, diet, etc., limits the usefulness of these measurements.

The anthropogenic sources have lower isoprene emission and are poorly quantified. They include combustion processes and evaporation of fuels (Borbon, 2003a; Borbon *et al.*, 2003b) in rural atmosphere (Burgess and Penkett, 1993) and urban environments (McLaren *et al.*, 1995; Derwent *et al.*, 1995). The anthropogenic contribution is minimal in summer, with estimated values of $5 - 10\%$. It was proposed that motor vehicles are responsible for a significant portion of the anthropogenic isoprene (Reimann *et al.*, 2000). Another anthropogenic sources of isoprene are cigarette smoking (Baek and Jenkins, 2004; Pouli *et al.*, 2003), biomass burning (Gaeggeler *et al.*, 2008), garden waste (Wilkins and Larsen, 1996) and chemical technology (Leber, 2001).

1.1.2 Importance of isoprene

Because of two double bonds, isoprene is highly reactive and is readily oxidized in the atmosphere by nitrate radicals ($NO_3^{\bullet}$), hydroxyl radicals ($OH^{\bullet}$), and ozone (O_3), with typical reaction lifetimes of 0.8 h, 1.7 h, and 1.3 days respectively (Seinfeld and Pandis, 1998). There is a wide range of products of these reactions such as methacrolein, methyl vinyl ketone, glycolaldehyde, hydroxyacetone, methylglyoxal, formaldehyde, organic acids, CO, peroxyacetyl nitrate (PAN) and methyl-peroxyacetyl nitrate (MPAN) which are volatile and well-soluble in water. Since isoprene is volatile and, in contrast to its products, hardly soluble in water, at first, it has been generally accepted that isoprene does not contribute to atmospheric Secondary Organic Aerosols (SOA) (Pandis *et al.*, 1991). However, (Claeys *et al.*, 2004a; Claeys *et al.*, 2004b; Edney *et al.*, 2005; Kleindienst *et al.*, 2007) and laboratory (Kroll *et al.*, 2006; Ng *et al.*, 2008) studies showed that isoprene one of the leading precursor of the SOA (formation and growth) in the atmosphere. Importance of atmospheric aerosols for environment is described in Section 1.5.

The reason isoprene emission by plants is still unclear. There are several hypotheses. One of them is thermotolerance – isoprene may protect plants against specific type of heat stress (Rodriguez-Concepcion and Boronat, 2002; Logan *et al.*, 2000). The hypothesis of

thermotolarance in a good agreement with the fact that isoprene emission form leaves at the top of canopy (higher heat fleck) are four times bigger than form leaves at the bottom of the canopy (Harley *et al.*, 1996; Sharkey *et al.*, 1996). Tolerance of heat flecks can help explain the distribution of the capacity to emit isoprene among plants (described in previous section).

The other hypothesis of plant isoprene emission is tolerance of ozone (Loreto and Velikova, 2001; Loreto *et al.*, 2001) and other reactive oxygen species (ROS) (Affek and Yakir, 2002; Peñuelas *et al.*, 2005). There is a suggestion that isoprene could reduce ROS by reducing heat damage directly rather than acting only through quenching of ROS generated by heating (Sharkey *et al.*, 2007).

Other hypotheses include: isoprene emission at high concentration speeds flowering in arabidopsis (Terry *et al.*, 1995), protects against herbivore (Laothawornkitkul *et al.*, 2008; Loivamäki *et al.*, 2008), influences the interactions between insects and plants, plays role in nutrient cycling, specifically by converting nitric oxide ($\cdot NO$) emitted from soils to plant available nitrogen (Klinger *et al.*, 1998).

Isoprene oxidation plays also an important role in modifying tropospheric O_3 (Chapter 1.4.1) and CH_4 amount depending on concentrations of nitrogen oxides ($NO_x = NO\cdot + \cdot NO_2$). At high-$NO_x$, there is hypothesis that isoprene oxidation produces NO_2 which increases levels of O_3, through photolysis (Sanderson *et al.*, 2003; Monson *et al.*, 2007). Another studies shown that reaction of isoprene atmospheric hydroxyl radicals ($OH^\bullet$) increasing ozone production through formation of hydroperoxides (RO_2) (Shirley *et al.*, 2006).

The situation is more complex in unpolluted conditions with low-NO_x: isoprene can react directly with O_3, and decreasing atmospheric concentrations of O_3, but there are suggestions that the OH-pathway is probably the more important isoprene oxidation pathway (Taraborelli *et al.*, 2009). Elimination of $OH^\bullet$ reduces the rate of conversion of $\cdot NO_2$ to nitric acid (HNO_3) and thus contributes to the efficacy of O_3 production. But the OH-oxidation pathways are not clearly understandable. $OH^\bullet$ is also the major atmospheric sink for CH_4 and thus an increase in isoprene concentration, by reducing $OH^\bullet$ concentration, will increase the lifetime of CH_4.

1.2 Sulfur dioxide

1.2.1 Sources of SO$_2$

Sulfur dioxide is the leading sulfur-containing pollutant of the atmosphere. The largest emission of SO$_2$ has anthropogenic origins (~ 75% (Zellner, 1999)). The main source is the combustion of fossil fuels in power plants, electricity generating stations, industrial boilers, road vehicles, aircraft, and ships. Other industrial facilities release SO$_2$ include iron and non-ferrous metal ore mines and smelters, oil refineries and natural gas scrubbers (Manahan, 2010; Zellner, 1999), sulfur mines and producing plants of sulfuric acid and paper.

Table 1.1. *Emission of SO$_2$ in some European countries (unit: Gg SO$_2$) (Vestreng et al., 2007).*

	1980	1990	2000	2004
Austria	344	74	32	29
Belarus	740	888	162	97
Czech Republic	2257	1876	264	227
Denmark	450	176	27	23
Estonia	287	274	96	90
Finland	584	259	74	83
France	3216	1333	613	484
Germany	7514	5289	630	559
Greece	400	487	493	537
Hungary	1633	1011	486	240
Norway	136	53	27	25
Poland	4100	3278	1507	1286
Russian Federation	7323	6113	2263	1858
Sweden	491	117	52	47
Turkey	1030	1519	2122	1792
Ukraine	3849	3921	1599	1145
United Kingdom	4838	3699	1173	833

Global SO$_2$ emissions from anthropogenic source increased steadily up to 1980 (Dignon and Hameed, 1989). Since 1980 the emission of sulfur dioxide has been progressively under control. For instance, European countries it decreased by 73% from 1980

to 2004 (Table 1.1) (Vestreng *et al.*, 2007), mostly due to policy regulation followed by realization of measures, and to economic decline. Physically, the reduction resulted from changes in the concentration of sulfur in fuels and introduction of catalytic exhaust pipes in transport. During aforementioned period the SO_2 emission decreased by 69% in Poland, by 70% in Ukraine, by 75% in Russian Federation and by 89% in Belarus.

Although most of sulfur dioxide emission has anthropogenic origins, there are natural sources of SO_2 such as volcanoes (Zellner, 1999) and biomass burning. Volcanoes can discharge several TgS during eruptions, which exceed their year production at calm state. For instance, The Mount Pinatubo eruption in June 1991 released an estimated 10 TgS (Fiocco and Fua, 1996) (a total annual volcanoes emission is 7.5 TgS (Berresheim and Jaeschke, 1983)). Other significant natural SO_2 source in the atmosphere is oxidation of dimethyl sulfide (DMS), $(CH_3)_2S$, the most abundant natural reduced sulfur species. An average global flux of DMS is $15 - 20$ TgS yr^{-1} (Bates *et al.*, 1992). It is mainly produced by biological and photochemical processes in the oceans. In particular, it is produced by some marine phytoplankton species (Andreae and Crutzen, 1997) during the cleavage of dimethylsulfoniopropionate. It forest fires, soils and vegetation in small amount also emit sulfur dioxide (Simpson *et al.*, 1999).

1.2.2 Importance of SO_2

Sulfur dioxide could be a dry deposition on Earth's surface or wet one, when SO_2 oxidize in the atmosphere (e.g., sulfate, sulfuric acid) (Pasiuk-Bronikowska *et al.*, 1992; Grgič *et al.*, 2003; Schurath *et al.*, 2003). This deposition influences the level of soils and freshwater acidification (Schöpp *et al.*, 2003), climate (Oden, 1968) and impacts the human health (World Health Organizations(Zellner, 1999; Vestreng *et al.*, 2007; Josipovic *et al.*, 2010). The latter problem has been increasingly emphasized during last years. Sulfur dioxide causes many respiratory and cardiovascular diseases. Its harmful effects on the lungs include:

- wheezing, shortness of breath and chest tightness, especially during exercise or physical activity;
- continued exposure at high levels increases respiratory symptoms and reduces the ability of the lungs to function;
- short exposures to peak levels of SO_2 in the air can make it difficult for people with asthma to breathe when they are active outdoors.

The risk is high for children, adults aged 65 and older, people with heart or lung disease, people with asthma who are active outdoors. Rapid breathing during exercise helps SO_2 reach the lower respiratory tract, as does breathing through the mouth.

Sulfur dioxide increases risk of the congenital heart disease such as aortic artery, valve, ventricular sepal defects (Manahan, 2010).

Deposition of SO_2 and products of its atmospheric transformation damages materials, soils and forests (Nellemann and Thomsen, 2001), and acidifies the surface waters. Acid rains bring about serious loss in fish stocks and in populations of other sensitive aquatic species (Oden, 1968).

Sulfur dioxide like isoprene, is a precursor of atmospheric aerosol (e.g., sulfate aerosols), which importance was discussed in Chapter 1.5.

1.2.3 Autoxidation of S(IV)

Autoxidation is a process of a compound oxidation in the presence of oxygen. Autoxidation of tetravalent sulfur (S(IV)) is an important process in the atmosphere, one of the pathways of the formation of acid rains. This process was extensively studied over last 20 years (Pasiuk-Bronikowska and Rudzinski, 1982; Berglund and Elding, 1995; Brandt and van Eldik, 1995; Fronaeus *et al.*, 1998). S(IV) autoxidation is catalyzed by transition metal such as iron(III) (Fe), manganese(II) (Mn), copper(I) (Cu) or cobalt (Co). In wide range of reaction acidity, the most efficient catalyst of the S(IV) autoxidation is an iron(III). However, there are a lot of hydrolytic species products (Baes and Mesmer, 1976) at different pH that complicates interpretations of the mechanism. Much smaller quantity of species has manganese. Nevertheless, ability of manganese to initialize the autoxidation of S(IV) is less than of Fe^{3+} but it is still an important sources of sulfate in atmospheric waters (Graedel *et al.*, 1986). Moreover, S(IV) conversion to O_2 conversion is reflect 2:1 stoichiometry of the overall autoxidation of S(IV) catalyzed by Mn(II) (Pasiuk-Bronikowska *et al.*, 1992).

There are several proposed mechanisms of the conversion of S(IV) into S(VI) catalyzed by Mn^{2+}. Berglund and Elding (1995) firstly proposed formation of manganese-sulfite complexes as a first step of oxidation of S(IV) by oxygen (Fig. 1.1). Then, $[Mn(HSO_3)^+]$ reacts with Mn^{3+} to form $SO_3^{\bullet-}$ radicals. These radicals rapidly react with dissolved molecular oxygen, producing $SO_5^{\bullet-}$ radicals. Reaction between $SO_5^{\bullet-}$ and Mn^{2+}

regenerates manganese(III) and forms $SO_5^{\bullet-}$. Hydrogen peroxymonosulfate oxidizes the complex $[Mn(HSO_3)^+]$ to produce sulfur(IV) as the final product.
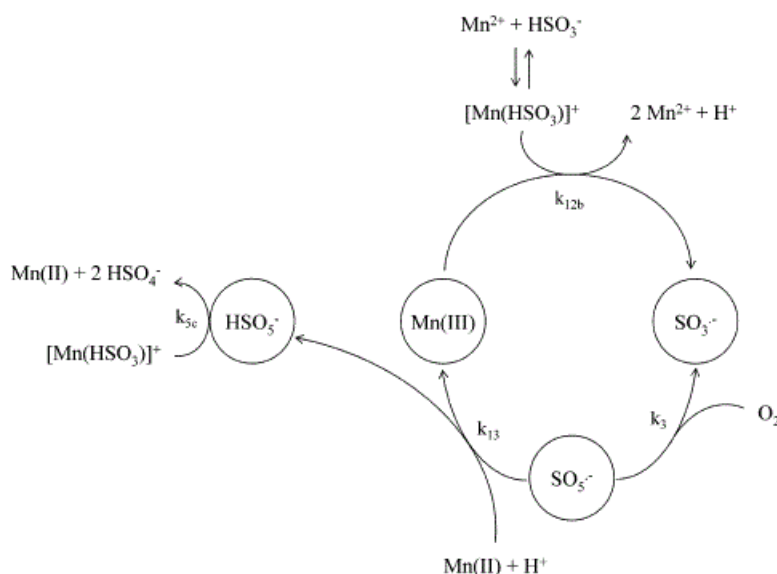
Fig. 1.1. *Proposed mechanism for the manganese(III/II)-catalyzed autoxidation of hydrogen sulfite (Berglund and Elding, 1995).*

This mechanism was corrected by Fronaeus *et al.* (1998). As catalytically active species, mixed-valence complex (OH)Mn(III)–O–Mn(II) was considered This complex reacts with HSO_3^- forming sulfoxy radical-anions $SO_3^{\bullet-}$, which propagate a chain reaction of autoxidation of S(IV) (Fig. 1.2). Formation of mixed-valence complex was confirmed with thermodynamic calculations based on redox equilibrium between Mn(II)/Mn(III) and Fe(II)/(III) systems. However, composition of the catalytic complex is still unknown.
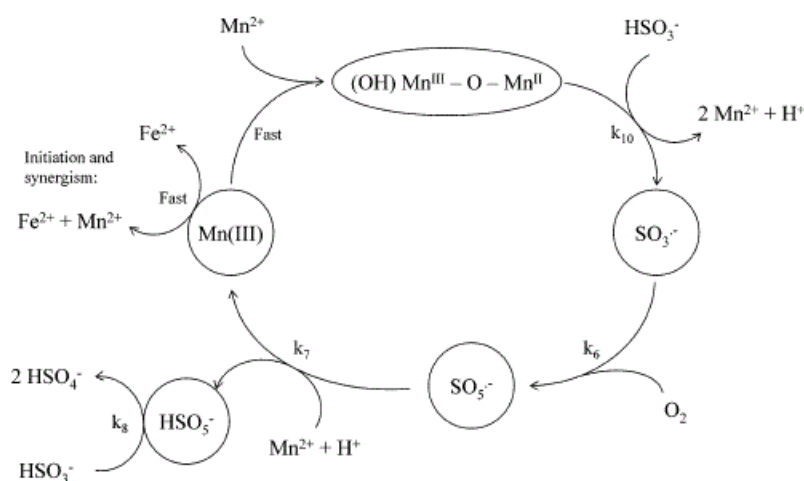
Fig. 1.2. *Catalytic cycle for manganese-catalyzed autoxidation of hydrogen sulfite, including Fe/Mn synergism and chain by trace concentration of Fe(III) (Fronaeus et al., 1998)*

Rudziński and Pasiuk-Bronikowska (2000) proposed and proved by modeling another mechanism of S(IV) autoxidation based on a scheme of the formation of organometallic complexes.

$$Mn(II)(OH_2)_6^{2+} + H_2O \rightarrow Mn(II)(OH)(OH_2)_5^+ + H_3O^+ \tag{1.1}$$

$$Mn(II)(OH_2)_5^+ + SO_3^{2-} \rightarrow (O_3S)Mn(II)(OH_2)_4^- + H_2O \tag{1.2}$$

$$(O_3S)Mn(II)(OH_2)_4^- + O_2 \rightarrow (H_2O)_4 (OH)(O_3S)Mn(III)O_2^- \tag{1.2}$$

$$(H_2O)_4 (OH)(O_3S)Mn(III)O_2^- + (O_3S)Mn(II)(OH)_4^- \rightarrow \tag{1.3}$$
$$\rightarrow (H_2O)_4(HO)(O_3S)Mn(III)OMn(III)(SO_3)(OH)(OH_2)_4^{2-}$$

$$(H_2O)_4(HO)(O_3S)Mn(III)OMn(III)(SO_3)(OH)(OH_2)_4^{2-} \tag{1.4}$$
$$\rightarrow 2Mn(III)^{3+} + 4OH^- + 2SO_3^{2-} + H_2O_2 + 6H_2O$$

$$SO_3^{2-} + H_2O_2 \rightarrow SO_4^{2-} + H_2O \tag{1.5}$$
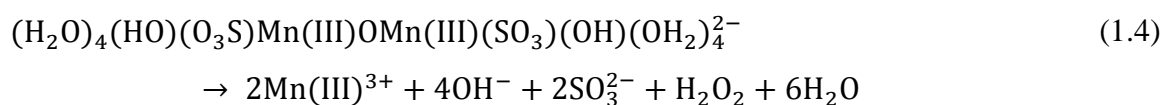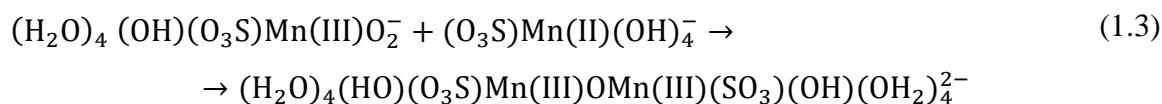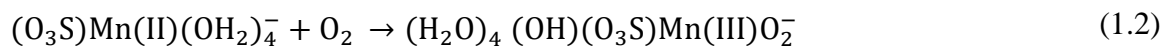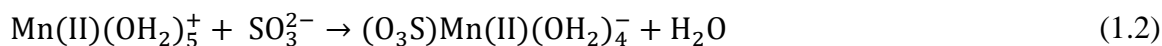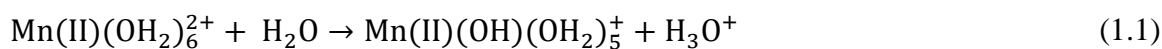
It was suggested that autoxidation of S(IV) is a complicated chain process propagated by sulfoxy-radical anions – sulfite, sulfate and peroxymonosulfate – forming during following reactions:

$$SO_3^{\bullet-} + O_2 \rightarrow SO_5^{\bullet-} \tag{1.6}$$

$$SO_5^{\bullet-} + SO_3^{2-}/HSO_3^- \rightarrow SO_3^{\bullet-} + SO_5^{2-}/HSO_5^- \tag{1.7}$$

$$SO_5^{\bullet-} + SO_3^{2-}/HSO_3^- \rightarrow SO_4^{\bullet-} + SO_4^{2-}/HSO_4^- \tag{1.8}$$

$$SO_4^{\bullet-} + SO_3^{2-}/HSO_3^- \rightarrow SO_3^{\bullet-} + SO_4^{2-}/HSO_4^- \tag{1.9}$$

$$SO_5^{\bullet-} + SO_5^{\bullet-} \rightarrow 2 SO_4^{\bullet-} + O_2 \tag{1.10}$$

$$SO_5^{\bullet-} + Mn(II)^{2+} \rightarrow SO_5^{2-} + Mn(III)^{3+} \tag{1.11}$$

$$SO_5^{\bullet-} + Mn(II)^{2+} \rightarrow SO_4^{2-} + 2 OH^- + Mn(III)^{3+} \tag{1.12}$$

$$SO_4^{\bullet-} + Mn(II)^{2+} \rightarrow SO_4^{2-} + Mn(III)^{3+} \tag{1.13}$$

$$SO_{2(g)} + H_2O \rightarrow SO_2 \times H_2O \tag{1.14}$$

$$SO_2 \times H_2O \rightarrow HSO_3^- + H^+ \tag{1.15}$$

$$HSO_3^- \rightarrow SO_3^{2-} + H^+ \tag{1.16}$$

$$2HSO_3^- \rightarrow S_2O_5^{2-} + H_2O \qquad (1.17)$$

$$SO_5^{2-} + SO_3^{2-} \rightarrow 2SO_4^{2-} \qquad (1.18)$$

$$HSO_5^- + HSO_3^- \rightarrow 2SO_4^{2-} + 2H^+ \qquad (1.19)$$
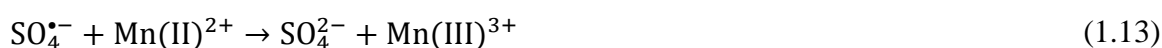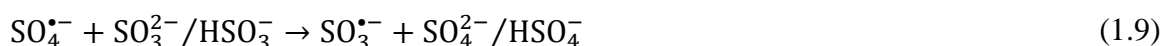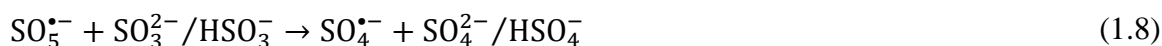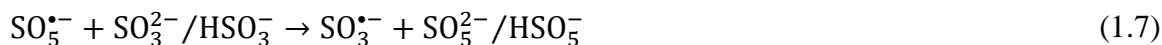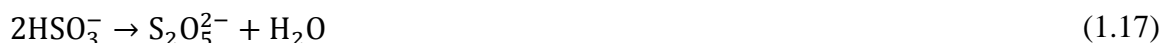
The termination of the process determine by reactions below:

$$SO_3^{\bullet-} + SO_3^{\bullet-} \rightarrow S_2O_6^{2-} \qquad (1.20)$$

$$SO_4^{\bullet-} + SO_4^{\bullet-} \rightarrow S_2O_8^{2-} \qquad (1.21)$$

$$SO_5^{\bullet-} + SO_5^{\bullet-} \rightarrow S_2O_8^{2-} + O_2 \qquad (1.22)$$

Nevertheless, there are still uncertainties in the mechanism of aqueous-phase sulfur(IV) oxidation by manganese-catalyzed oxygen.

1.3 Nitrous acid

1.3.1 Sources of nitrous acid

Nitrous acid (HONO) is an important trace component of the atmosphere. Although it was detected for the first time in ambient air in 1979 (Acker *et al.*, 2006), the source and the formation mechanisms of HONO in the atmosphere are not yet well known (Lammel and Cape, 1996). It is believed that nitrous acid is directly emitted from its sources such as vehicles (Djehiche *et al.*, 2011), aircrafts (Arnold *et al.*, 1992), combustion process (Pitts *et al.*, 1989) and cigarette smoking (Eatough *et al.*, 1989). Nitrous acid is also chemically formed in the atmosphere during daytime and nighttime. HONO daytime source strength is 500pptv/h but nighttime is only 8 pptv/h (Kleffmann *et al.*, 1998).

Daytime sources of the formation of HONO include heterogeneous processes and reactions in gas phase.

The most significant gas-phase reaction is fast reaction of NO· with OH˙ in the presence of metal (M):

$$\cdot NO + OH^{\cdot} + M \rightarrow HONO + M \qquad (1.23)$$

HONO can be formed upon the gas-phase reaction of photolytically excited $\cdot NO_2$ with water (Li *et al.*, 2008a). Importance of these sources is not estimated.

The reaction of $\cdot NO_2$ with $HO_2\cdot$ occurs at high concentration of substrates and low yield of nitrous acid (Stockwell and Calvert, 1983) has only a negligible importance too.

$$\cdot NO_2 + HO_2\cdot \rightarrow HONO + O_2 \tag{1.24}$$

Photolysis of aromatic compounds with *ortho*-nitrophenol unit can also explain high concentration of HONO in urban atmosphere (Bejan *et al.*, 2006).

Recent study has shown that photolysis of methyl nitrite is a source of HONO in air too (Djehiche *et al.*, 2011).

$$CH_3ONO + OH\cdot \rightarrow CH_3O + HONO \tag{1.25}$$

Daytime heterogeneous processes are the most probable sources of nitrous acid in the atmosphere, especially heterogeneous conversion of $\cdot NO_2$ on either the ground or the aerosol surface. Some of photochemical sources are a photo-enhanced reaction of gaseous $\cdot NO_2$ on solid organic compounds like aromatic hydrocarbons (George *et al.*, 2005) and conversion of $\cdot NO_2$ on humic acid aerosols (Stemmler *et al.*, 2007). However, it is difficult to make estimations about course of the reaction of the creation of nitrous acid under real atmosphere conditions and to explain mechanism of the formation of HONO near the ground in rural and urban areas (Kleffmann, 2007).

The photolysis of nitrate or nitric acid adsorbed on ground and vegetation surfaces is a main daytime source of HONO in polar regions (Zhou *et al.*, 2001; Zhou *et al.*, 2002b) and a significant one in rural areas, which was proved directly and indirectly (Zhou *et al.*, 2002b; Zhou *et al.*, 2002a; Kleffmann, 2007). Though, the detailed mechanism of HONO formation is still unknown.

The photolytic reduction of $\cdot NO_2$ on TiO_2 aerosols surfaces was revealed as a new source of HONO (Gustafsson *et al.*, 2006) based on the Reaction 1.26:

$$2\cdot NO_2 + H_2O \rightarrow HONO + HNO_3 \tag{1.26}$$

More recently it was proved that Reaction 1.26 occurs also on mineral dust surfaces during dust storms (Gustafsson *et al.*, 2008).

Nighttime sources of the formation of nitrous acid include conversions of $\cdot NO_2$ on humid surfaces during heterogeneous Reaction 1.26 and directly emitted from it sources (Lammel and Cape, 1996; Vogel *et al.*, 2003). The mechanism of this reaction is still unclear.

There are some studies where different hydrocarbons were absorbed on humid surfaces such as soot (Ammann *et al.*, 1998) or aqueous solutions containing phenolic compounds (Ammann *et al.*, 2005) but it has proved that this of minor importance (Kleffmann, 2007).

Reaction 1.27 was suggested a source of nitrous acid (Calvert *et al.*, 1994) but it was shown unimportant for the atmosphere (Kleffmann *et al.*, 1998). That also the case with Reaction 1.28 (Saliba *et al.*, 2000).

$$NO\cdot + \cdot NO_2 + H_2O \rightarrow 2\ HONO \tag{1.27}$$

$$HNO_3 + NO \rightarrow HONO + \cdot NO_2 \tag{1.28}$$

1.3.2 Importance of HONO

Nitrous acid plays an important role in photochemical air pollution. The photolysis of HONO under solar UV radiation leads to the formation of hydroxyl radicals (OH$^{\cdot}$), the key oxidant in the degradation of most air pollutants in the troposphere.

$$HONO + hv \rightarrow NO\cdot + OH^{\cdot} \tag{1.29}$$

This reaction explains the daily OH$^{\cdot}$ production. It was confirmed that HONO is the dominant precursor of OH$^{\cdot}$ during early hours of the morning in the lowest part of the troposphere in urban area in Rome (Acker *et al.*, 2006). At morning, up to 80% of OH$^{\cdot}$ is produced during Reaction 1.29. The "OH morning peak" could be explained by accumulation of HONO during the night. At noon, only 30% of OH$^{\cdot}$ comes from photolysis of HONO. Other sources of hydroxyl radicals at that time of the day are ozone and formaldehyde photolysis which contribute similar amounts about 30% (Platt *et al.*, 2002).

The discovery of HONO over sunlit snow surface showed that its photolysis is also important in polar regions (Dibb *et al.*, 2004).

Nitrous acid is a crucial intermediate in the formation of photochemical smog in the troposphere. The formation and photolysis of HONO accelerate the production of ozone, the oxidation of various pollutants and the formation of atmospheric aerosols (Aumont *et al.*, 2003; Harris *et al.*, 1982). It was proved that HONO has a direct impact on stratospheric ozone due to its heterogeneous reaction with HCl on sulfuric acid aerosols (Zhang *et al.*, 1996).

Therefore, photolysis of nitrous acid not only acts as the initiator of photochemistry in the early morning hours, but also plays a significant role as a precursor of photooxidants throughout the day. Very often HONO is regarded a typical trace compound of the polluted urban air whose amount depend on the level of the pollution (Acker *et al.*, 2006; Stutz *et al.*, 2010).

Emission of nitrous acid causes atmospheric acidification. Its formation of nitrous acid on surfaces leads to the acidification of the biosphere and the materials. Deposition of HONO was found on vegetation (Neftel *et al.*, 1996) and wet sandstone.

HONO is often present in indoor environments. Moreover, indoor concentration is higher than outdoor one. Typical indoor levels are $5 - 15$ ppbv (sometimes up to 100 ppbv), with [HONO]/[NO_2] ratios $0.15 - 0.4$ while for outdoor one is 0.03. The main indoor sources of HONO are direct emissions from invented combustion appliances (Spengler *et al.*, 1993; Eatough *et al.*, 1989), smoking and surface conversion of $\cdot NO_2$ and $NO\cdot$ (described above). Heterogeneous formation of HONO inside was also found in automobiles (Febo and Perrino, 1995). Level of nitrous acid inside the car was 30 ppbv and [HONO]/[NO_2] 0.4 in polluted urban areas. Lower outdoor level of nitrous acid comparing to indoor one is explained of photolytic instability of HONO (Reaction 1.29).

Nitrous acid affects also human health and life. It forms mutagenic (Kirchner and Hopkins, 1991) and carcinogenic nitrosamines (Pitts *et al.*, 1978) in the reaction with amines or residual nicotine from tobacco smoke sorbed to indoor surfaces (Sleiman *et al.*, 2010). Exposure of person to high concentration of HONO during short period of time has adverse effects to mucous membranes and lung function (Beckett *et al.*, 1995; Rasmussen *et al.*, 1995).

1.4 Transformations of isoprene

1.4.1 Gas-phase reactions

Reactions in gas phase are the most examined transformations of isoprene. Oxidation of isoprene in the air consists in reactions with the most reactive atmospheric species such as hydroxyl radicals ($OH^{\cdot}$), nitrate radicals ($NO_3^{\cdot}$), and ozone (O_3) (Le Bras *et al.*, 1997; Fan and Zhang, 2004; Paulot *et al.*, 2009; Taraborelli *et al.*, 2009). These reactions lead to formation of wide range of oxygen containing products with one or more oxygenated functional groups.

The possible products are alcohols (–OH), diols, polyols, aldehyde (–C(=O)H), hydroxyacetones (–C(OH)–R–C(=O)H), ketone (–C(=O)−), carboxylic acid (–C(=O)OH), hydroxycarboxylic acid (–C(OH)–R–C(=O)OH), dicarboxylic acids (HO(O=)C–R–C(=O)OH), nitrate esters (–ONO$_2$), peroxyacyl nitrate esters (–C(=O)OONO2), sulfate esters (–OSO$_3$), sulfate-nitrates esters (O$_3$SO–R–ONO$_2$), percarboxylic acid (–C(=O)OOH). Further reactions of these compounds give products with more complicated structure and are less volatile and more soluble in water than isoprene. The eventual products of gas-phase transformation of isoprene are carbon monoxide and dioxide.

Figure 1.3 – 1.5 presents shortened mechanism of the isoprene oxidation by OH$^{.}$, NO$_3^{.}$ and O$_3$, respectively. For simplicity, only 2 possible isomers were showed for all cases.
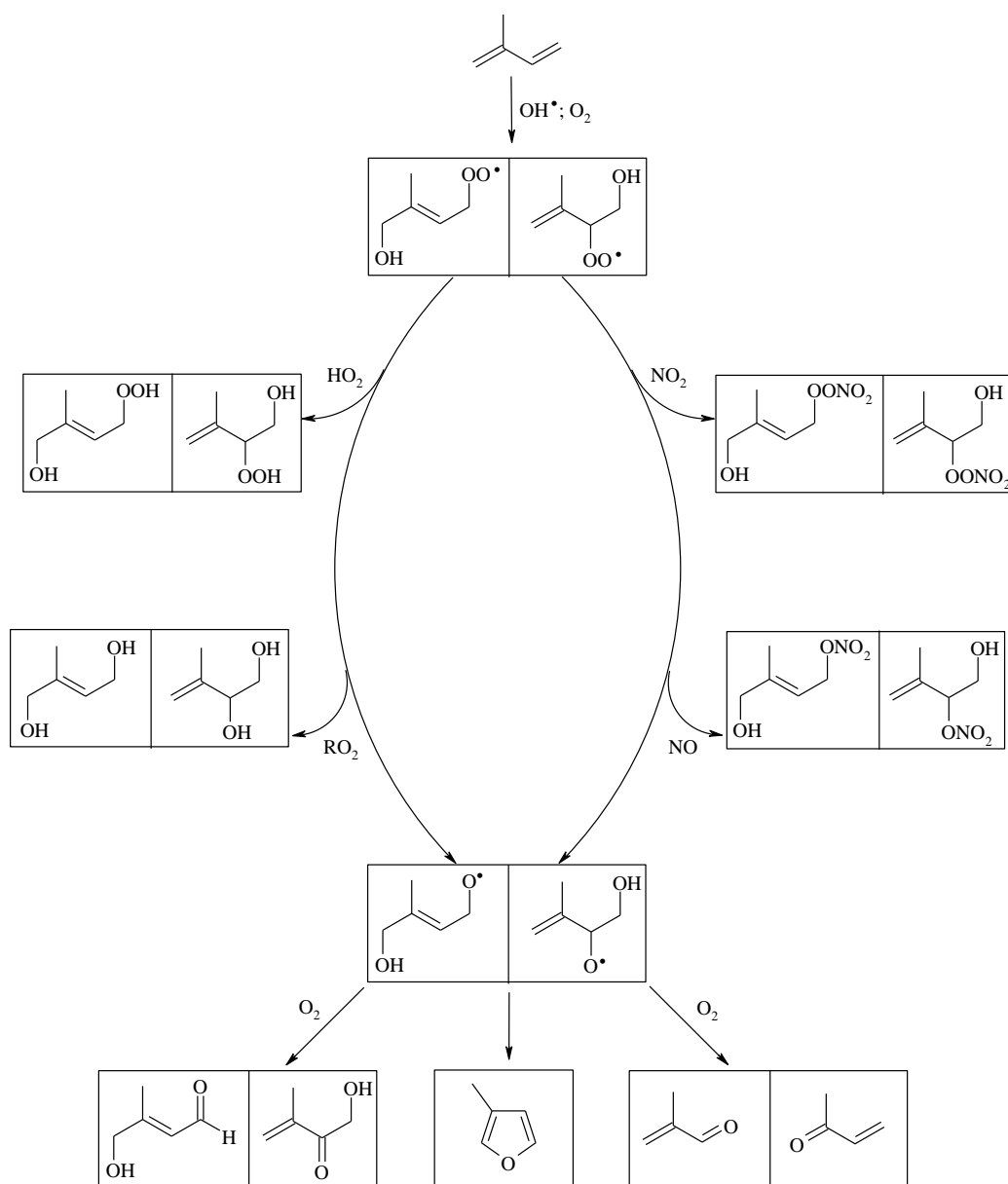
Fig. 1.3. *Simplified mechanism for the OH$^{.}$ initiated oxidation of isoprene.*

Isoprene in the presents of oxygen is attacked by OH· giving six possible isomers with one double bond in structure (Fig. 1.3). The peroxy-hydroxy radicals could react with ·NO₂, RO₂, and NO· forming variety products including methyl vinyl ketone, and methacrolein and 3-methylfuran. The contribution of these products to the carbon balance still needs improvement.
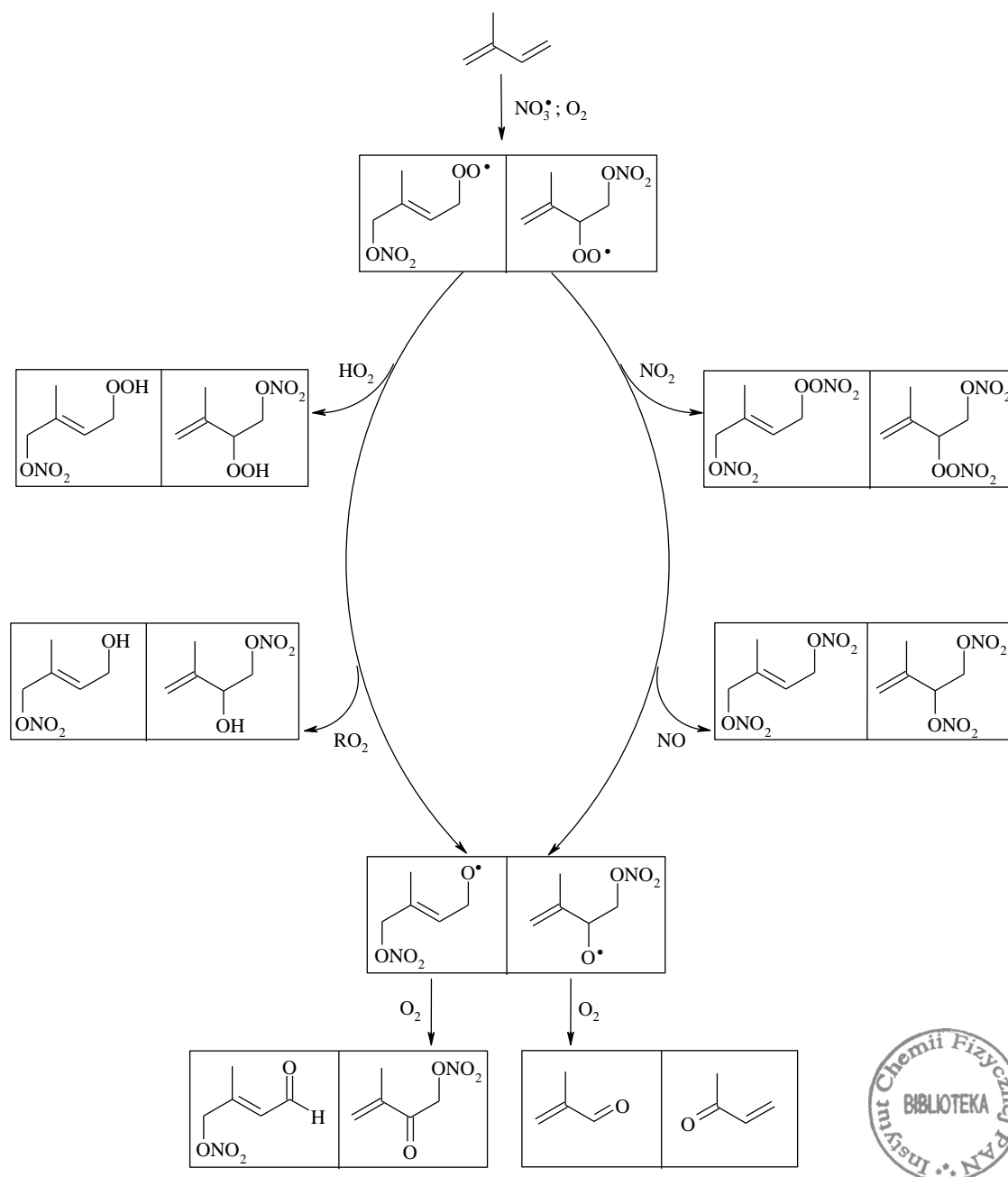

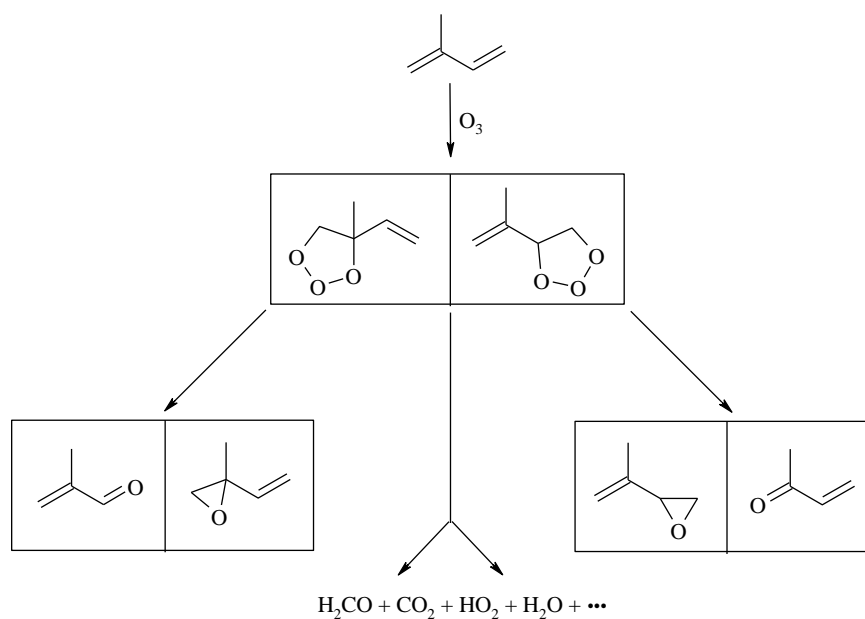**Fig. 1.4.** *Simplified mechanism for the NO₃ initiated oxidation of isoprene.*

Nitrite radicals in the presence of oxygen react with isoprene giving also six isomers of nitro-oxy-peroxy radicals similar to OH-initiated process. However, this addition is preferable in 1 position giving as a main product 3-mehyl-4-nitoxy-2-butenal. All other products are also needed for carbon balance.

Fig. 1.5. *Simplified mechanism for the O₃ initiated oxidation of isoprene.*

Isoprene reaction with ozone has distinguished pathway. During this transformation, O_3 adds to one of the isoprene double bond forming ozonides, which fragment in several ways giving as main products methacrolein, methyl vinyl ketone, and formaldehyde.

Although investigation of gas-phase transformation of isoprene is in progress, there remain uncertainties about the degradation pathways.
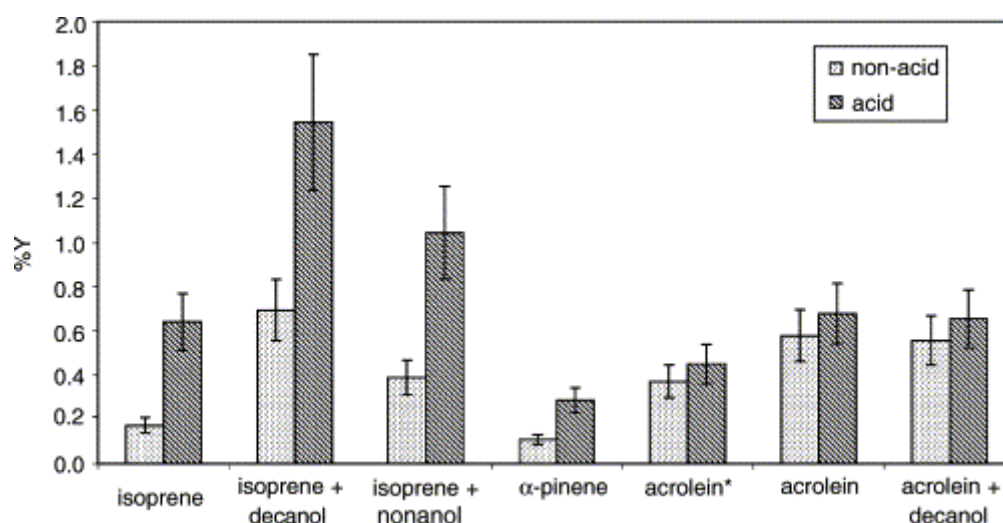
1.4.2 Heterogeneous reactions

As I mentioned before isoprene hadn't been considered as a significant precursor of secondary organic aerosols. Nevertheless, last laboratory, smog chamber and field studies showed that it makes considerable contribution to the formation of SOA.

Firstly, it was proposed to consider the role of heterogeneous reactions in SOA formation in climate change prediction models by Jang *et al.* (2002). The investigation showed that some atmospheric organic compounds including isoprene react heterogeneously on acidic surfaces of atmospheric aerosol, increasing yield of secondary organic aerosols. However, the importance of these reactions for atmosphere wasn't suggested in this study.

Importance of heterogeneous reaction of isoprene in atmosphere was shown by Limbeck *et al.* (2003). They demonstrated that particle-phase reaction of some dienes including isoprene in the presents of a sulfuric acid aerosol catalyst could be additional

sources of Humic-Like Substances (HULIS) in the troposphere. It had been investigated before that (HULIS) is a substantial constituent of water-soluble fraction of atmospheric organic aerosols. In rural and polluted areas the concentration of HULIS is from 20% to 50% (Zappoli *et al.*, 1998). The majority of these compounds have structure similar to humic and fulvic acid, that's why it were named humic-like substances. Molecular mass of HULIS is between 150 – 500 Da (Kiss *et al.*, 2003).These are polyacidic compounds of aliphatic and aromatic structures. Because HULIS were found in fog waters and aqueous extract of fine aerosols (Zappoli *et al.*, 1998; Facchini *et al.*, 1999) it was suggested it's may influence the hygroscopicity, cloud condensation nuclei (CCN) forming ability, surface tension and optical parameters of aerosol particles.

The same results were received by Czoschke *et al.* (2003). They used a twin Teflon bags and flow reactor to investigate reaction of isoprene, acrolein and α-pinene with ozone in presence of acid or non-acid inorganic seed aerosols. For all compounds there was an increasing yield of secondary organic aerosols in case of using acid seed catalyst comparing to non-acid ones (Fig. 1.6).


Fig. 1.6. *Percent yields of aerosol from twin bag experiments. (These values have been divided by 10 to fit the chart) (Czoschke et al., 2003).*

These studies triggered comprehensive investigations of isoprene heterogeneous reaction in the atmosphere. The influence of the presents of SO_2 on irradiated of isoprene/NO_x/air mixture was researched by Edney *et al.* (2005). The results showed that appearance of sulfur dioxide significantly boost the acid-catalyzed photooxidation of isoprene in presents of NO_x from ~ 0 to 2.8%. The main products of this oxidation were 2-methylthreitol, 2-methylerythritol and 2-methylglyceric acid which had been observed in the natural aerosol from the Amazonian rain forest and at K-puszta, Hungary (Chapter 1.3.2.)

(Claeys *et al.*, 2004a; Claeys *et al.*, 2004b). These compounds among some others were suggested to call "markers" of the oxidation of isoprene in the atmosphere. Importance of the photooxidation of isoprene with NO_x in the presents of SO_2 for atmosphere wasn't established. The mechanism of the formation of 2-methyltetrols and 2-methylglyceric acid was not presented.

This investigation was continued by Kleindienst *et al.* (2006). It was widened by studying of impact the different concentration of sulfur dioxide on the irradiation of isoprene and α-pinene in presence of NO_x. The initial concentration of isoprene was $3600 \pm 10 \mu gCm^{-3}$, NO_x – 492 or 475 ppb, SO_2 – from 0 to 291 ppb. The yield of SOA formation was from 0.11 %, in case of absence of SO_2, to 0.71 %, in case of maximum one concentration. In other words, this study proved increasing the SOA formation of isoprene SOA in the presence of SO_2 (Fig. 1.7). It was also suggested importance of these reactions for areas impacted by biogenic oxidation products and SO_2.
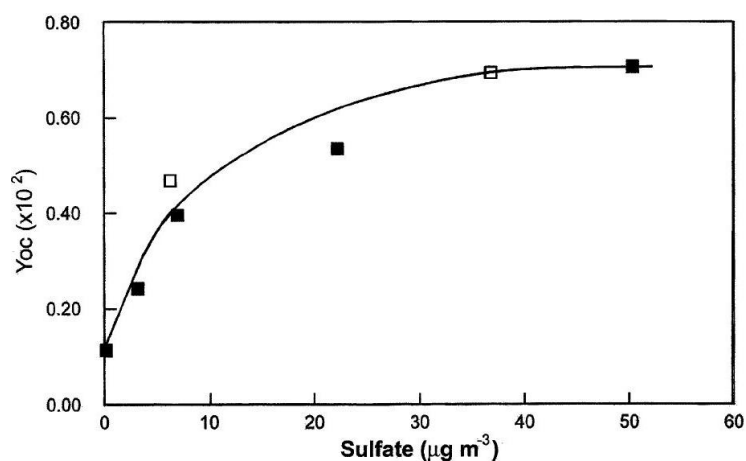
Fig. 1.7. *Secondary organic carbon yield of isoprene with increasing levels of sulfate (Kleindienst et al., 2006).*

The influence of different initial concentrations of NO_x was probed too. Kroll *et al.* (2006) studied photooxidation of isoprene with $OH^•$ radical at different NO_x regimes. The products formation was checked by Atmospheric Mass Spectrometer (AMS). It was proved that forming products were organic compounds (Fig. 1.8) because of typical AMS spectra. Experiments at high-NO_x conditions showed decreasing of SOA yield with increasing $[NO_x]$. Low-NO_x ones, leads to the rapid decreasing of SOA what could be explain by reactions of semi-volatile SOA components.

20
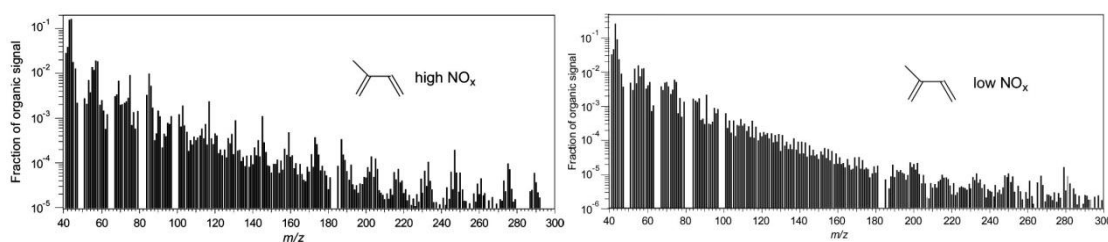
Fig. 1.8. *Typical AMS spectrum of SOA formed from isoprene photooxidation under high- and low-NO_x conditions (Kroll et al., 2006).*

The direct oligomers formation was also observed on acidic sulfate aerosols from isoprene and α-pinene (Liggio *et al.*, 2007). These oligomers contained 4 and 2 repeating units, respectively.

The main parameters that affect the yield of SOA formation from isoprene were summarized by some model (Ervens and Kreidenweis, 2007). So, low-NO_x conditions enhance isoprene SOA formation. Acid-catalyzed reactions increase the yield of it up to 50% comparing to neutral ones (Pun and Seigneur, 2007). The concentration ratio of organics/NO_x, relative humidity, and absorbing mass are more significant parameters for efficiency of the heterogeneously oxidation of isoprene.

Vivanco *et al.* (2011) performed chamber experiments in both presence and absence of SO_2 and HONO comparing properties of mixture of biogenic parent organic gases (isoprene, α-pinene and limonene) with anthropogenic ones (1,3,5-trimethylbenzen, o-xylene, octane, and toluene). The results showed higher yield of SOA formation, larger particle and its rapid growth in the case of the first mixture.

Polyols, the markers of oxidation of isoprene, formation were observed in another chamber study. There were reactions of isoprene with H_2O_2 on or in acidic particles which lead to the formation of 2-methyltetrols (Böge *et al.*, 2006). The mechanism of polyols formation from isoprene was proposed (Fig. 1.9). The laboratory data showed that isoprene gives low amounts of 2-methyltetrols. Nevertheless, estimations were able to explain high concentrations of the 2-methyltetrols origin from isoprene oxidation in forest aerosols from Amazonia under high-NO_x conditions during the biomass burning period compared to those under low-NO_x conditions during the wet season.
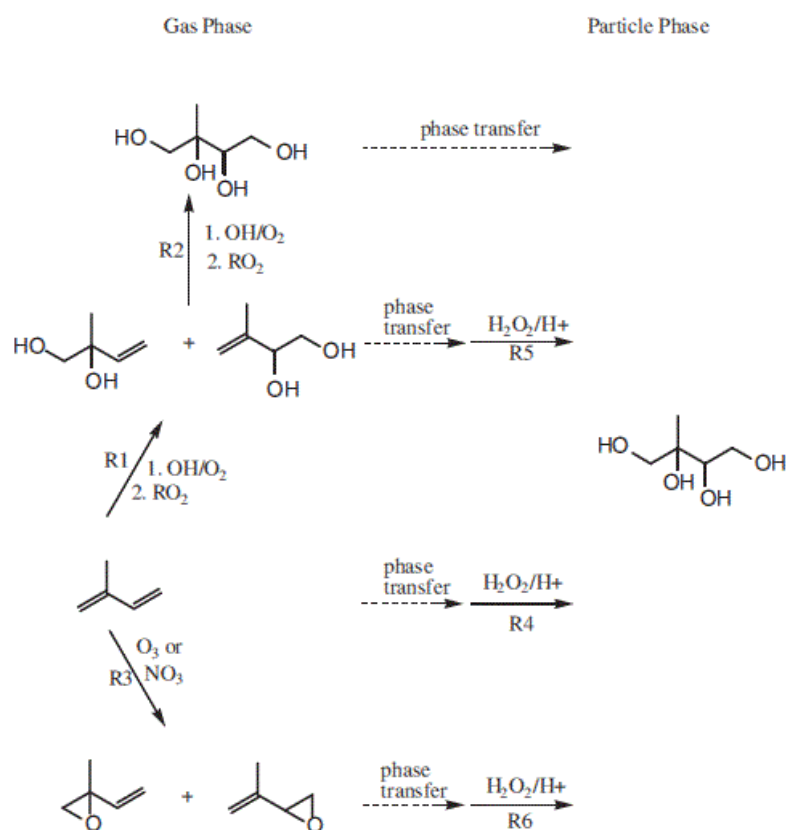
Fig. 1.9. *Proposed reaction pathways for the atmospheric formation of 2-methyltetrols from isoprene (Böge et al., 2006).*

Another markers of isoprene such as glyoxal and methylglyoxal were recently identified in aerosol collected at K-puszta (Gómez-González *et al.*, 2008) and in laboratory studies (Healy *et al.*, 2008). Moreover, laboratory data showed higher yield of SOA formation then it was proposed by modeling studies.

The average concentration of isoprene markers was recently shown about 250 ngm^{-3} during the dry period, 157 ngm^{-3} during the transition period and 52 ngm^{-3} during the wet period (Claeys *et al.*, 2010). The average concentrations of 2-methyltetrols were 54 ngm^{-3}, 34 ngm^{-3}, and 27 ngm^{-3}, respectively. In dry period, the acidity of the aerosols and NO$_x$ concentration increased while the wet deposition decreased, which could lead to the enhanced SOA formation from isoprene.

Another important products of heterogeneous transformation of isoprene it atmosphere are esters, especially organosulfates. First evidence of it was presented by Surratt *et al.* (2006). Moreover, the esters that form during photooxidation of isoprene in presents of OH radicals under different NO$_x$ conditions had oligomeric structure. The chemical composition of secondary organic aerosols strongly depended on the NO$_x$ concentrations. It was suggested that under high-NO$_x$ conditions monomeric units of polyesters is 2-methylglyceric acid with

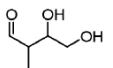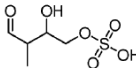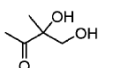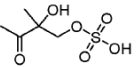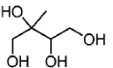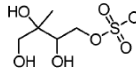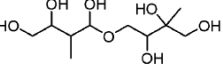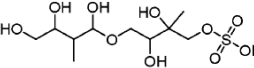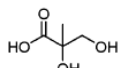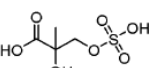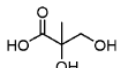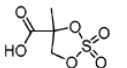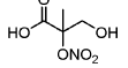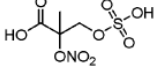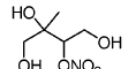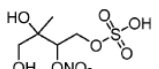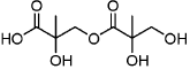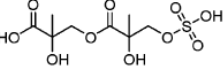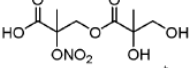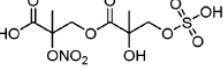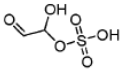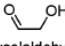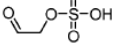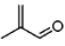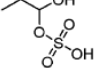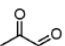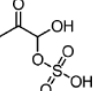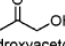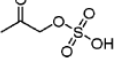102 Da differences which is a further product of oxidation of methacrolein, first-generated product of isoprene oxidation. Other compounds of SOA had acidic nature too. Under low-NO_x conditions, organic peroxides and hemiacetal dimers are the main products of the oxidation of isoprene. It was suggested that oligomers consist of a peroxyhemiacetal units. Simplified mechanism of the transformation of isoprene under high- and low-NO_x conditions was proposed too (Fig. 1.10).

Lately, this author (Surratt *et al.*, 2007b) identified structure of sulfate esters (Table 1.2) produced in chamber experiments and showed that these esters were found in samples of atmospheric aerosol. It was proved that these organosulfates hadn't been artifacts and these pathways of SOA formation were important for atmosphere. It was shown that acidity of sulfate aerosols enhanced yield of sulfate esters formation and explained uncertainties from earlier studies.
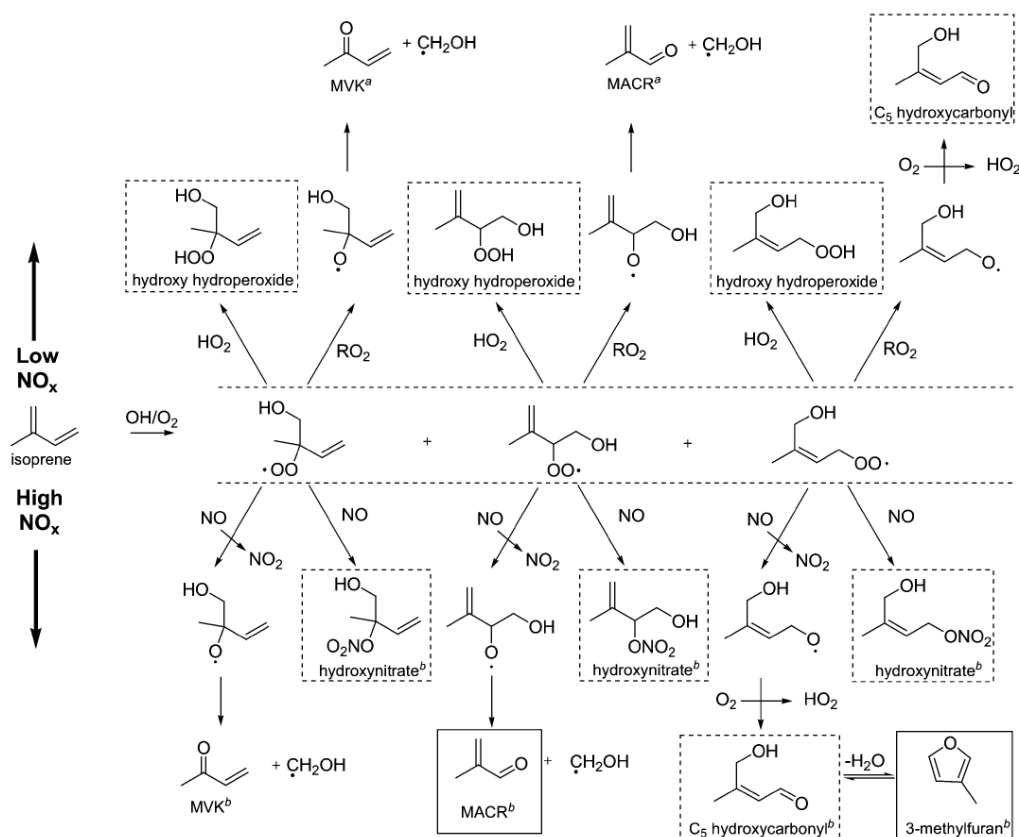
Fig. 1.10. *Reaction mechanism of isoprene oxidation under low- and high-NO_x conditions. Dotted boxes indicate possible SOA precursors, whereas black boxes indicate known SOA precursors (Surratt et al., 2006).*

Table 1.2. *Proposed isoprene sulfate ester SOA products.*

previously identified isoprene SOA product[a]	MW	proposed sulfate ester structure[a]	observed [M − H]⁻ ion (m/z)	major [M − H]⁻ product ions (m/z)
Low-NOₓ				
C₅ alkene triol / ald form[b]	118		197	97 80
C₅ alkene triol / keto form[b]	118		197	97 80
2-methyltetrols[b]	136		215[c,d]	97 80
hemiacetal dimer[b]	254		333[d]	315 (- H₂O)[e] 215 (- C₅ alkene triol) 197 (- 2-methyltetrol) 97 80
High-NOₓ				
2-methylglyceric acid (2-MG)[b]	120		199[c]	119 (- 2-MG) 97 80
2-methylglyceric acid (2-MG)[b]	120		181	97 80
2-MG acid nitrate[b]	165		244	226 (- H₂O) 197 (- HONO) 153 (- [CO₂ + HONO]) 97
C₅ trihydroxy nitrate[f]	181		260[d]	197 (- HNO₃) 183 (- CH₃NO₃) 97 80
2-MG dimer[b]	222		301	257 (- CO₂) 119 97 80
2-MG nitrate dimer[b]	267		346	[g]
Highest Acidity Conditions				
glyoxal	58		155	[g]
glycolaldehyde[h]	60		139	[g]
methacrolein	70		167	[g]
methylglyoxal[h]	72		169	[g]
hydroxyacetone[h]	74		153	[g]

The first tentative estimation of the mass concentration of organosulfates in ambient rural aerosols was performed by Lukács *et al.* (2009). The results showed that up to 12% of total sulfur concentration were organosulfates, with the lower concentration limit in water-soluble fine aerosol estimated at $0.02\,\mu gSm^{-3}$ to $0.09\,\mu gSm^{-3}$. The connection between sulfates and organosulfates in aerosol phase was also proposed in more recent studies (Vivanco *et al.*, 2011).

1.4.3 Aqueous-phase reactions

Atmospheric aqueous-phase reactions are a potentially important source of Secondary Organic Aerosols (SOA) (Blando and Turpin, 2000; Fu *et al.*, 2009). These processes could explain the atmospheric presents of some compounds (Carlton *et al.*, 2006). It occurs in suspended water droplets in clouds, fogs, mists, hazes and aerosols. Formation of SOA through cloud processing requires: (1) the uptake of organic compounds into water droplets, (2) its chemical reaction with other dissolved species and/or water, (3) the evaporation of droplets, leaving low-volatility products in the particle phase. Solubility of precursor compound is an important condition because of first step of the process. Isoprene was regarded as insoluble in water compound and, thus, has not been shown to contribute to SOA formation through aqueous-phase mechanism. However, isoprene solubility is 0.940×10^{-2} M and its concentration in water may be significant for the atmosphere (Rudziński, 2004). For instance, it was found up to 94 pmol l^{-1} isoprene in the ocean and up to 100 parts-per-trillion (pptv) of isoprene in marine air which partly explained by sea-to-air fluxes (Matsunaga *et al.*, 2002).

Pedersen and Sehested (2001) estimated rate constants, activation energies for the aqueous-phase ozonation of isoprene and some of it first-generation products – methyl-vinyl-ketone and methacrolein. Overall lifetimes of these compounds in a cloud environment were also calculated. But results showed that transformations of isoprene in clouds are of minor importance in all it atmospheric processes.

Rudziński (2004) showed that isoprene inhibited the autoxidation of SO_2, or S(IV) in weakly alkaline solutions (pH ~ 8.5). Tentative mechanism of the reaction of isoprene coupled with autoxidation of S(IV) were proposed and suggested that this transformation could be important for rain forest, sea-coastal regions and urban areas.

Claeys *et al.* (2004a) found for the first time diastereoisomers of a polyols, particularly 2-methylthreitol and 2-methylerythritol, in natural aerosols from the Amazonian rain forest. It was suggested that these compounds formed through OH˙ radical-initiated photooxidation of isoprene that just condensed to aerosol. Mechanism that was proposed requires low-NO$_x$ conditions like natural tropic ones (Fig. 1.11). Samples also contained mono- and dihydroxydicarboxylic acids, for example, malic, α-hydroxyglutaric, tartaric acid. Some saccharidic compounds such as levoglucosan, arabitol, mannitol and glucose were identified too. The same polyols were found in rural aerosols from the continental forest at K-puszta, Hungary (Claeys *et al.*, 2004b). Nevertheless, in this paper authors proposed that 2 methyl-tetrols are formed under high-NO$_x$ conditions which happen during the biomass burning period. Homogeneous mechanism of its formation was also reexamined and acid-catalyzed reactions with hydrogen peroxide in the aqueous aerosols phase have been proposed.
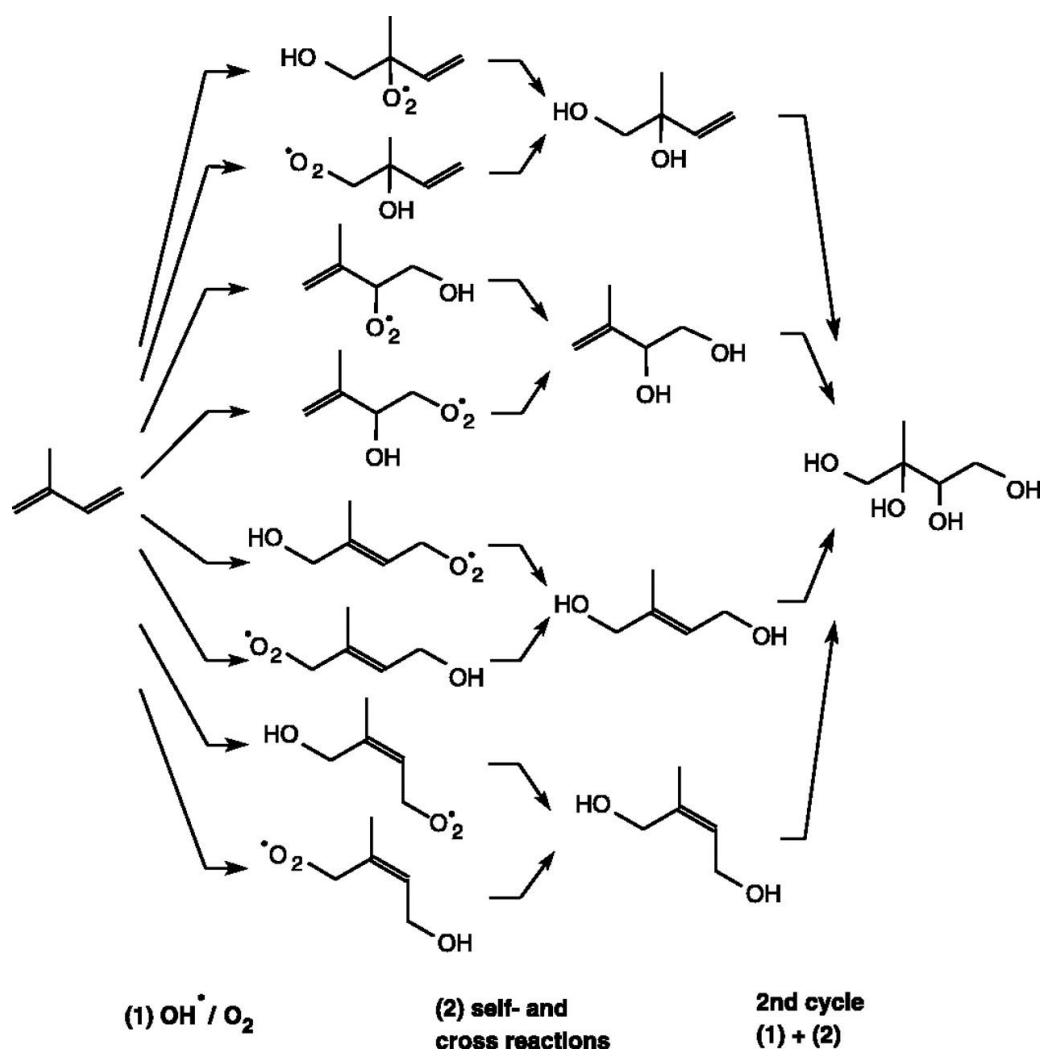
Fig. 1.11. *Believed mechanism of 2-methyltetrol formation from photooxidation of isoprene in the presence of acidic particles (Claeys et al., 2004a).*

Sato (2008) investigated photooxidation of four conjugated dienes including isoprene under high-NO_x conditions. The major products in the aqueous solutions of the SOA were 2-methyltetrols, nitrooxypolyols, 2-methylglyceric acid, and nitric acid for isoprene photooxidation. It was concluded that NO_x suppressed the gas-phase formation of 2-methyltetrols (Fig. 1.12).
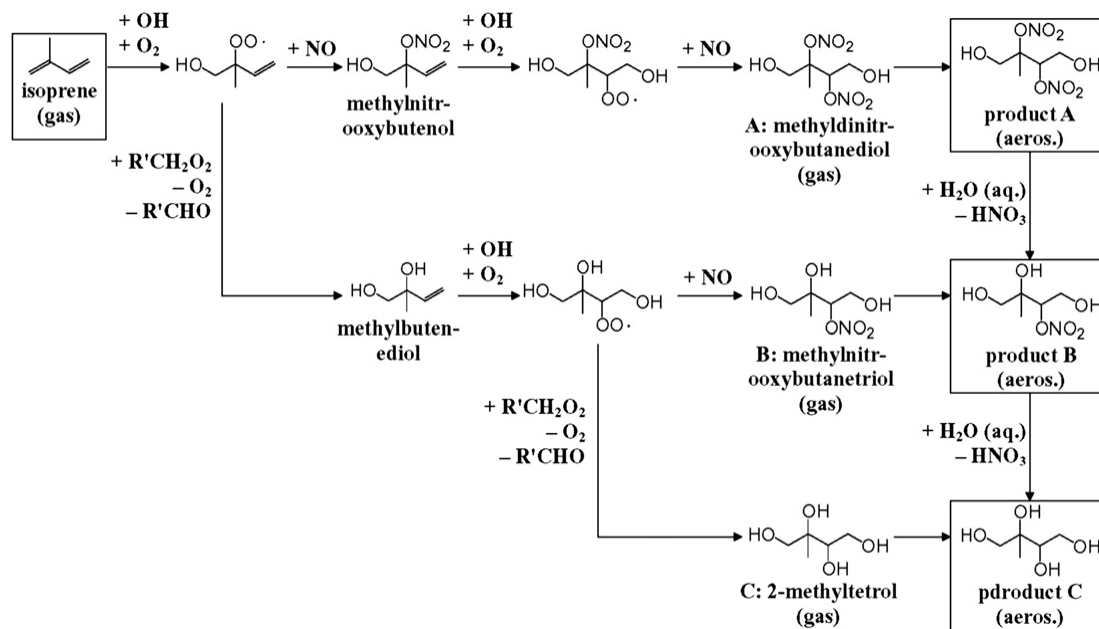
Fig. 1.12. *Proposed mechanism of methyldinitroxybutenediols, methylnitrooxybutentoriols and 2-methyltetrol formation from photooxidation of isoprene in the presence of NO_x (Sato, 2008).*

Rudziński *et al.* (2009) investigated autoxidation of isoprene with sulfoxy radical-anions in wide range of solution acidity (from 3 to 9). Different influence of isoprene on S(IV) autoxidation at different pH was observed. Isoprene slowed down the chain of oxidation of SO_2 in acidic and alkaline solutions and accelerated in neutral ones. Data obtained from experiments were compared with chemical-kinetic modeling. It was suggested that these reactions capable reduce acidification of atmospheric waters and aerosols.

Although isoprene has low solubility in water some of its products of gas-phase oxidation in the atmosphere become more soluble. Gas-phase oxidation of isoprene was discussed in Chapter 1.4.1.

Couvidat and Seigneur (2011) developed a new model for the formation of secondary organic aerosol (SOA) from isoprene. It were concluded that 1) SOA formed under low-NO_x conditions are highly hydrophilic which prefer aqueous phase rather than organic one; 2) under high-NO_x conditions form compounds with different solubility; 3) highly hygroscopic

SOA formed from isoprene would likely partition between an aqueous phase and the gas phase at high humidity in the atmosphere.

Water-soluble carbonyl compounds from isoprene oxidation could further oxidized in droplets forming different compounds including oligomers. Moreover, it is believed that aqueous-phase reaction could explain of the formation of high-molecule-weight compounds. Oligomers were found in ambient atmospheric aerosols, cloud and fog water (Limbeck *et al.*, 2003; Gelencsér *et al.*, 2002). Most of the second- and next-generation products of isoprene oxidation are water-soluble low-volatility organics that remain in cloud droplets upon its evaporation. These processes are one of the additional sources of SOA in the atmosphere – multiphase reactions. I'm going to talk about it in Chapter 1.5.

Aqueous-phase oligomer formation reduces the vapor pressure of products and enhancing SOA formation.

Formation of hygroscopic secondary organic aerosols from isoprene in atmospheric droplets could hand out as cloud condensation nuclei (CCN). It is very important in polluted areas because pollutants are a large source of water-soluble aldehydes and ketones.

Recent studies showed that isoprene is an important precursor of SOA formation through in-cloud processing. It was concluded because of high emission, concentration, reactivity, and yield of water-soluble products of isoprene oxidations.

Lim *et al.* (2005) predicted using a box model that typical emission of isoprene in the Amazon gives about 50 ngm^{-3} organic acid (Fig. 1.13). Isoprene forms in cloud 1.6 Tg yr^{-1} SOA that is a significant contribution to global source strength of biogenic SOA of 8 – 40 Tg yr^{-1}.
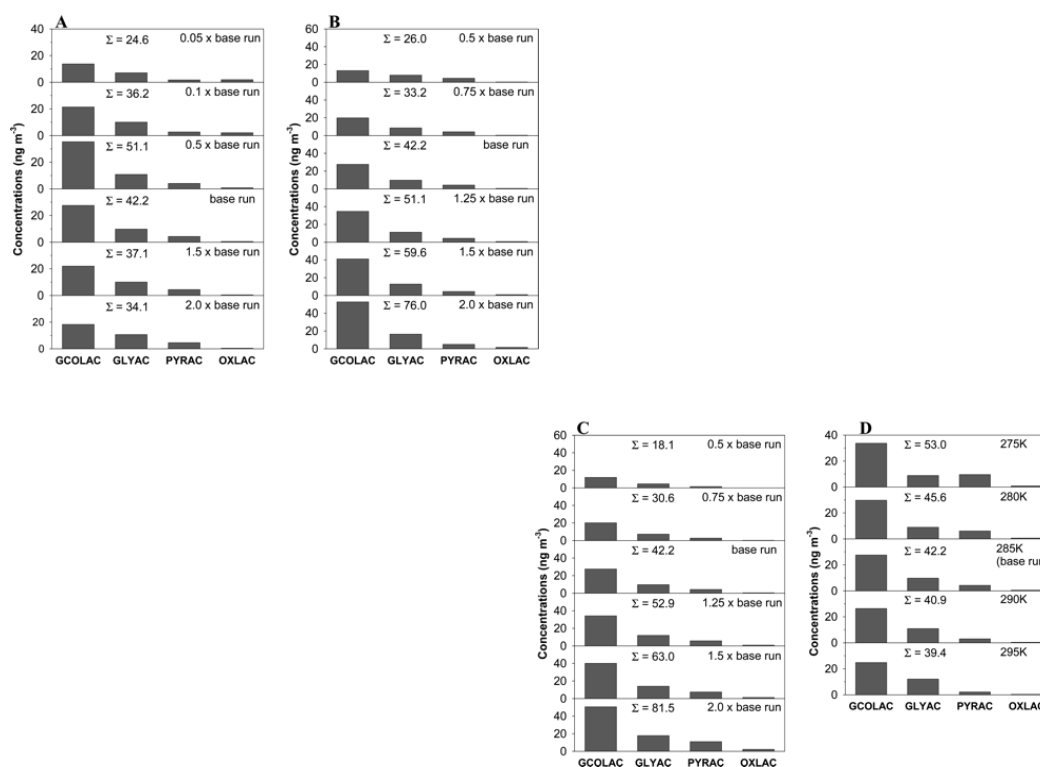
Fig. 1.13. *Particulate concentrations of glycolic acid (GCOLAC), glyoxylic acid (GLYAC), pyruvic acid (PYRAC), and oxalic acid (OXLAC) after three cloud processing with increasing (A) isoprene emission flux, (B) photolysis frequency, (C) liquid water content, and (D) temperature (Lim et al., 2005).*

Modeling investigations performed by Ervens (2008) showed that isoprene forms up to 42% of SOA under high-NO_x conditions. This could explain enhanced formation of SOA from isoprene in aircraft measurements of cloud-processed particles.

1.5 Atmospheric aerosols

Atmospheric aerosols are colloids or suspensions of fine particles or liquid droplets dispersed in the air. Examples of liquid droplets suspended in the air are mist, fog, and haze. On the other hand, smoke, fume, fly ash, dust, smoke, soot, and smog represent solid particles in the air. Diameters of the aerosol particles, Ø, fall in the range from 1 nm to 10 μm. Depending on their size, particles are classified by fractions: ultrafine or PM_1 (Ø < 1 μm), fine or $PM_{2.5}$ (1 μm > Ø < 2.5 μm) and course or PM_{10} (2.5 μm > Ø < 10 μm), where PM means "particulate matter".

Organic matter is a significant fraction of the total mass of tropospheric fine aerosols. It amounts to 20% − 50% at continental mid-latitudes (Saxena and Hildemann, 1996), and

close to 90% in tropical forests (Roberts *et al.*, 2001; Andreae and Crutzen, 1997). Cycling of atmospheric aerosols is presented in Fig. 1.14.
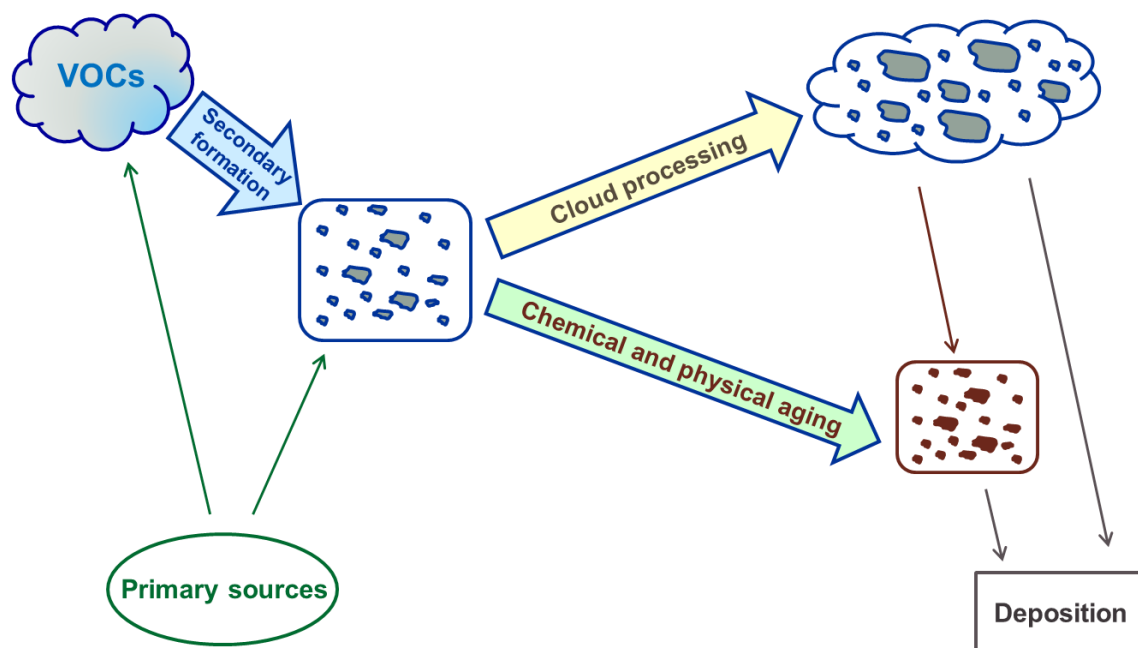
Fig. 1.14. *Cycling of atmospheric aerosols.*

There are primary and secondary organic aerosols. Primary organic aerosols (POA) originate from wide range of natural and anthropogenic sources. Natural sources include volcanic eruptions, dust storms, forest and grassland fires, living vegetation, sea spray, and mineral dust. Anthropogenic sources include industry, agriculture, transport, construction, and biomass burning.

Original understanding of Secondary Organic Aerosols formation is that Volatile Organic Compounds (VOCs) – directly emitted by terrestrial vegetation into the air – react photochemically with atmospheric oxidants in the gas phase to produce first-generation gaseous products which are more polar than their precursors and partition into particulate organic matter or liquid water (Seinfeld and Pankow, 2003).

However, there are many observations which cannot be explained by traditional view of SOA formation. The most important are: 1) formation of polyfunctional and high-molecular-weight organic compounds; and 2) higher oxygen-to-carbon (O/C) ratio in ambient low-volatility oxygenated organic aerosols than in aerosols from traditional smog chambers (Aiken *et al.*, 2008). Recent studies showed that these discrepancies could be explained by chemical and photochemical processes in atmospheric aqueous phase (Jang *et al.*, 2002; Tolocka *et al.*, 2004). According to this "modern theory" VOCs react via photochemistry, acid catalysis, and with inorganic constituents in the aqueous phase forming organic acids,

oligomers, and organosulfates (Carlton *et al.*, 2006; Surratt *et al.*, 2007b). After water evaporation, some of the products part into gas phase and some, less volatile remain in particles (Loeffler *et al.*, 2006). However, the present understanding of aqueous-phase mechanisms of SOA formations is far from completes.

Atmospheric aerosols have direct and indirect effect on Earth's climate. Aerosols reflect and absorb incoming solar radiation and terrestrial radiation. As a result, atmospheric aerosols modify Earth's radiation budget, therefore, have the "direct" cooling or warming effect on the Earth. Indirect effect of aerosols bases on their capacity to act as Cloud Condensation Nuclei (CCN) and thus to induce cloud formation. Moreover, fogs are formed by a similar mechanism (Kanakidou *et al.*, 2005).

Atmospheric aerosols also impact the air quality and human health. They influence atmospheric circulation and the abundance of greenhouse and reactive trace gases (Kanakidou *et al.*, 2005; Hallquist *et al.*, 2009). Airborne particles play important roles in spreading of biological organisms, reproductive materials, and pathogens (bacteria, pollen, spores, and viruses). Aerosols and bioaerosols affect human health causing respiratory, cardiovascular, infectious, and allergic diseases (Pope and Dockery, 2006).

Because of many existing uncertainties and gaps in our knowledge of sources, compositions, properties and mechanisms of atmospheric aerosol, in particular SOA, formation and transformation (Poschl, 2005), its true impact on the global climate and human health is not clear yet.

The most significant SOA precursors are biogenic hydrocarbons: aromatic hydrocarbons, most of terpenes, cycloalkenes and some acyclic compounds (Table 1.3). Isoprene, the main biogenic VOC, was at first not considered a direct precursor of SOA. However, in 2004 the products of the aqueous phase oxidation of isoprene – 2-methyltetrols, 2-methylglyceric acid and 3 isomeric C_5-alkene triols – were identified in field samples of aerosol from the Amazon rainforest in Brazil and from a forest site at K-puszta, Hungary (Claeys *et al.*, 2004b; Claeys *et al.*, 2004a). Since then, heterogeneous and aqueous-phase transformations of isoprene have been considered sources of SOA components. (Reactions of isoprene in the atmosphere were discussed in previous chapter.)

Table 1.3. *The main SOA precursors (Seinfeld and Pandis, 1998)*

Aromatic hydrocarbons	Monoterpenes	Other reactive VOCs
Toluene	α-Pinene	Cycloalkenes
m-,o-,p-Xylene	β-Pinene	Alkenes
1,2,4-Trimethylbenzene	Δ^3-Carene	Isoprene [a]
1,3,5- Trimethylbenzene	Sabinene	Linalool
m-Ethyltoluene	Myrcene	Terpenoid alcohols
o- Ethyltoluene	Limonen	Sesquiterpenes
	Ocimene	
	α-Terpinene	

[a] (Hallquist *et al.*, 2009)

This thesis deals with reactions of isoprene with inorganic compounds, namely dissolved forms of sulfur dioxide and nitrous acid that can lead to formation of SOA components.

2 Goal

The presented thesis aims to provide insight into aqueous-phase reactions which can significantly influence the production of new components of the atmospheric air, secondary aerosols, and precipitation that affect the air quality. Specifically, the thesis aims to describe the kinetics, mechanisms and products of aqueous-phase reactions of isoprene, C_5H_8, in the presence of oxygen, O_2, and dissolved forms of sulfur dioxide, SO_2, nitrous acid, HONO, and manganese(II) sulfate, $MnSO_4$.

The aims of the thesis are justified by a large gap between field measurement and model predictions of the composition and concentration of secondary organic aerosols as well as its properties. The aqueous-phase reactions in clouds, fogs, and deliquescent aerosols provide an additional important pathway of SOA formation. Studies of aqueous-phase transformations of atmospheric trace compound can provide missing formation routes of several components of SOA and rainwater, and therewith, help to evaluate the regional and global impact of atmospheric aerosols on visibility, climate, and human health and life, and solve some problems connected with it.

3 Experimental part

3.1 Methods

3.1.1 Mass Spectrometry

Mass spectrometry is an analytical technique used for qualitative studies of organic compounds. This method studies the masses of atoms or molecules or fragments of molecules. To obtain a mass spectrum, the sample molecules are ionized, the ions are accelerated by an electric field and then separated according to their mass-to-charge ratio, *m/z*. The area of each peak is proportional to the abundance of each isotope. That is why, MS technique gives also quantitative information (Hesse *et al.*, 1997). The accuracies of measuring mass are 0.01% for big organic molecules. Mass spectrometry is used for determination of:

- masses of particles;
- elemental composition of sample or molecules;
- the chemical structures of molecules such as the amino acid sequence in a protein, the nucleic acid in DNA, structure of a complex carbohydrate, and the types of lipids in a single organism;
- purity of the compound;
- composition of the mixture of chemical compounds;
- masses of individual cells and viruses.

Mass spectrometers have three basic parts such as the ionization source, the analyzer and the detector. The samples are first introduced into the ionization source of the instrument, where they are ionized to acquire positive or negative charges. In analyzer ions are separated according to their mass-to-charge ratios (*m/z*) and arrive at different parts of the detector.

Electrospray Ionization (ESI) is one of the types of ionization sources in mass spectrometers. The ESI are operated at/or near atmospheric pressure and, thus is also called Atmospheric Pressure Ionization (API). It is a sensitive (ng-pg), robust, and reliable technique. The ESI let to form charged ions (also multiply) from relatively non-volatile, polar, thermally labile compounds that are not willing to analyze by other conventional techniques. The ranging of analyzing molecule masses is from less than 10 Da to more than 100 000 Da.

Mass spectrometry is the most powerful detector for chromatography (Chapter 3.1.4). Example of this is Gas Chromatography/Mass Spectrometry (GC/MS). It is actually two techniques that are combined to form a single method of analyzing mixtures of chemicals.

Analyzing mixture of compounds is initially injected into the GC where the mixture is vaporized and separated on the column. Each component of the mixture then immediately is characterized by mass spectroscopy.

The GC/MS allows separating, quantifying, and identifying complex mixture and uses in the medical, pharmacological, environmental, and law enforcement fields.

3.1.2 Nuclear Magnetic Resonance

Nuclear magnetic resonance (NMR) is an analytic technique which based on ability of magnetic nuclei in a magnetic field absorbs and reemits electromagnetic radiation. Under appropriate conditions a sample can absorb light in the radio frequency region – 60 ÷ 1000 MHz at frequencies governed by the characteristics of the sample (Hesse *et al.*, 1997).

It could be explained by that many nuclei have an overall spin and all nuclei are electrically charged. If an external magnetic field is applied, the spin changes its orientation and emits energy at appropriative frequency. This frequency depends on different things such as the type, chemical environment of the nuclei, its spatial location in the magnetic field and strength of that field. There are many nuclei with non-zero spin, but the most commonly studied ones are ^{1}H and ^{13}C.

The ^{1}H NMR spectrum of an organic compound provides information concerning the number of different types of hydrogen atoms present in the molecule, their relative number, their electronic environment, and the number of their "neighbors".

This technique is used for:

- determination or proving of the chemical structure of organic compounds;
- determination of the stereochemistry of organic compounds;
- determination the purity of a sample;
- kinetic investigations;
- determination of the amount of compounds in solution of a sample;

NMR is also routinely used in advanced medical imaging techniques.

3.1.3 UV-VIS Spectrophotometry

Ultraviolet-visible spectrophotometry (UV-VIS) is an analytic technique based on measurement of the interaction of electromagnetic radiation and matter. Spectrophotometry investigates the absorption of the different substances in gas or vapor state or dissolved molecules and ions. The investigative range of light wavelength is from 190 nm to 780 nm where 190 – 400 nm is an ultraviolet and 400 – 780 nm – visible regions (Hesse *et al.*, 1997).

Spectrophotometry is used for both qualitative and quantitative determination of different analytes.

Wavelengths at the maximum of the compound's absorption are important data for qualitative investigation. They give information about numbers and types of absorption bands corresponding to structural groups within the molecule or ion. Different molecules absorb radiation of different wavelengths.

The quantitative determination shows that the extent of the absorption is proportional with the amount of the species absorbing the light. These methods are based on Lambert-Beer Law:

$$A = log_{10}(I_0/I) = \varepsilon cl \qquad (3.1)$$

where, A is absorbance, I_0 – the incident light's intensity at given wavelength, I – the light intensity after it passes through the sample, ε – molar extinction coefficients, c – concentration of the compound in the solution, l – path length of light through the sample.

Absorbance is an additive function that's mean that absorbance of a mixture is a sum of the absorbance of the components:

$$A = A_1 + A_2 + A_3 + \cdots + An = \varepsilon_1 c_1 l + \varepsilon_2 c_2 l + \varepsilon_3 c_3 l + \cdots + \varepsilon_n c_n l \qquad (3.2)$$

The number of wavelength used to determine the absorbance is equal with the number of the constituents. If multicomponent mixture follows additive law, and each component follows the Lambert-Beer's Law, then the spectra of the mixture can be decomposed into the spectra of its components to reveal the composition of the mixture.

Spectrophotometric method is used for:
- identification of compounds such as transition metal ions, highly conjugated organic compounds and biological macromolecules;
- determination of substances purity;

- determination of presence and amount of double and triple bonds in molecule or ion;
- kinetic investigations;
- determination of the amount of compounds in solution.

A UV/VIS spectrophotometer may be used as a detector for HPLC (Chapter 3.1.4.).

3.1.3.1 Woodward –Fieser rules

Woodward-Fieser rules allow predicting position of absorption maximum wavelength of the longest $\pi \rightarrow \pi^*$ transitions in UV spectrum of open-chain, homo- and heteroannular dienes and trienes (Hesse *et al.*, 1997).

The incremental rules start from specific base values for dienes of different configurations (Fig. 3.1).
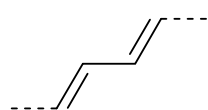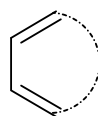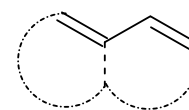
| (acyclic) | (homoannular) | (heteroannular) |
| 217 nm | 253 nm | 214 nm |

Fig. 3.1. *Basic compound for Woodward – Fieser estimation of long wavelength absorption maximum.*

Each increments spread basic value with quantity given in Table 3.1.

Table 3.1. *Values of increment in nm.*

Increments	
Conjugated double bond	+30 nm
Exocyclic position of a double bond	+5 nm
Alkyl or aryl group	+5 nm
Auxochromic group:	
O-alkyl	+6 nm
O-acyl	0 nm
S-alkyl	+30 nm
$N(alkyl)_2$	+60 nm
Cl	+5 nm
Br	+5 nm

Extended Woodward-Fieser rule lets calculate absorption maximum of for α, β - unsaturated carbonyl compounds.

Precision of the empirical rules is 2 – 3 nm between experimental λ_{max} and calculated values. The basic value for the establishment is for compound below (Fig. 3.2) in methanol or ethanol as solvent depending on type of X-substitution (Table 3.2).
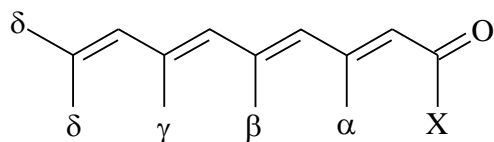
Fig. 3.2. *Basic compound for Woodward – Fieser estimation of α, β – unsaturated carbonyl substances.*

Each further conjugated C=C bond, it exocyclic position and homoannular diene component brings quantity given in Table 3.2.

Table 3.2. *Values of different substitution and increment in nm.*

Substitutions			Increments		
	X		*C=C*	*C=C*	
H	Alkyl (or 6-membered ring)	OH, O-alkyl	conjugated bond	exocyclic position	Homoannular diene
207	215	193	+30	+ 5	+ 39

Different substitutions in different position according to carbonyl group bring further correction in the value of wavelength of maximum absorption (Table 3.3). Absorption depends on type and polarity of solvent and it correction should also be taken into account (Table 3.3).

Table 3.3. *Values of different substitutions and solvent corrections in nm.*

Substitutions					Solvent correction	
	α	*β*	*γ*	*≥δ*		
Alkyl (open- chain)	10	12	18	18	Water	+ 8
Cl	15	12			Chloroform	-1
Br	25	30			Dioxane	-5
OH	35	30		50	Ether	-7
O-alkyl	35	30	17	31	Hexane	-11
O-acyl	6	6	6	6	Cyclohexane	-11
N(alkyl)$_2$		95				

Calculating quantity of λ_{max} is a sum of basic value, and correction of each substitution in every position and solvent.

3.1.4 High-Performance Liquid Chromatography

Chromatography is a sophisticated method for separating and quantifying components in mixture of chemical compounds. The separation is result of the different interaction of the mixture between two phases: one of that is stationary and other – mobile. As stationary phase, could be a solid or liquid supported on a solid, whereas mobile phase is a liquid or gas. The stationary phase is defined as the immobile packing material in the column. The mobile phase flows through the stationary phase and carries the components of the mixture with it. The interactions of the analyte with mobile and stationary phases can be manipulated through different choices of both solvents and stationary phases. Depending on specific physical and chemical properties, mixture of analytes interacts with the stationary phase in different way. Each analyte elutes from column at characteristic time, and resulting peak can be used to confirm its identity and quantify it (Harris *et al.*, 2010).

High performance liquid chromatography (HPLC) is one of the types of chromatography.

HPLC uses a liquid mobile phase to separate the components of a mixture. The stationary phase can be a liquid or a solid phase. These components are first dissolved in a solvent, and then forced to flow through a chromatographic column under a high pressure where separate.

These stationary-phase particles have specific properties which depend on the type of HPLC which is being performed – reversed-phase (RP), normal-phase (NP), ion-exchange (IEX), size-exclusion (SEC), and hydrophobic (HIC) and hydrophilic (HILIC) interaction chromatography, among other.

Normal-phase chromatography (NP-HPLC) separates molecules on the basis of differences in the strength of their interaction with a polar stationary phase. Mobile phase is nonpolar. The components of the analyte mixture interact with the polar surface that removes them from the flowing mobile-phase stream.

Reversed-phase chromatography (RP-HPLC) utilizes polar mobile phase and nonpolar stationary phase. Separates molecules are based on differences in their hydrophobicity and polarity.

HPLC can be used to detect, purify, isolate, quantify, and characterize the individual components of the mixture. This method is applicable to samples with components ranging

from small organic and inorganic molecules and ions to polymers and proteins with high molecular weights.

3.1.5 pH measurements

The pH measurement belongs to a potentiometric measurement. It is made by comparing the potential of measuring pH electrode in a sample with the readings in standards whose pH has been defined by buffers. The pH electrode consists of an H^+ selective membrane, and internal and external reference electrodes, usually combined in one housing. Potential difference builds up on the sides of thin glass in the bubble thanks to the difference between H^+ activities on both sides (Atkins, 2007).

A pH meters are readout device that precisely measure the voltage and translate them into pH values at the correct temperature under the most adverse conditions according to Nernst equation.

$$E = E_o + (2.3\ RT/nF)\ log\ (aH^+) \tag{3.3}$$

where, E is measured potential from the sensing electrode, E_o – related to the potential of the reference electrode, $(2.3\ RT/nF)$ – the Nernst factor, log (aH^+) – the pH, $R,\ F$ – Gas Law and Faraday's constant, respectively, T – temperature, n – charge of the ion.

Electrode behavior is dependent on temperature.

3.1.6 Dissolved oxygen measurements

Dissolved oxygen electrode is a polarographic device of the type first described by Clark in 1956. It consists of a pair polarized silver electrodes and an electrolyte separated from the sample by a gas-permeable membrane and is reduced to hydroxyl ions at a silver cathode according to the reaction:

$$O_2 + 2H_2O + 4e^- \rightarrow 4OH^- \tag{3.4}$$

The electrons necessary for this process are provided by a reaction at the silver anode. Because the electrolyte contains chloride ions, this reaction occurs as:

$$Ag + Cl^- \rightarrow AgCl + e^- \tag{3.5}$$

3.1.7 Chemical reaction kinetics

For kinetic measurements, the simplest method as isothermal batch type of the reactor was chosen. This reactor type is a closed system with a fixed total mass. All constituents of the liquid phase are mixed with together in the initial moment (time = 0). Composition of batch changes with respect to time, however, it is constant in any points of the system at any instant because of efficient stirring. As well temperature of the fluid is unchangeable at each point of the reactor. Batch reactor is commonly used for interpretation of reaction rate for various types of reacting systems.

Thus, if we assume that there are n reactants and products S, which participate in k reactions:

$$\sum_{i=1}^{n} r_{ij} S_j = 0; \quad i=1, 2, \ldots, k \tag{3.6}$$

where, r_{ij} are stoichiometric coefficients of reactants,

then, the change of the concentration of each species (reactants or products) is given by

$$\frac{dC_i}{dt} = \sum_{i=1}^{k} r_{ij} r_j; \quad i=1, 2, \ldots, k \tag{3.7}$$

where, r_j is a rate law for the reaction j.

In addition, we assumed that all considered reaction were elementary, so that

$$r_j = k_j \, c_i \, c_{k \neq i} \tag{3.8}$$

or

$$r_j = k_j \, c_i^2 \tag{3.9}$$

in case of 2 nd order self-reaction,

or

$$r_j = k_j \, c_i \tag{3.10}$$

in case of hydrolysis of a single molecule.

where, k_i – rate constants for reaction j.

One of the most common methods for estimation of kinetics parameters is test of integrated form of rate law. The system of equations (3.7) can be solved provided the rate laws (3.8) are known or assumed. Exact analytical solutions are usually not available for larger systems. Numerical solutions can be obtained using commercial or self-written solvers. If the rate constants in the rate laws (3.8) differ by several orders of magnitudes, the system (3.7) requires solvers capable of handling so called stiff systems of ordinary differential equations.

3.1.8 Computational quantum chemical calculations

Quantum chemical calculations were performed using density Gaussian 03 (Frisch *et al.*, 2003) suite of programs. First, an attempt to predict equilibrium structures of molecular systems was made via locating global minima on the potential energy surface (PES). Different minima correspond to different conformations or structural isomers of a single molecule. The optimization is based on step by step calculation of the energy at sequential points of the PES and determination of the gradient at these points. The optimization is finished when the forces are zero (gradient is negative) and the next step is very small – it has converged. The second step was to check if the geometry corresponds to the global energy minimum or to a saddle point. This can be done by calculation frequencies for all found stationary points. If there are no imaginary frequencies the optimized structure is a minimum, but if there is at least one imaginary frequency the structure is a saddle point (a transition state if there is only one). These calculations were carried out using harmonic approximation. This procedure was used for both ground and excited state modeling (Foresman and Frish, 1996).

Two methods were used in this work. The first one was Density Functional Theory (DFT) – an approach that is based on a strategy of modeling electron correlation via general functionals (a function whose definition is itself a function) of the electronic density. It was chosen because of its quite balanced accuracy-to-cost correlation for medium-sized molecules. This method was applied for ground state geometry optimization and vibrational transitions predictions.

B3LYP (Becke, Lee, Yang and Parr three-parameter) (Lee *et al.*, 1988; Becke, 1988, 1993) functional with 6-31++G(2df, 3pd) basis set were applied in both cases. This is a split-

valence basis set (allowing orbitals to change size) with addition of polarization functions to both heavy atoms and hydrogen atoms, and with diffuse functions added to heavy atoms (important for the excited states). This functional with such a basis set is again quite commonly used in the study of related molecules. For frequency assignment, a scaling coefficient of 0.9648 was used to correct for the method used (Merrick *et al.*, 2007). Estimated errors in the determination of energies of optimized structures were ~ 1 kcal/mol.

The solvent effects in the quantum chemical calculation were estimated using Polarized Continuum Model (PCM). It is a family of solvent effects models in computational chemistry that is among the most widely used. The PCM allows reducing the complexity of free energy calculations due to considering solvent as a polarizable continuum but not as separate molecules.

3.2 Chemical reagents and solvents

All chemical reagents and solvents were used as purchased without further purification. They are listed in alphabetical order along with corresponding makers and purring grade.

Basic reagents

Kinetics study:

- manganese(II) sulfate monohydrate – $MnSO_4 \times H_2O$ – (> 99% pro analysis grade), *ACS*
- 2-methyl-1,3-butadiene – C_5H_8 – (> 98% syntheses grade, stabilized with 100 ppm of 4-tert-butylpyrocatechol), *MERC*
- sodium disulfite – $Na_2S_2O_5$ – (> 98% pro analysis grade), *ACS*
- sodium nitrite – $NaNO_2$ – (98% pure p.a.), *CHEMPUR*
- sodium sulfite – Na_2SO_3 – (98% pro analysis grade), *ACS*

Synthesis:

- allyl alcohol – C_3H_6O – (≥ 99.5%), *BDH Laboratory Reagent*

- benzyl alcohol – C_7H_8O – ($\geq$ 99.5%), *BDH Laboratory Reagent*

- 3-bromopropen– C_3H_5Br – (99%), *Sigma-Aldrich*

- citraconic acid dimethyl ester – $C_7H_{10}O_4$ – (99%), *ABCR*

- diisobutylaluminum hydride – $C_8H_{19}Al$ – (Dibal-H, 1 M in hexane), *Acros Organics*

Auxiliary:

Solvents and gases

- acetonitril-3d – CD_3CN – (99.8 atom%D), *ARMAR Chemicals*

- argon – Ar_2 – (N 5.0), *Multax*

- *tert*-butyl methyl ether – $C_5H_{12}O$ – ($\geq$ 99.5% for synthesis), *ROTH*

- ethyl acetate – $C_4H_8O_2$ – ($\geq$ 99.8% for spectroscopy), *POCH*

- ethyl alcohol absolute – C_2H_5OH – (99.8% pure p.a.- basic), *POCH*

- methanol – CH_4O – ($\geq$ 99.9% for HPLC), *POCH*

- sodium sulfate anhydrous – Na_2SO_4 – ($\geq$ 99.5% pure p.a.), *ChemPur*

- sulfuric acid – H_2SO_4 – (93%), *Cheman*

- tetrahydrofuran – C_4H_8O – (99.5%, dry), *Acros Organics*

- water – H_2O – (> 18 Ω cm) purified with Milli-Qplus, *Millipore*

3.3 Instrumentation

Spectrophotometer

- V-570 UV/VIS/NIR spectrophotometer, NCP-508 (Jasco)

- quartz micro-cells (Hellma Suprasil)

Electrodes

- Ross Ultra glass combination pH electrode (Thermo Electron)

- 9708-99 O_2 electrode, Clark-type (Orion, now also Thermo Electron)

pH-meter

- 525A+ pH-meter (Thermo Electron)

- 920 pH-meter (Orion, now also Thermo Electron)

Voltage signals from both pH-meters were recorded every 0.1 s, and converted to pH and oxygen concentration in mol dm^{-3}, using a computer system equipped with a M6281 data acquisition card and a Lab View application, both from National Instruments.

Mass spectrometer
- QTRAP 4000 (Applied Biosystems)
- API 365 (PE-Sciex)

Nuclear magnetic resonance
- Bruker Avance II 300 NMR spectrometer (Bruker)

High-performance liquid chromatography
- Prominence LC-20 HPLC system (Shimadzu)
- Atlantis$^®$T3 column (Waters)
- QTRAP 4000 (Applied Biosystems)

Evaporation chamber
- Rotary vacuum evaporater (Unipan)

Ultraconic bath
- Transsonic 470/H (Elma)

Thermostat
- U7^c model, Höppler type (VEB MLW Prüfgeräte-Werk)

3.4 Procedures

3.4.1 Kinetic reactor setup

The aim of the thesis was to describe the kinetics, mechanisms and products of aqueous-phase reactions of isoprene in the presence of dissolved forms of SO_2 and HONO, oxygen and manganese(II) sulfate. For better imitation of scenarios possible in real atmospheric systems, the experiments were planned basing on the knowledge that dissolved

46

forms of SO_2 ($SO_2 \times H_2O$, HSO_3^-, SO_3^{2-}) react with oxygen via chain-reaction route catalyzed by cations of transition metals in a way depending on the acidity of solutions (Section 1.2.3). Thus, to meet the aim of the thesis, the following set of experiments were carried out at several fixed initial acidities:

- MOS   – Mn, O_2, S(IV);
- MON   – Mn, O_2, NO_2;
- MOSN   – Mn, O_2, S(IV), NO_2;
- MOSC   – Mn, O_2, S(IV), C_5H_8;
- MOCN   – Mn, O_2, C_5H_8, NO_2;
- MOSCN   – Mn, O_2, S(IV), C_5H_8, NO_2.

All experiments were carried out at 25 ± 0.2 $^\circ$C. The initial concentrations of reactants were: $(7.8 \pm 0.02) \times 10^{-4}$ M S(IV); $(2.50 \pm 0.30) \times 10^{-4}$ M O_2; $(8.68 \pm 0.30) \times 10^{-5}$ M C_5H_8; 1×10^{-5} M $MnSO_4$; 1×10^{-4} M $NaNO_2$. The initial acidity of reaction solutions ranged from 2 to 8.7.

The experimental method used to investigate reactions of isoprene coupled with autoxidation of S(IV) in the presence of sodium nitrite was used as described by Rudziński (2004, 2009). The reactor used had a 0.752 dm^3 volume, Teflon cover, and water jacket for thermostating the reacting solutions. The reactor was well stirred and operated without gas phase − homogeneously and in batch manner (Fig. 3.3). At the beginning, the solution of the manganese(II) sulfate and oxygen in water was poured in the reactor. After that, the reactor was sealed.

An aliquot of aqueous solution of isoprene and sodium nitrite were added to the solution in reactor. The reaction was triggered by the adding of aliquot of aqueous solution of sodium sulfite prepared from Na_2SO_3 and $Na_2S_2O_5$. Different initial acidities of the reacting solutions were obtained by varying the proportion of the latter compounds (Reactions 3.11 − 3.13). For initial acidities low than 5.2, dilute sulfuric acid was used to acidify the reaction solution.

$$C_5H_8$$

$$S(IV) + O_2$$

$$MnSO_4 \qquad NaNO_2$$

[O$_2$]   on - line   off - line   ESI-MS

UV   CID-MS

pH   HPLC

$$25\ ^oC$$

$$pH_o = 2 \div 9$$
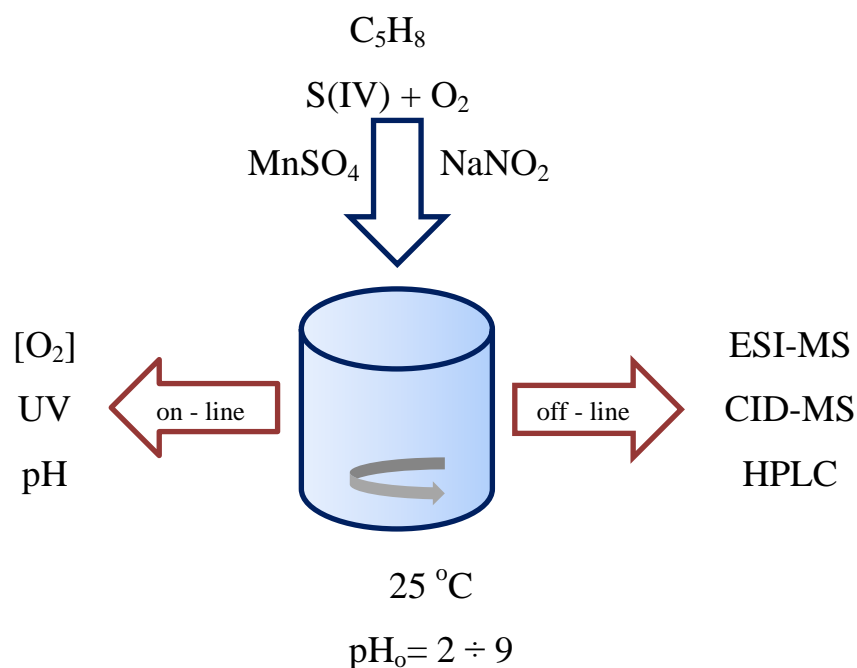
Fig. 3.3. *A schematic diagram of experimental setup for kinetics studies.*

$$(Na_2SO_3)_s \rightarrow 2Na^+ + SO_3^{2-} + H_2O \qquad (3.11)$$

$$(Na_2S_2O_3)_s + H_2O \rightarrow 2Na^+ + HSO_3^- \qquad (3.12)$$

$$HSO_3^- \rightarrow H^+ + SO_3^{2-} \qquad (3.13)$$

During the experimental course, pH, concentration of dissolved oxygen and high-resolution UV spectra of reacting solutions were recorded. Figure 3.4 shows changes of pH and decay of reactants during a reaction run in neutral solution, with isoprene present.
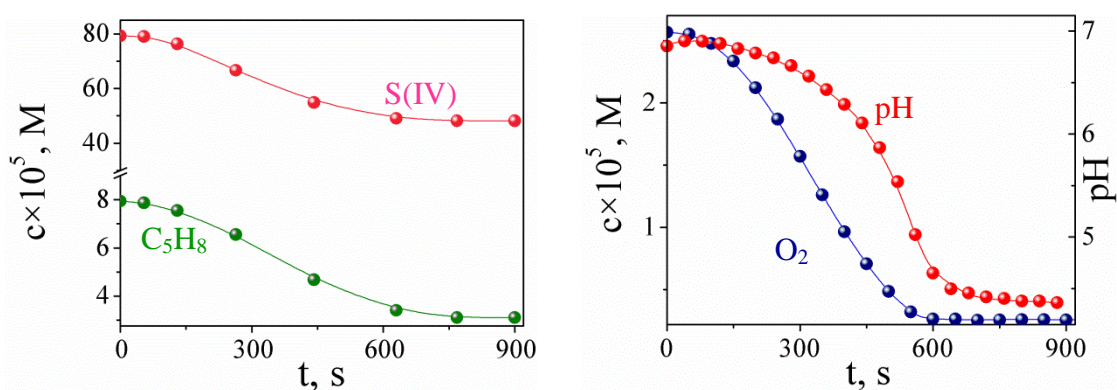
Fig. 3.4. *Changes of the concentration of substrates and pH during the reaction run.*

Temperature in the reactor was measured with a mercury thermometer. Concentrations of isoprene and sulfite, bisulfate, and nitrite ions in the reacting solution were obtained by

manual deconvolution of recorded UV spectra of reacting solutions using the reference spectra of these species. Post-reaction solutions were analyzed off-line by mass spectrometry, high performance liquid chromatography, and nuclear magnetic resonance.

3.4.1.1 pH and O_2 measurements

The pH and concentration of O_2 were measured continuously with pH electrode and a Clark-type electrode connected to pH-meters (Chapter 3.3). Both electrodes were calibrated before each experiment: the pH one – against two different buffers and the O_2 one – against the electronic zero and the local atmospheric pressure, using a built-in circuitry. Voltage signals from both pH-meters were recorded every 0.1 s, and converted to pH and oxygen concentration in mol dm^{-3}, using a computer system equipped with a M6281 data acquisition card and a Lab View application, both from National Instruments.

The changes of concentration of dissolved O_2 and acidity of reaction solution during the experimental course were obtained directly from the measurements. Oxygen concentration were shown as $ppmO_2$ (parts per million O_2) by the pH-meter without any corrections for the electrode characteristics. The response of O_2-electrode was 95% in less than 15 s, sufficiently fast for the reaction times considered:

- > 150 s – Mn, O_2, S(IV);
- > 600 s – Mn, O_2, S(IV), C_5H_8;
- > 150 s – Mn, O_2, S(IV), C_5H_8, NO_2;
- > 700 s – Mn, O_2, S(IV), NO_2;
- > 2500 s – Mn, O_2, C_5H_8, NO_2.

3.4.1.2 UV measurements

During reactions the UV spectra of the solution were periodically recorded (Fig. 3.5) by a spectrophotometer (Chapter 3.3), using a closed sampling loop constructed from a T-valve, a syringe and a quartz flow-through micro-cell. Other parameters that were used in UV measurements were:

- wavelength: 200 – 300 nm
- bandwidth: 0.2 nm

- data pitch: 0.5 nm
- light path: 1 cm

Table 3.4. *Molar absorption coefficients of the reagents in aqueous solutions at 25 °C.*

Absorbing species	Wavelength (nm)	Absorption molar coefficient (M^{-1} cm^{-1})	Concentration range (M)
SO_3^{2-}	205	3926.9 ± 18.9	$1 \times 10^{-4} - 7 \times 10^{-4}$
	215	2231.4 ± 40	
	225	968.6 ± 18.2	
HSO_3^-	205	869.5 ± 6.8	$2 \times 10^{-4} - 2 \times 10^{-3}$
	215	87.01 ± 1.60	$2 \times 10^{-4} - 5 \times 10^{-3}$
Isoprene	225	17425 ± 227	$2 \times 10^{-5} - 8 \times 10^{-4}$
NO_2^-	209.5	5260.3 ± 353.7	$5 \times 10^{-6} - 1 \times 10^{-4}$
	230	1690.8 ± 76.8	$5 \times 10^{-5} - 1 \times 10^{-3}$

The absorption molar coefficients and reference UV spectra of substrates were already shown (Rudziński, 2004). This information was completed with nitrite ion data. Figure 3.6 presents these spectra, Table 3.4 – absorption molar coefficients. The reagents absorbed UV light of the wavelength from 200 to 235 nm and obeyed the Lambert-Beer Law (Section 3.1.3).
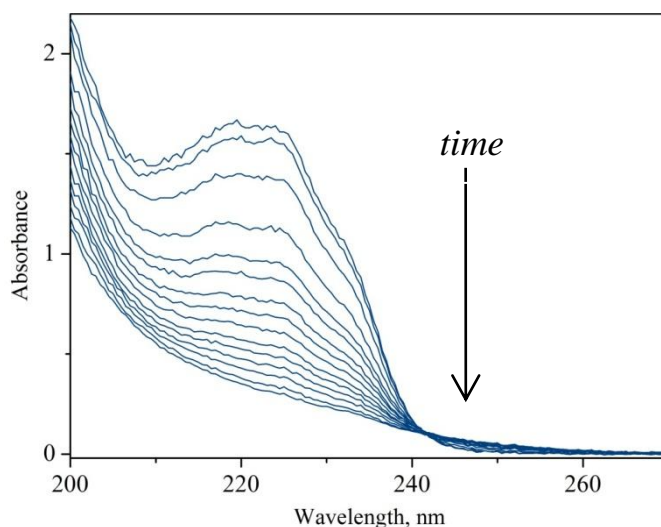
Fig. 3.5. *Raw UV spectra of a reacting solution at pH_o =4.0. Initial concentrations of reactants were: $MnSO_4$ – 1×10^{-5} M; S(IV) – 7.8×10^{-4} M; O_2 – 2.53×10^{-4} M; C_5H_8 – 7.63×10^{-5} M and $NaNO2$ – 1×10^{-4} M.*
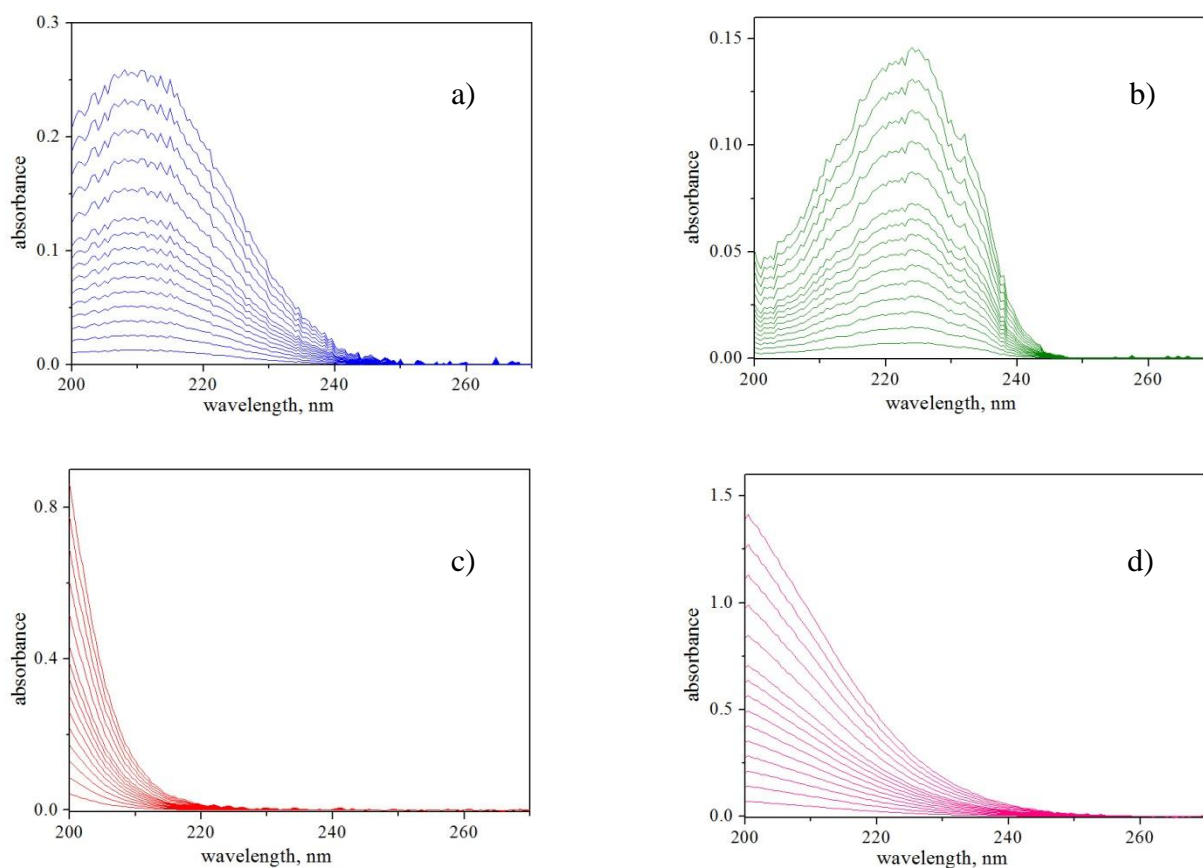
Fig. 3.6. *Reference spectra of: a) nitrite $((5.00 \div 0.25) \times 10^{-5}$ M); b) isoprene $((7.95 \div 0.4) \times 10^{-6}$ M); c) bisulfite $((4.00 \div 0.2) \times 10^{-4}$ M) and d) sulfite ions $((3.00 \div 0.15) \times 10^{-4}$ M) in aqueous solutions at 25 ^{o}C.*

Deconvolution of UV spectra recorded during reaction runs was applied to determine the concentrations of reagents and their change during the reactions. It was based on manual subtraction of reference spectra using a custom-built MS excel application. This application lets subtract several spectra and previews of the raw, the approximated and the residual spectra. The raw spectra were composed of the spectra of absorbing substrates and spectra of absorbing products. Ultraviolet absorption of sodium sulfate and manganese(II) sulfate was negligible. Concentration-time profiles of each absorbing component were calculated from the respective series of subtraction factors and the calibration data for the reference spectra. This required all absorbing species followed the Lambert-Beer Law. The condition was checked for sulfite, bisulfite, nitrite ions, and isoprene. The standard errors of subtraction factor for reactants were determined by Rudziński (2004): SO_3^{2-} less than 3%; HSO_3^- – < 10%, isoprene – < 12% and NO_2^- – 15%.

3.4.1.3 Chemical-kinetic simulations

Mathematica 2.3 package were used for solving a set of ordinary differential equations raised on the mechanism of the reactions (Section 4.2, MOSC experiments). Reversible reactions were treated kinetically, each one as a pair of independent reactions. Rate constants for modeling were collected in Table 4.4 (Chapter 4.2). Constants, for which no experimental estimates were available, were adjusted using trial and error guesses.

3.4.2 Mass spectrometry

Post-reaction solutions were analyzed off-line in a triple-quadruple negative electrospray mass spectrometer (Applied Biosystem, API 365; Applied Biosystem, QTRAP 4000). The samples – were taken directly after some experiment, using a gas-tight syringe to prevent the access of air, and diluted with methanol before injection to the MS apparatus. Samples were introduced into mass spectrometer using a direct infusion technique.

During each mass spectrometry run a number of instrument setting such as declustering potential, focusing potential, collision energy level, rate of collision gas, source temperature were optimized. A typical setting for mass spectrometry ranged as specified below:

- declustering potential (DP): $50 – 400$ V
- focusing potential (FP): $10 – 30$ V
- collision energy (CE): $0 – 35$ eV
- rate of collision gas: $1 – 12$ a.u.
- time of single scan: $1 – 3$ s
- infusion rate: 10 μl/s
- source temperature: $100 – 400\ ^{o}$C

All mass spectra were recorded using the Analyst 1.4 software from Applied Biosystems. Treatment of spectra consisted of averaging and smoothing of signals in spectra. After acquisition mass spectra processed using the Corel Draw 12 software whereupon transferred into Microsoft Word. Molecular structures of compound of interest were drawn using MDL ISIS Draw 2.5 platform.

3.4.3 Nuclear magnetic resonance

^{1}H NMR spectra were recorded on a Bruker Avance II 300 spectrometer operating at 300 MHz with relaxation delay 6 sec. The NMR samples were concentrated in *vacuo* and dissolved in acetonitrile-d3 (CD_3CN, *ARMAR Chemicals*) at 298 K. 5 mm glass NMR tubes were sealed under argon in order to avoid condensation of water from air.

3.4.4 High-performance liquid chromatography

The post-reaction samples were subjected to HPLC analysis (HLPC system, Shimadzu) without any further treatment. The following parameters were setup for LC/MC analysis runs:

- type: Reversed Phase (RP)
- column: Atlantis[®]T3 C18 µ3
- dimension: 150×2.1 mm
- eluents: Acetonitrile (B) – 0.1% acetic acid in water (A)
- elution type: gradient
- column temperature: ambient
- flow rate: 5 mL/min
- detection: triple quadruple mass spectrometer
                                (QTRAP4000, Applied Biosystems)

Total ion chromatogram was treated as was described in Section 3.4.2.

3.4.5 Syntheses of reference compounds

The structural identification with mass spectrometry was supported by the synthesis of reference material. The procedures applied are stated below.

3.4.5.1 Sodium allyl/benzyl sulfonate
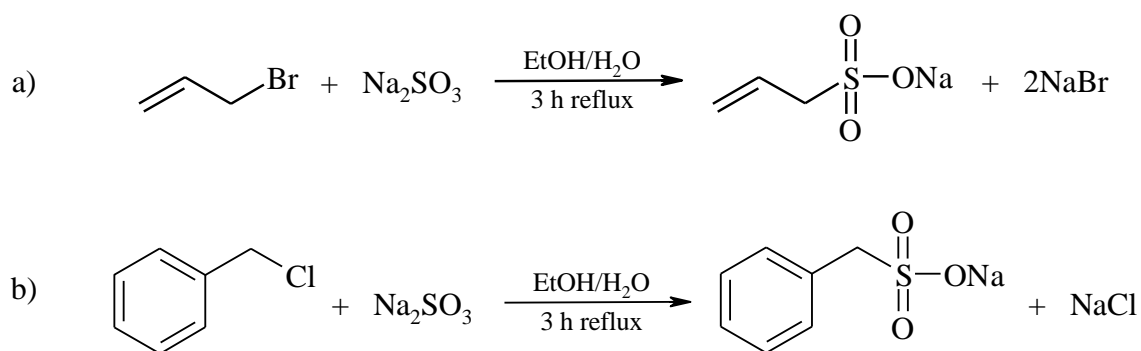
Scheme 3.1 *Synthesis of a) sodium prop-2-ene sulfonate (MW 144); b) sodium phenylmethanesulfonate (MW 194).*

This compound was prepared by the same method as described by (Jiang *et al.*, 1999). In round-bottomed flask were placed 7 ml of 99.8% ethanol, 2 ml of H_2O (MilliQ) and 1.43 ml of 3-bromopropen (16.6 mmol) or benzyl chloride (12.4 mmol). Then stirrer was started and the mixture heated to boiling. To this well-stirred and boiling solution was added dropwise a solution of 731.2 mg (5.8 mmol) of sodium sulfite in 3 ml of H_2O (MilliQ). After that the solution mixture was refluxed for 3 h. The solution was concentrated in *vacuo*. The remaining water solution was taken out on a vacuum line. The boiling 13 ml of 99.8% ethanol was used to purify the crude products. On cooling the solution to room temperature, the crystallized products were collected by filtration. The mother liquor was used for second extraction of the residue. The final product (white powder) was obtained in 67%.

3.4.5.2 Mono-prop-2-ene-1-yl sulfate/ mono(phenylmethyl) sulfate
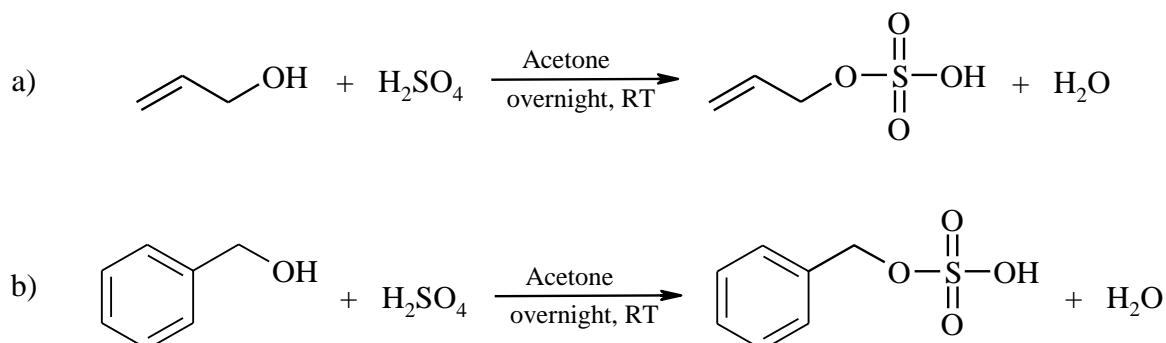

Scheme 3.2. *Synthesis of a) mono-prop-2-ene-1-yl sulfate (MW 138); b) mono(phenylmethyl) sulfate (MW 188).*

The synthesis of ester standards was carried out in round-bottom flask where were placed 5 ml of acetone and 50 µl allyl alcohol (42.7 mg; 0.7 mmol) or benzyl alcohol

(52.2 mg; 0.5 mmol) (Reinning *et al.*, 2008). After that this solution was acidified with a drop of concentrated sulfuric acid. It was left overnight with stirring at ambient temperature. Then mixture was diluted with methanol as 1:100 without purification or isolation before that.

3.4.5.3 *O*-sulfonyl-4-hydroxy-2-methylbut-2-ene
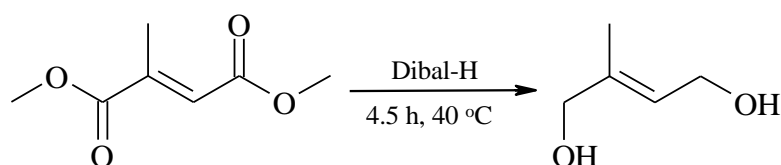
Scheme 3.3. *Synthesis of 2-methylbut-2-ene-1,4-diol.*

In 3-neck flask were placed 0.91 ml (6.33 mmol) citraconic acid dimethyl ester and ~20 ml of dry tetrahydrofuran (THF) under an argon atmosphere and cooled to -70 °C. After that, 28 ml of diisobutylaluminum hydride (Dibal-H, 1 M in hexane) was added dropwise to that cooled mixture. Ratio of dimethyl citraconate to Dubal-H is 1:4.4. The solution was warmed to -40 °C in 4.5 hour. Then, mixture of 15 ml of methanol and 2 ml of H_2O was added dropwise to the solution and left with stirring overnight. On warming to room temperature, anhydrous Na_2SO_4 was added and the solids were removed by filtration on Al_2O_3 and washed with a small amount of *tert*-butyl methyl ether. The solvent was removed in *vacuo*. The total yield of a yellow oily liquid is 324.8 mg; 3.18 mmol, 50% (van Wijk and Lugtenburg, 2002).
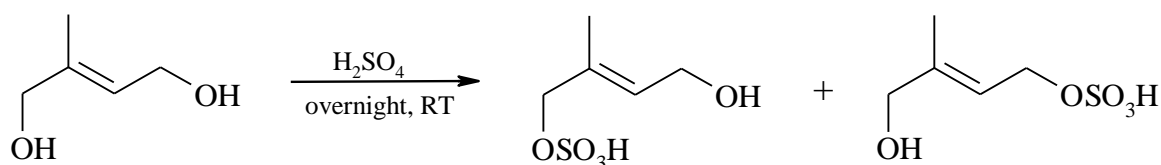
Scheme 3.4. *Synthesis of the isobaric O-sulfonyl-4-hydroxy-2-methylbut-2-enes.*

The rude product without further purification was used for mono esterification. The solution of 176.8 µl of products in 10 ml acetone was acidified with a drop of concentrated sulfuric acid. The reaction was stirred 3.5 h at room temperature. No further work-up was conducted. The reaction aliquot was diluted by a factor 1:100 with methanol and applied in the further structural analysis with mass spectrometry.

4 Results and discussion

The aim of the thesis was to describe the kinetics, mechanisms and products of aqueous-phase reactions of isoprene in the presence of dissolved form of SO_2 and HONO, oxygen and manganese(II) sulfate. The obtained results are comprised in several parts. In the first Chapters 4.1, the kinetic data obtained for set experiments shown in Section 3.4.1 are presented. In the Chapter 4.2, chemical mechanisms of investigated reactions are proposed. Section 4.3 deals with the comparison of kinetics results obtained experimentally and on theoretical base. The Chapter 4.4 presents a broad discussion on the structural elucidation of novel products formed in the reactions of isoprene with sulfoxy-radical anions based on the mass spectrometry and related techniques. Finally, the Section 4.5 provides the computational calculations for the proposed reaction products with Gaussian package program.

4.1 Kinetics study

Figure 4.1 summarizes the results of chemical-kinetic experiments carried out to gain insight into possible transformations of isoprene in atmospheric-like solutions. It shows the variation in time of the reactant concentrations measured directly or determined from measured quantities in the range of reaction runs arranged to cover a wide span of solution acidities and several combinations of substrate compounds already mentioned in the Procedures section:

- MOS   – Mn, O_2, S(IV);
- MON   – Mn, O_2, NO_2;
- MOSN   – Mn, O_2, S(IV), NO_2;
- MOSC   – Mn, O_2, S(IV), C_5H_8;
- MOCN   – Mn, O_2, C_5H_8, NO_2;
- MOSCN   – Mn, O_2, S(IV), C_5H_8, NO_2.

Initial acidity pH = 8.7
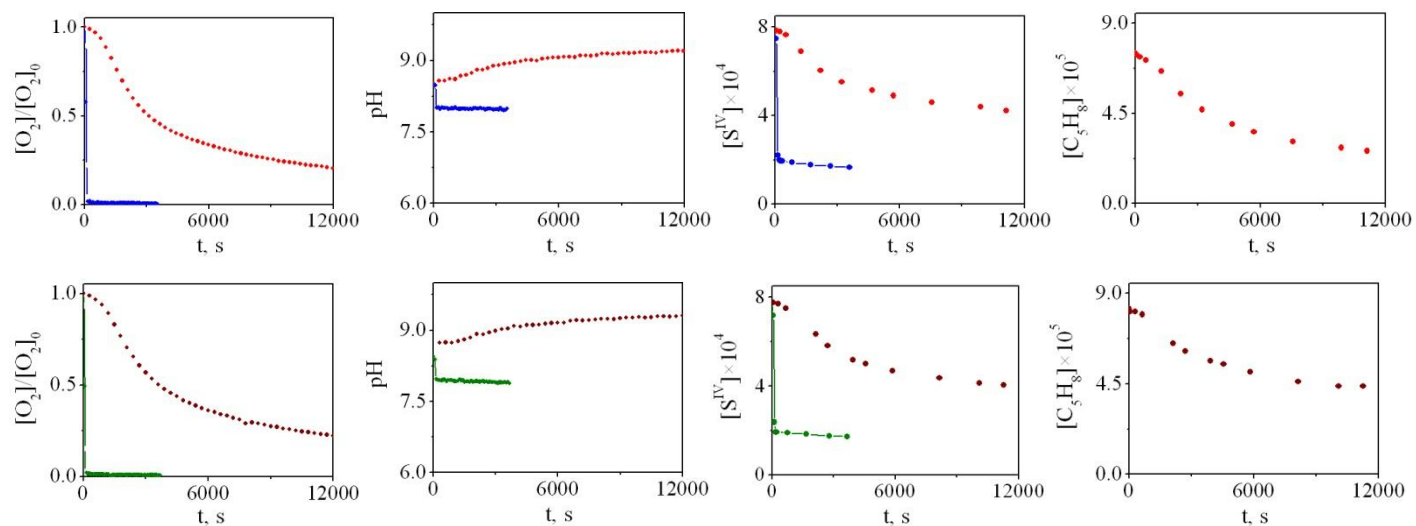
Initial acidity pH = 6.9
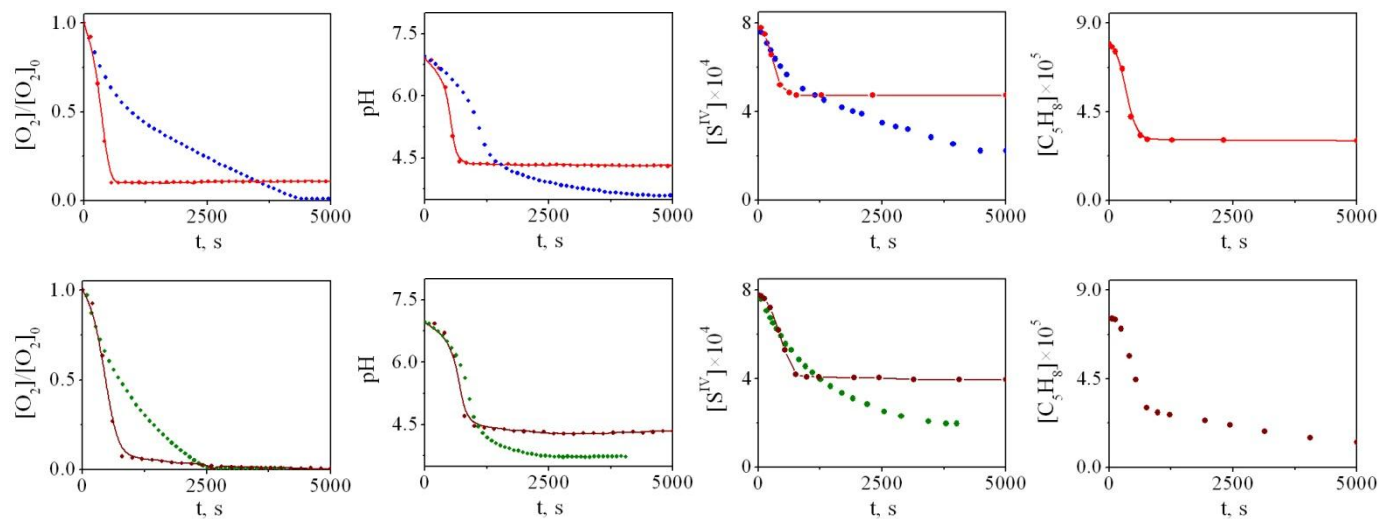
Initial acidity pH = 6
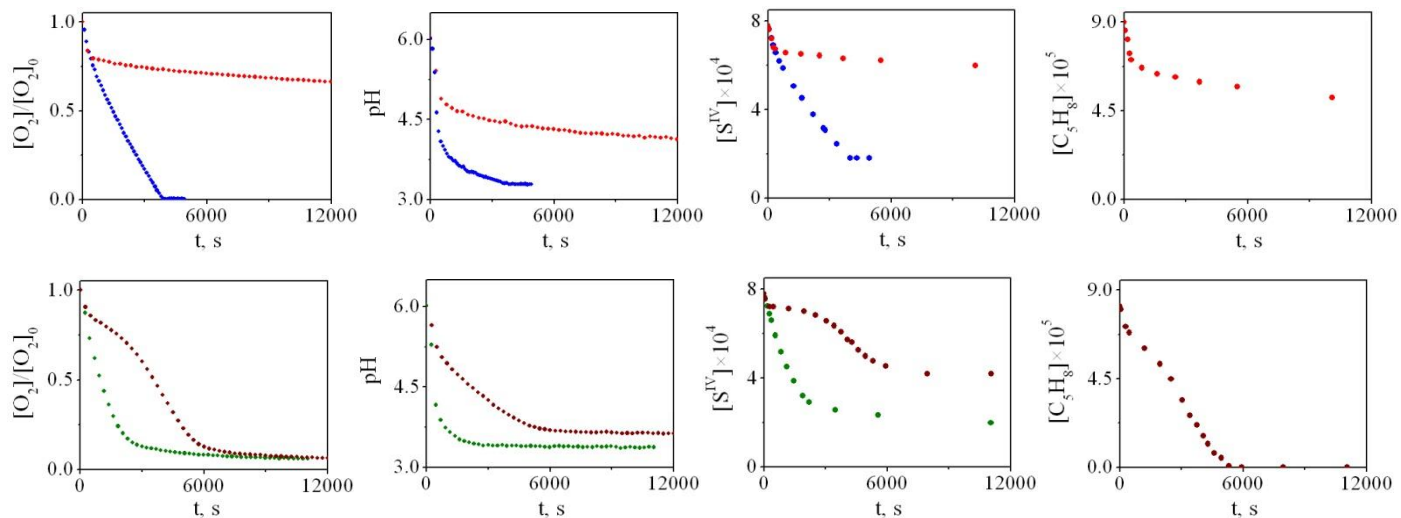
Initial acidity pH = 5.2
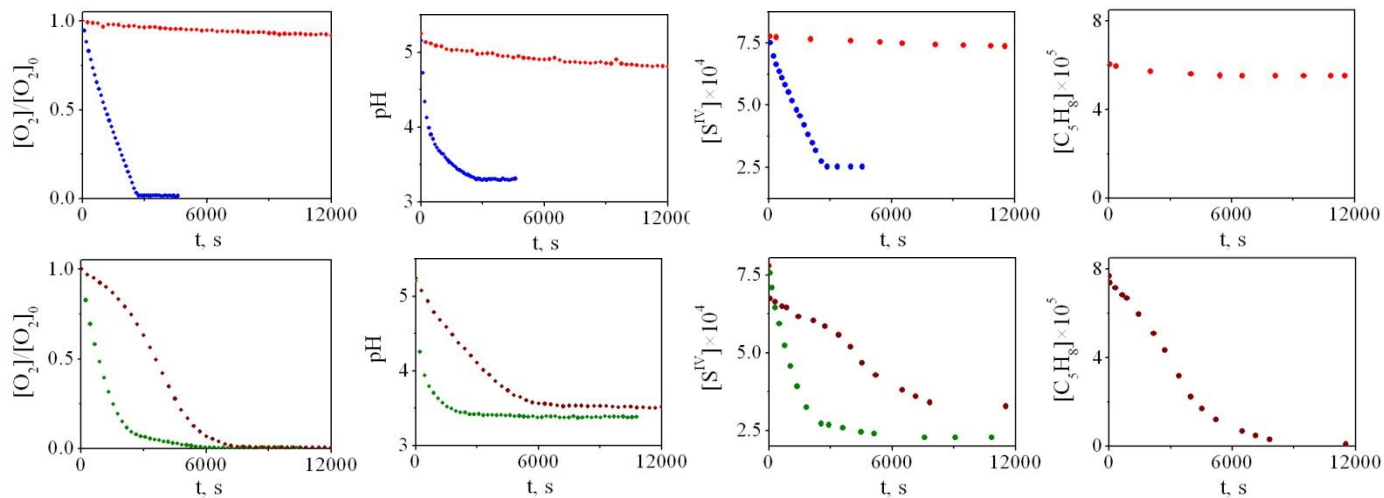
Initial acidity pH = 4
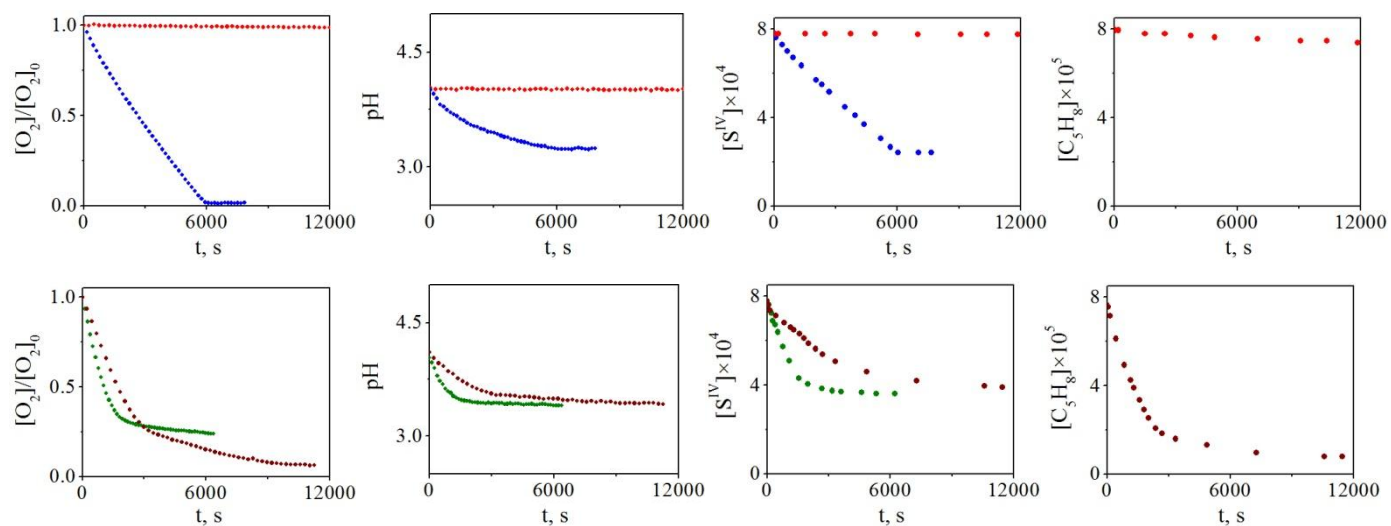
Initial acidity pH = 3
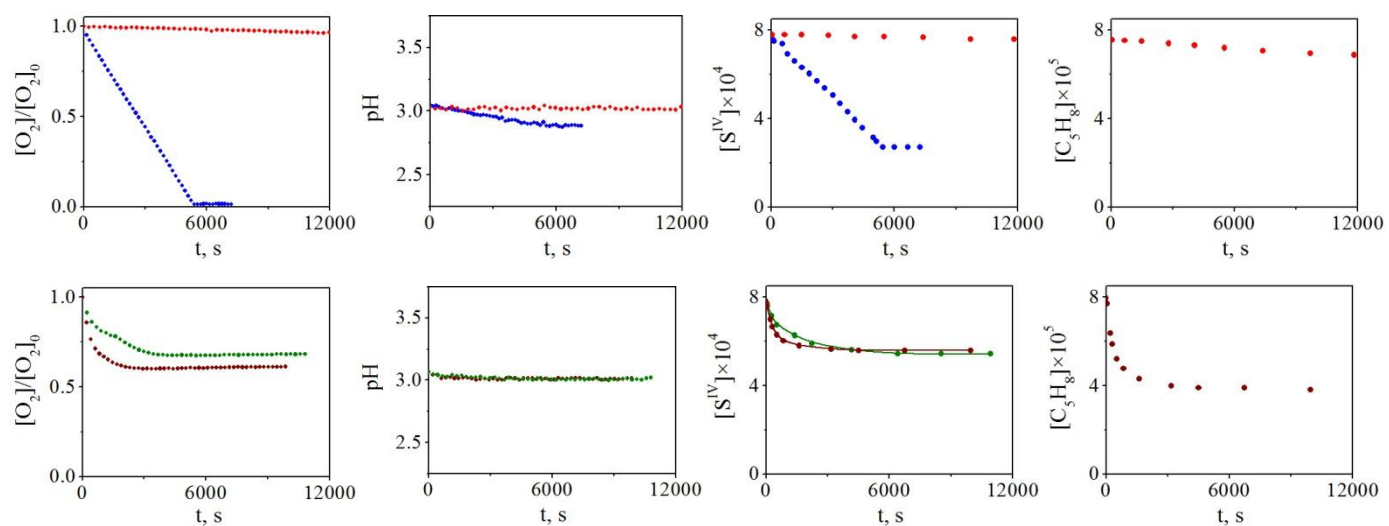
Initial acidity pH = 2.2
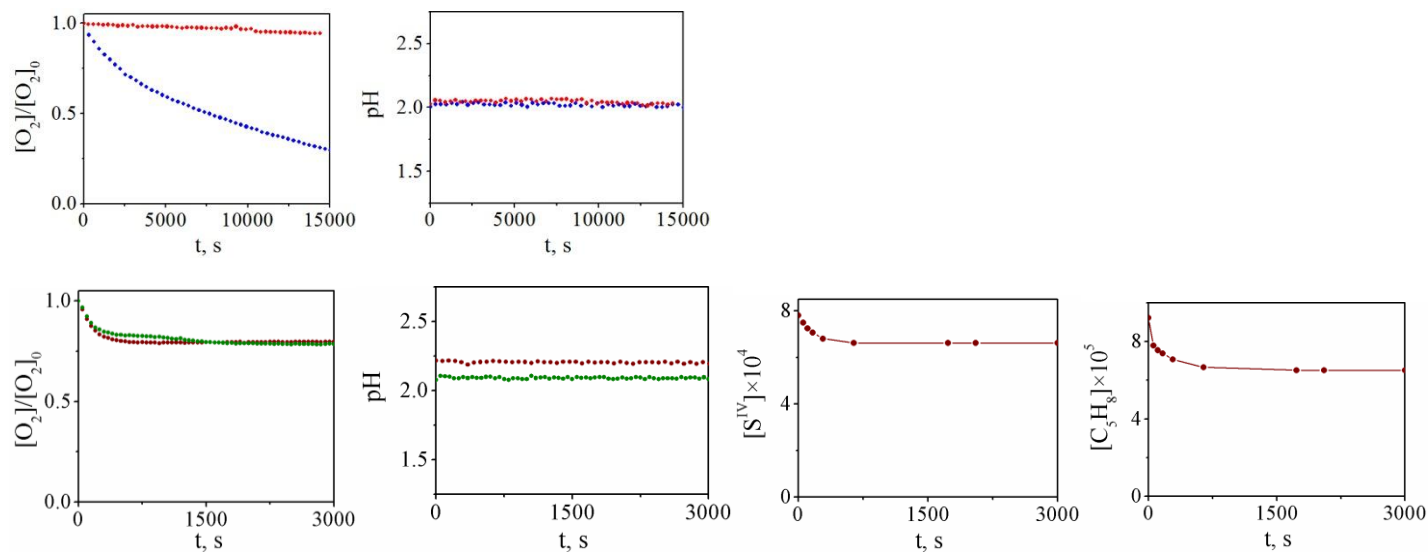
Fig. 4.1. *Variation in time of reactant concentration during S(IV) autoxidation at different initial acidities: blue dots indicate autoxidation of S(IV) alone (MOS expt); red dots – in the presence of isoprene (MOSC expt); green dots – in the presence of NO_2^- ions (MOSN expt); wine dots – in the presence of isoprene and NO_2^- ions (MOSCN expt).*

In the following sections, the reaction courses of all reactions are presented and discussed as time profiles of O_2 concentration normalized against the initial values of this concentration ($[O_2]/[O_2]_o$). In case of pure autoxidation of S(IV) catalyzed by manganese(II) ions (MOS), the overall stoichiometry of reactions makes the conversion of S(IV) strictly twice larger than the conversion of oxygen (Pasiuk-Bronikowska *et al.*, 1992). In other cases, the overall stoichiometry may vary slightly and needs specific discussion.

4.1.1 Experiments without isoprene

- **MOS experiments** *(manganese, oxygen and sulfite)*
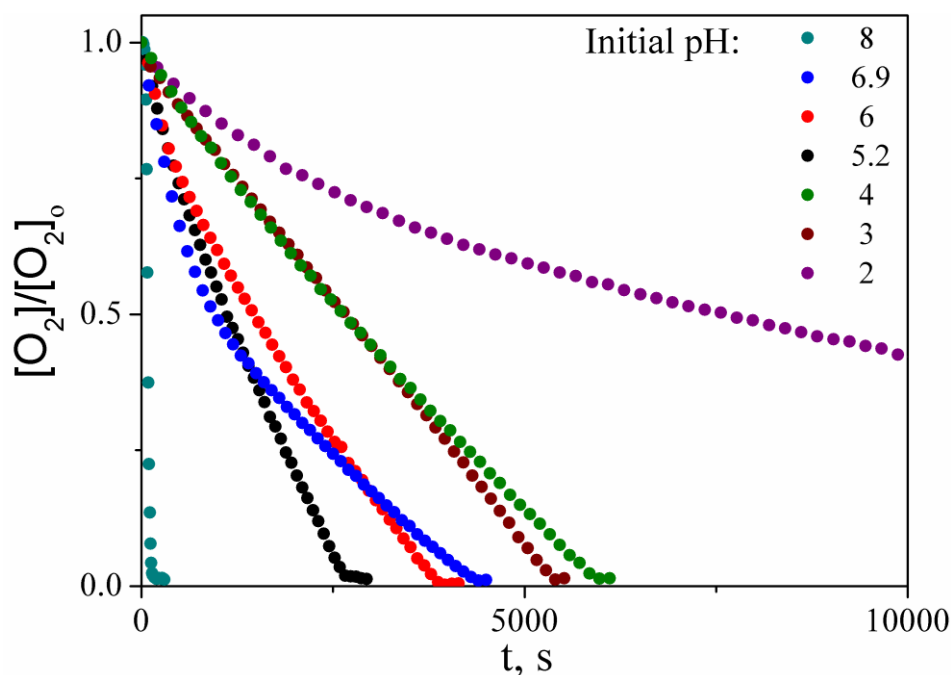
Fig. 4.2. *Decay of oxygen during autoxidation of S(IV) (MOS expt) at different initial acidities of reaction solutions: dark cyan – pH$_o$=8; blue – 6.9; red – 6; black – 5.2, olive – 4; wine – 3; purple – 2.*

Rate of autoxidation of tetravalent sulfur catalyzed by Mn^{2+} depended on the initial acidity of the reaction solution (Fig. 4.2). Increasing the acidity generally decreased the rate of the process. This is consistent with the chain-radical mechanism of the S(IV) autoxidation (Pasiuk-Bronikowska *et al.*, 1992) and the fact that radical-anions propagating the chain, react much faster with SO_3^{2-} ions than with HSO_3^- ions as shown by the corresponding rate constants at 25°C (Huie and Neta, 1987):

$$SO_5^{\bullet-} + HSO_3^- \rightarrow SO_3^{\bullet-} + SO_5^{2-} \qquad\qquad k = 2.5\times10^4 \ dm^3/(Ms) \qquad (4.1)$$

$$SO_5^{\bullet-} + HSO_3^- \rightarrow SO_4^{\bullet-} + SO_4^{2-} \qquad\qquad k = 7.5\times10^4 \ dm^3/(Ms) \qquad (4.2)$$

$$SO_5^{\bullet-} + SO_3^{2-} \rightarrow SO_3^{\bullet-} + SO_5^{2-} \qquad\qquad k = 3.25\times10^6 \ dm^3/(Ms) \qquad (4.3)$$

$$SO_5^{\bullet-} + SO_3^{2-} \rightarrow SO_4^{\bullet-} + SO_4^{2-} \qquad\qquad k = 9.75\times10^4 \ dm^3/(Ms) \qquad (4.4)$$
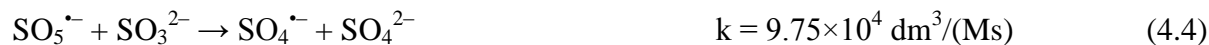
The distribution of S(IV) species in solution depends on the solution acidity. Figure 4.3 shows molar fraction of SO_3^{2-} and HSO_3^- ions as well as hydrated sulfur dioxide $SO_2\times H_2O$ in a 7.8×10^{-4} mol dm^{-3} solution sodium sulfite at 25^oC calculated using the literature equilibrium dissociated constants. It is evident that the fraction of fast-reacting SO_3^{2-} ions decreases sharply with increasing acidity of solutions down to a practically null value at pH $\approx$ 5, so that, there are no these ion type in solutions of pH < 5. At pH = 3 − 5, the slow-reacting HSO_3^- practically dominate in solutions.
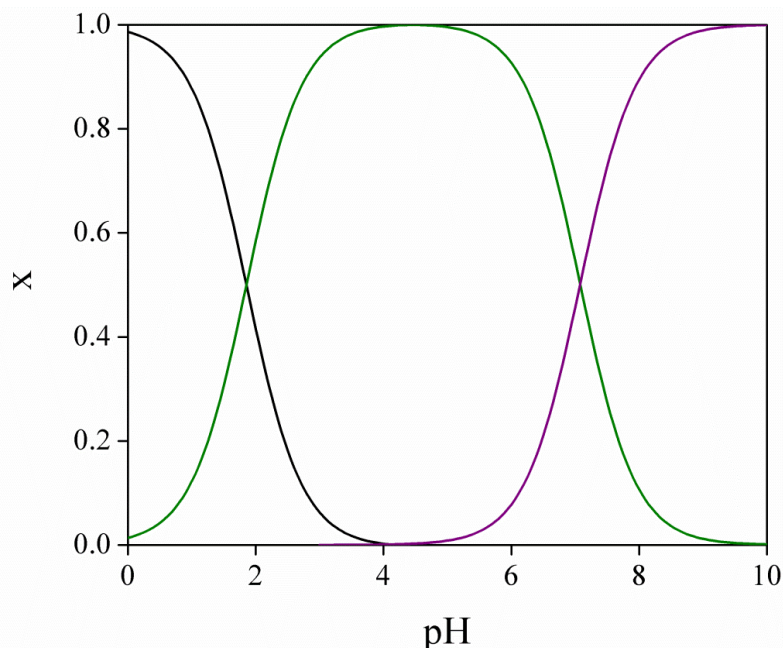
Fig. 4.3. *Molar fractions of hydrolytic species in a 7.8×10^{-4} mol dm^{-3} solution of Na_2SO_3 (or SO_2) at 25^oC calculated using the dissociation equilibrium constants $K(SO_2\times H_2O) = 1.39\times10^{-2}$ mol dm^{-3}, $K(HSO_3^-) = 8.40\times10^{-8}$ mol dm^{-3}: olive line corresponds to HSO_3^- ions; purple line– to SO_3^{2-} ions; black line – to undissociated $SO_2\times H_2O$.*

- **MON experiments** *(manganese, oxygen and nitrite)*

At 25°C, aqueous solutions containing initially the manganese(II) sulfate catalyst, oxygen and sodium nitrite at various initial acidities (pH$_o$ = 2 − 8) showed no O$_2$ consumption and no changes in high resolution UV spectra (200 − 300 nm). This means N(III) was not oxidized in aqueous solutions at the conditions given.

- **MOSN experiments** *(manganese, oxygen, sulfite and nitrite)*
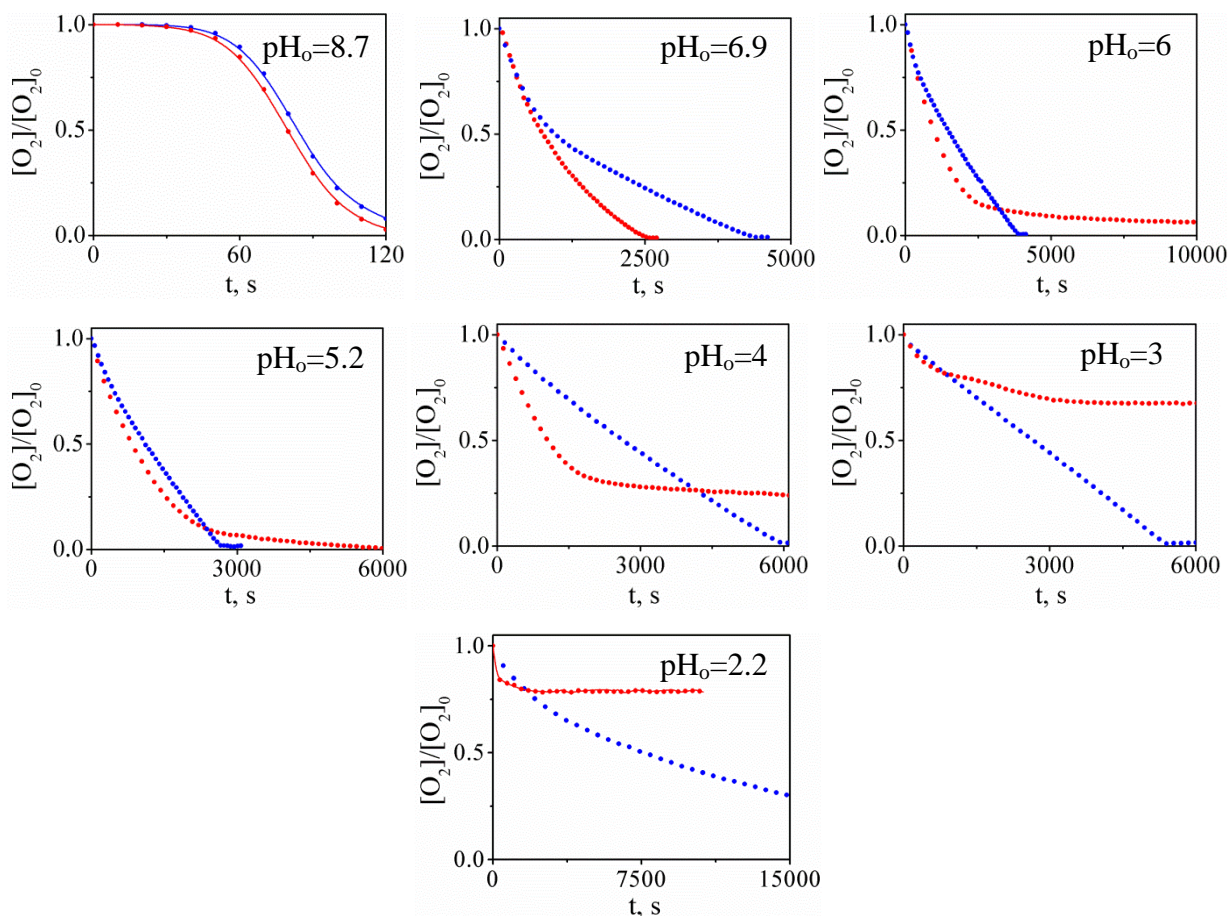
Fig. 4.4. *Influence of nitrite on the decay of oxygen during S(IV) autoxidation at different initial acidities: blue dots correspond to the autoxidation of S(IV) alone (MOS expt); red dots – to the autoxidation in the presence of NO$_2^-$ ions or HONO (MOSN expt).*

Addition of NaNO$_2$ to the S(IV) autoxidation system increased the rate of the reaction in neutral and slightly alkaline solutions (pH ≥ 6.9) (Fig. 4.4). The conversion of oxygen in these experiments was 100%. Similar influence was observed in slightly acidic solutions (6 ≥ pH ≤ 5), with the exception that at the end of each process the rate of O$_2$ significantly slowed down. The conversion of oxygen was still close to complete, albeit after prolonged time. In acidic solutions

$(4 \geq pH \leq 2)$, the initially fast decay of oxygen slowed down significantly after relatively short time or even stopped (experiments at $pH = 2.2$) leaving $20 \div 80\%$ of the element unreacted –more in more acidic solutions. Similar observation was reported by Ellison and Eckert (1984) who studied the influence of NO_2 and nitrous acid on the Mn-catalyzed oxidation of aqueous SO_2 for flue gas scrubbing purposes. They concluded that nitrous acid reacted nearly instantaneously with the S(IV) and produced some inhibitor that greatly slowed the later rate. They suggested that $\cdot NO_2{}^*$ was oxidizing S(IV) directly, while the plausible inhibitor was $NO\cdot^*$, because of its ability to scavenge radicals propagating the oxidation.

This simple mechanism may not suffice to explain the results presented in Fig. 4.4. Firstly, direct oxidation of S(IV) by $\cdot NO_2$ does not require molecular oxygen and regenerates nitrite or nitrous acid from which it originated (Chen *et al.*, 2002; Clifton *et al.*, 1988; Davies and Kustin, 1969):

$$HONO/NO_2^- + Mn^{3+} \rightarrow \cdot NO_2 + Mn^{2+} (+ H^+) \tag{4.5}$$

$$2\cdot NO_2 + SO_3^{2-} + H_2O \rightarrow 2NO_2^- + SO_4^{2-} + 2H^+ \tag{4.6}$$

In the present experiments, oxygen was consumed in the course of reaction along with sulfite (molar ratio of consumed species, $\Delta S/\Delta O_2$, was 2). Moreover, if the experiment at $pH = 2.2$ was continued by adding a new aliquot of $NaNO_2$ solution, the decay of oxygen was restarted for some time and then stopped, exactly like at the beginning of the experiment. Figure 4.5 shows the addition could be repeated several times with the same effect. The molar ratio of N and O_2 consumed was always 2.
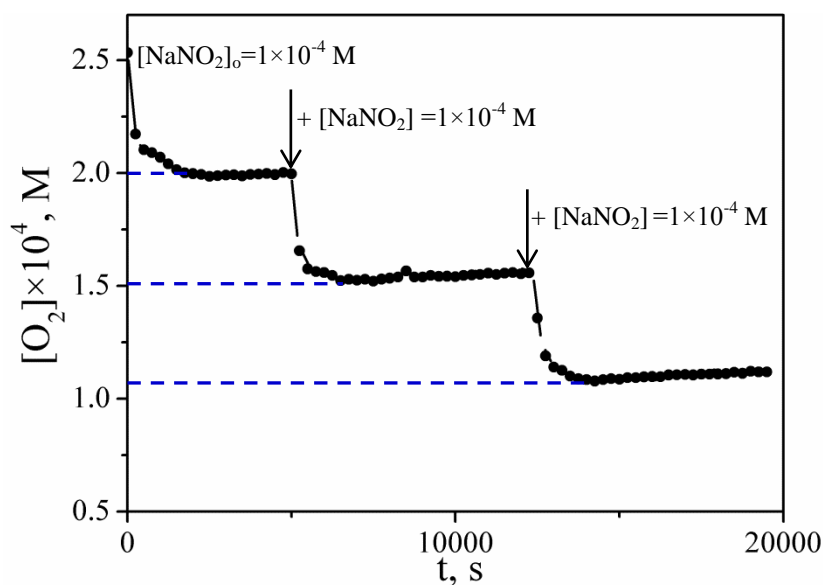
Fig. 4.5. *Course of the autoxidation of S(IV) in the presence of nitrite ions (MOSN expt) at pH_o = 2.2 with marking of the time of each addition of sodium nitrite solution.*

Therefore, a more plausible mechanism of the reaction is that the oxidation of S(IV) proceeds via a regular radical chain (Section 1.2.3) which is enhanced by nitrite and nitrous acid providing additional and more efficient production of sulfite radicals (references are listed in Table 4.5, Chapter 4.2, MOSCN experiments):

$$HONO + Mn^{3+} \rightarrow \cdot NO_2 + Mn^{2+} + H^+ \qquad k = 2.2\times10^4 \ 1/(Ms) \qquad (4.7)$$

$$NO_2^- + Mn^{3+} \rightarrow \cdot NO_2 + Mn^{2+} \qquad \text{very fast} \qquad (4.8)$$

$$\cdot NO_2 + HSO_3^- \rightarrow NO_2^- + SO_3^{\bullet -} + H^+ \qquad k = 2.8\times10^4 \ 1/(Ms) \qquad (4.9)$$

$$\cdot NO_2 + SO_3^{2-} \rightarrow NO_2^- + SO_3^{\bullet -} \qquad k = 1.12\times10^6 \ 1/(Ms) \qquad (4.10)$$

versus less efficient

$$HSO_3^- + Mn^{3+} \rightarrow Mn^{2+} + SO_3^{\bullet -} + H^+ \qquad k = 3\times10^1 \ 1/(Ms) \qquad (4.11)$$

$$SO_3^{2-} + Mn^{3+} \rightarrow Mn^{2+} + SO_3^{\bullet -} \qquad k = 1\times10^3 \ 1/(Ms) \qquad (4.12)$$

The concept is additionally supported by the fact that nitrite and nitrous acid were not oxidized in the $MnSO_4 - O_2$ system, i.e. when sulfite was not present (vide MON experiments).

When the concentration of nitrite or nitrous acid in a reacting solution gets smaller, the generation of sulfite radicals naturally slows down and so does the autoxidation of S(IV) and consumption of oxygen. The reaction becomes even slower than the autoxidation of S(IV) in the

absence of nitrite because NO_2 competitively consumes Mn^{3+} ions necessary for reactions 4.11 and 4.12, turning itself into nitrate (Davies and Kustin, 1969):

$$\cdot NO_2 + Mn^{3+} + H_2O \rightarrow NO_3^- + Mn^{2+} + 2H^+ \qquad \text{very fast} \qquad (4.13)$$

In addition, a self-reaction of NO_2 leads directly to nitric and nitrous acid (Rayson *et al.*, 2012; Shen and Rochelle, 1998):

$$2\cdot NO_2 + H_2O \rightarrow HNO_3 + HNO_2 \qquad k = 8.46\times10^7; 1.6\times10^7 \ 1/(Ms) \qquad (4.14)$$
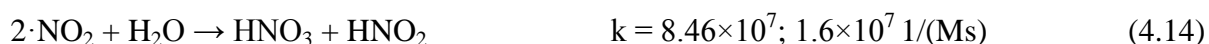
The slow-down effect of nitrite and nitrous acid is stronger in acidic media because HONO is a weaker generator of sulfite radicals than nitrous ions (Reactions 4.7 and 4.10), while it is a dominant species of the two at low pH (Fig. 4.6) calculated on the basis of the reaction below (SC-Database, 1997, 2000):

$$HONO \rightleftharpoons NO_2^- + H^+ \qquad K = 7.08\times10^{-4} \ M \qquad (4.15)$$
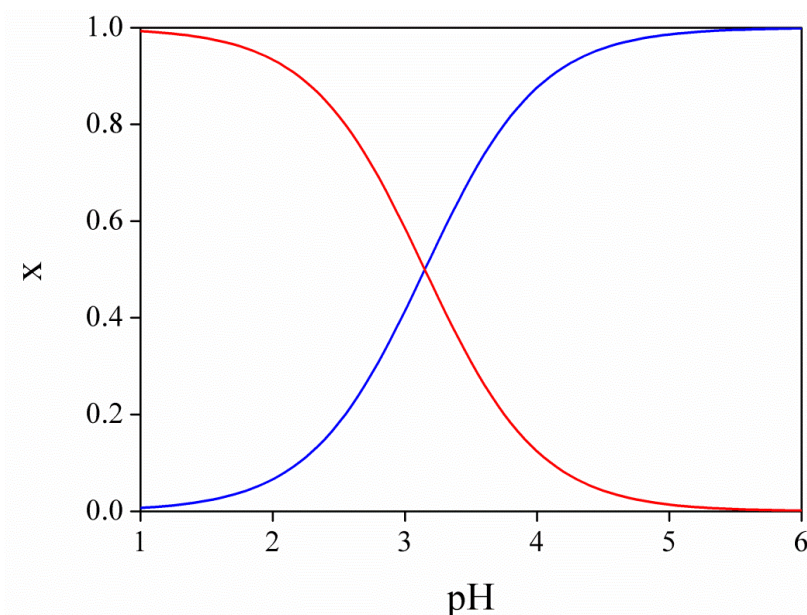
Fig. 4.6. *Molar fractions of hydrolytic species in a 1×10^{-4} mol dm^{-3} solution NaNO$_2$ at 25°C calculated using the dissociation equilibrium constants K(HONO) = 7.08×10^{-4} mol dm^{-3}: red line corresponds to HONO; blue line – to NO$_2^-$ ions.*

For simplicity and as a first approximation, the presented discussion did not include the formation of peroxynitrites initiated by NO· which forms from HONO very slowly under presented conditions (Rayson *et al.*, 2012). Formation of S–N compounds, such as nitrilo- and hydroxyl-sulfonates was skipped as well, because it was extremely slow under the conditions

66

considered (Pasiuk-Bronikowska and Rudzinski, 1982; Susianto *et al.*, 2001). An otherwise complete mechanism by which nitrite and nitrous acid participate in the autoxidation of S(IV) is presented in Figure 4.7.
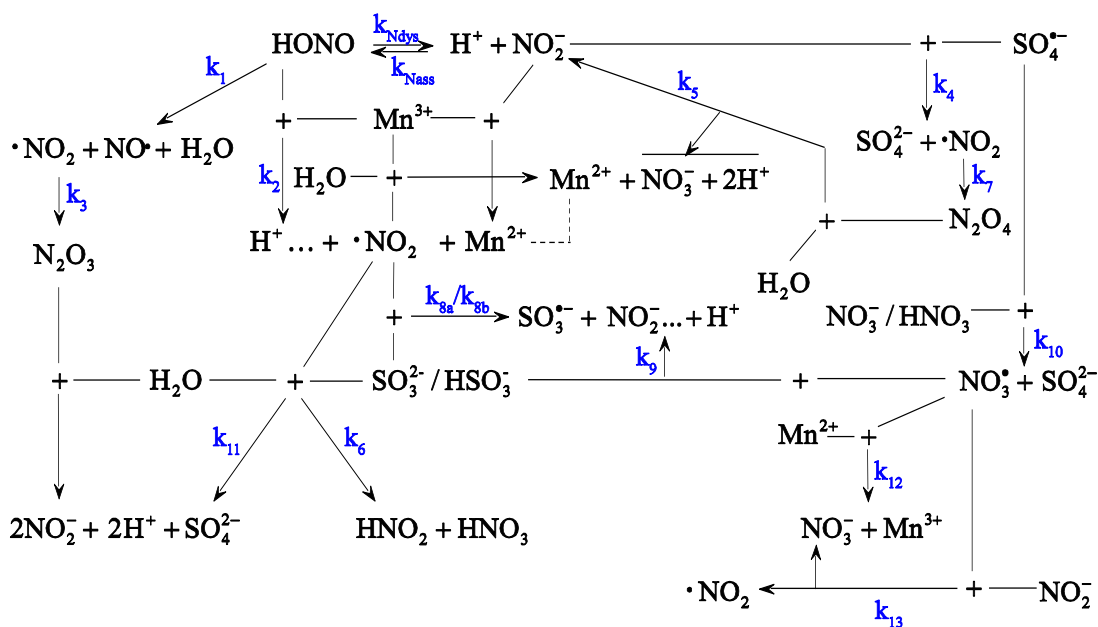
Fig. 4.7. *Mechanism of S(IV) autoxidation catalyzed by Mn $^{3+}$ in the presence of nitrous acid and nitrite ions.*

4.1.2 Experiments with isoprene

- **MOSC experiments** *(manganese, oxygen, sulfite and isoprene)*
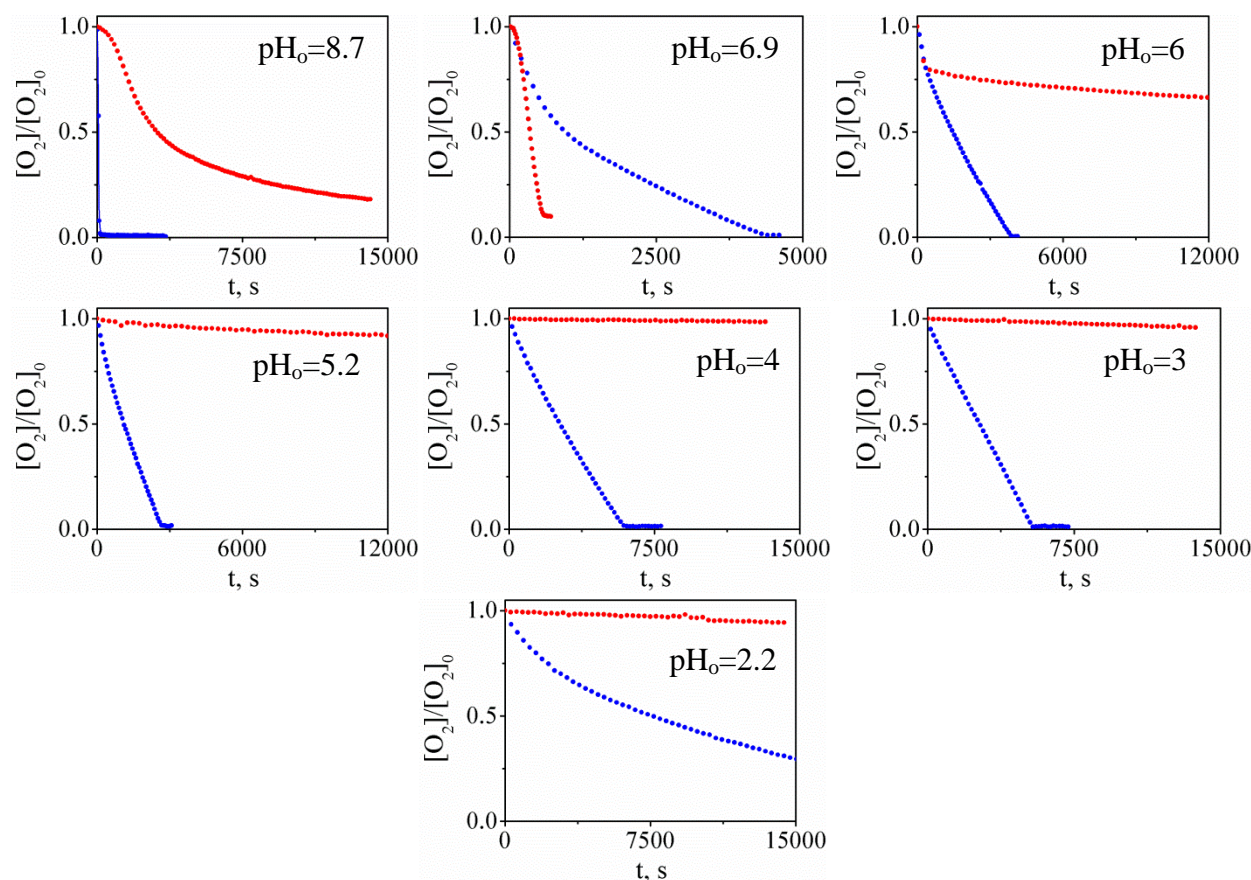
Fig. 4.8. *Influence of isoprene on the autoxidation of S(IV) at different initial acidity of the reaction solution. Red points correspond to the experiments with isoprene (MOSC expt); blue points – to the experiments without isoprene (MOS expt).*

Isoprene influences the autoxidation of S(IV) catalyzed by manganese(II) ions in different ways which depend on the initial acidity of reacting solutions (Fig.4.8). In the acidic ($pH_o = 2.2 \div 6$) and alkaline ($pH_o = 8.7$) solutions, isoprene inhibits the autoxidation. In neutral ($pH_o = 7 \div 8$) solutions, it accelerates the reaction. In solution of $pH_o = 5.2 \div 6$, and $pH_o = 8.7$ isoprene strongly slows down the autoxidation of S(IV). In the acidic solution $pH \leq 4$, it almost stops the reaction with the overall conversion of oxygen less than 10%. This difference of isoprene impact on the autoxidation of S(VI) which in different way are depended on initial acidity of the reaction solution was explained by Rudziński *et al.* (2009):

- different rates of reactions of SO_3^{2-} and HSO_3^- ions with $SO_5^{\bullet-}$ radical-anions arising during the autoxidation of S(IV), as it was mentioned before (see Chapter 4.1.1, MOS experiments);

- scavenging of sulfoxy radicals such as $SO_4^{\bullet-}$ and $SO_3^{\bullet-}$ by isoprene;

- regeneration of $SO_3^{\bullet-}$ radical during further oxidation of isoprene.

Other thing is that ratio of S(IV) conversion to O_2 conversion is fixed for autoxidation of S(IV) without inhibitors. It is equal 2:1 for the overall reaction (Reaction 4.16).

$$2Na_2SO_3 + O_2 \xrightarrow{MnSO_4} 2Na_2SO_4 \tag{4.16}$$

Conversion ratio $\Delta[S(IV)]/\Delta[O_2]$ in experiments with isoprene decreases to ~ 1.53:1 in alkaline solution, drops to 1.28:1 at $pH_o = 7.7$ and increases up to ~ 1.6 in acidic solutions.

The ratios of isoprene conversion to O_2 conversion is about 0.25:1 in alkaline solutions, and increases in slightly acidic solutions (Table 4.1). The value at $pH_o = 4.0$ is rather uncertain as calculated from total conversions lower than 1%.

The reduction of conversion ratios in the presence of isoprene could be explained by formation of its oxygenated products.

Table 4.1. *Experimental conversion ratios in transformation of isoprene coupled with autoxidation of S(IV).*

Initial pH	Experimental conversion ratios	
	$\Delta[S(IV)]/\Delta[O_2]$	$\Delta[C_5H_8]/\Delta[S(IV)]$
8.3	1.53	0.21
7.7	1.28	0.25
7.0	1.52	0.25
5.8	1.63	0.40
4.0	1.61[a]	1.21[a]

[a] the values have increased uncertainty, because conversion of each reactants was lower than 1%

- **MOCN experiments** *(manganese, oxygen, isoprene and nitrite)*

The MOCN experiments comprised runs in which nitrite ions/nitrous acid, oxygen, manganese(II) sulfate and isoprene were brought together in aqueous solutions of various acidities. In solutions of $pH \geq 5$, no consumption of oxygen and no changes in UV spectra were observed. At more acidic conditions, up to 20% of oxygen and up to 60% of isoprene was consumed in about 4 hours – more in more acidic solutions (Fig. 4.9). Unfortunately, the

consumption of nitrite/nitrous acid could not be determined because of high inaccuracy of the UV-spectra analysis.
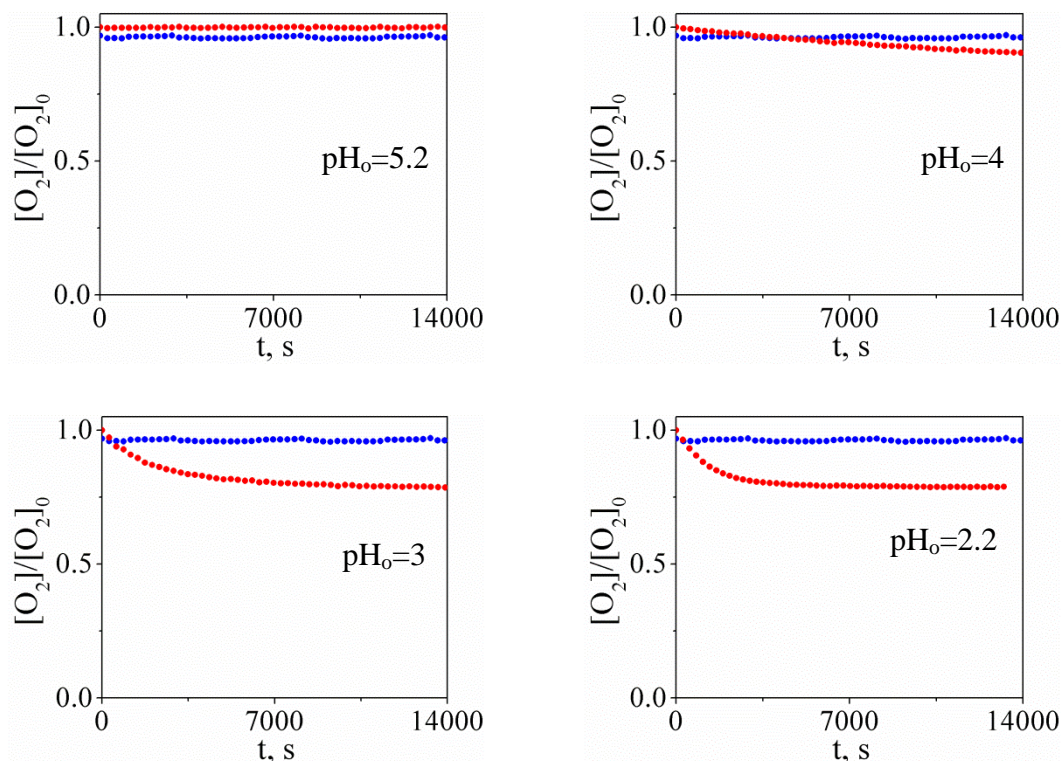
Fig. 4.9. *Decay of oxygen at different initial acidities of reaction solutions in MON (blue dot)s and MOCN (red dots) experiments.*
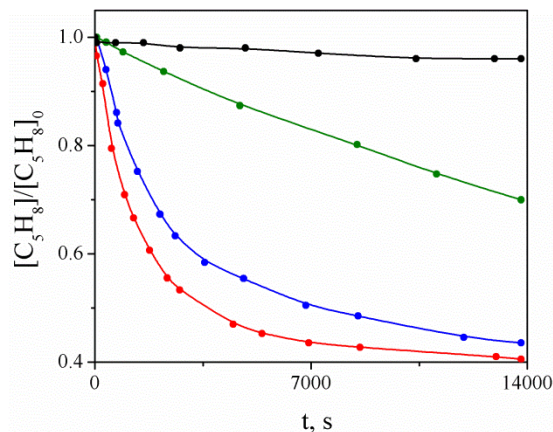
Fig. 4.10. *Decay of isoprene during MOCN experiments at different initial acidities of reaction solutions: black dots correspond to $pH_o = 5.2$; olive – 4; blue – 3 and red – 2.2.*

Figure 4.10 shows isoprene decay in acidic solutions ($pH_o = 5.2 \div 2.2$). The highest isoprene conversion (~ 60%) is observed for $pH_o = 2.2$. The profile of isoprene decaying is not identical to that of oxygen (Fig.4.9). It is similar at the beginning of the experimental run, but, at the second part of the reaction course, the concentration of isoprene still decreases while the

concentration of oxygen stays unchanged. The same situation is observed for $pH_o = 3$ albeit with smaller C_5H_8 conversion – 55%. Shapes of isoprene concentration profiles at $pH_o = 4$ and 5.2 are analogous to these of O_2 with $\Delta[C_5H_8] \sim 30\%$ and 10%, respectively.

Table 4.2. *Molar conversions and conversion ratio of oxygen and isoprene in MOCN experiments at acidic conditions, after about 4 hours.*

pH_o	$[O_2]_o$ mol dm^{-3}	$\Delta[O_2]$ mol dm^{-3}	$[C_5H_8]_o$ mol dm^{-3}	$\Delta[C_5H_8]$ mol dm^{-3}	$\Delta[C_5H_8]/\Delta[O_2]$
4.0	2.5×10^{-4}	2.6×10^{-5}	8.82×10^{-5}	2.78×10^{-5}	1.07
3.0	2.5×10^{-4}	5.3×10^{-5}	8.03×10^{-5}	4.53×10^{-5}	0.85
2.2	2.65×10^{-4}	1.1×10^{-5}	8.19×10^{-5}	3.98×10^{-5}	1.02

Table 4.2 shows the molar conversions of oxygen and isoprene in the MOCN experiments at pH 4, 3 and 2.2, as well as the ratio of these conversions which appeared close to 1. This implies a possible overall reaction involved could be:

$$HONO + O_2 + H_2C=C(CH_3)–CH=CH_2 \rightarrow H_2C(NO_2)–C(CH_3)=CH–C(O)H + H_2O \qquad (4.17)$$

Reaction 4.17 would be initiated by slow decomposition of HONO into nitroxide radicals (Rayson *et al.*, 2012):

$$2HONO \rightarrow \cdot NO_2 + NO\cdot + H_2O \qquad\qquad k = 2.8\times10^1 \ dm^3/(mol\ s) \qquad\qquad (4.18)$$
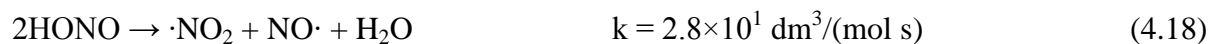
Figure 4.11 shows a complete mechanism behind, which includes the addition of $\cdot NO_2$ to a double bond in isoprene followed by the addition of oxygen to the organic radical formed.
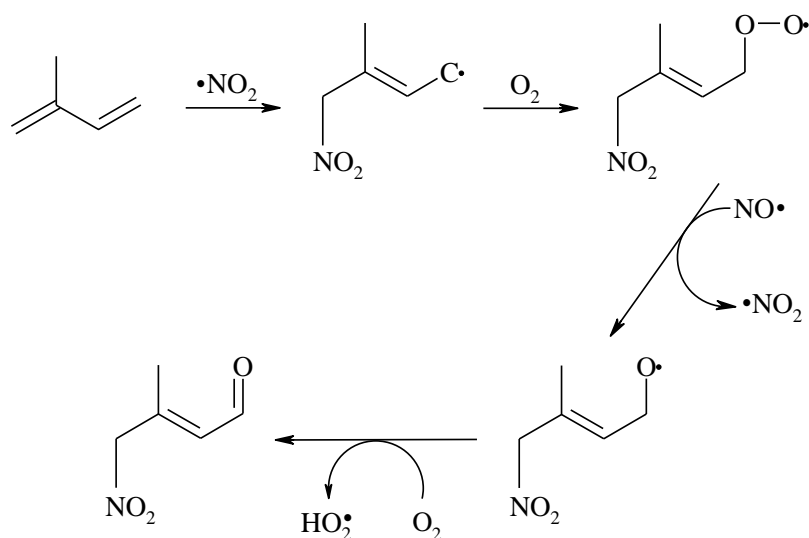
Fig. 4.11. *Mechanism of transformation of isoprene initiated by nitrate radicals.*

The chain reaction terminates by following reactions:

$$\cdot NO_2 + HO_2^{\bullet} \rightarrow HO_2NO_2 \tag{4.19}$$

$$HO_2NO_2 \rightarrow NO_2^- + O_2 + H^+ \tag{4.20}$$

$$HO_2NO_2 \rightarrow HONO + O_2 \tag{4.21}$$

$$\cdot NO_2 + \cdot NO_2 + H_2O \rightarrow H^+ + NO_3^- + HONO \tag{4.22}$$

Additional support to the concept mechanism in Figure 4.11 came from the preliminary mass spectrometric analysis (direct infusion, electrospray ionization, positive-ion mode) which revealed a reasonably significant peak at $m/z = 129$ that can represent protonated $H_2C(NO_2)$–$C(CH_3)=CH$–$C(O)H$ ions (MH^+).

- **MOSCN experiments** *(manganese, oxygen, sulfite, isoprene and nitrite)*

The addition of sodium nitrite to the reacting system with isoprene and autoxidation of S(IV) had little influence in alkaline and neutral solutions, but changed significantly the course of the reactions in acidic media (Fig. 4.12 – 4.13).
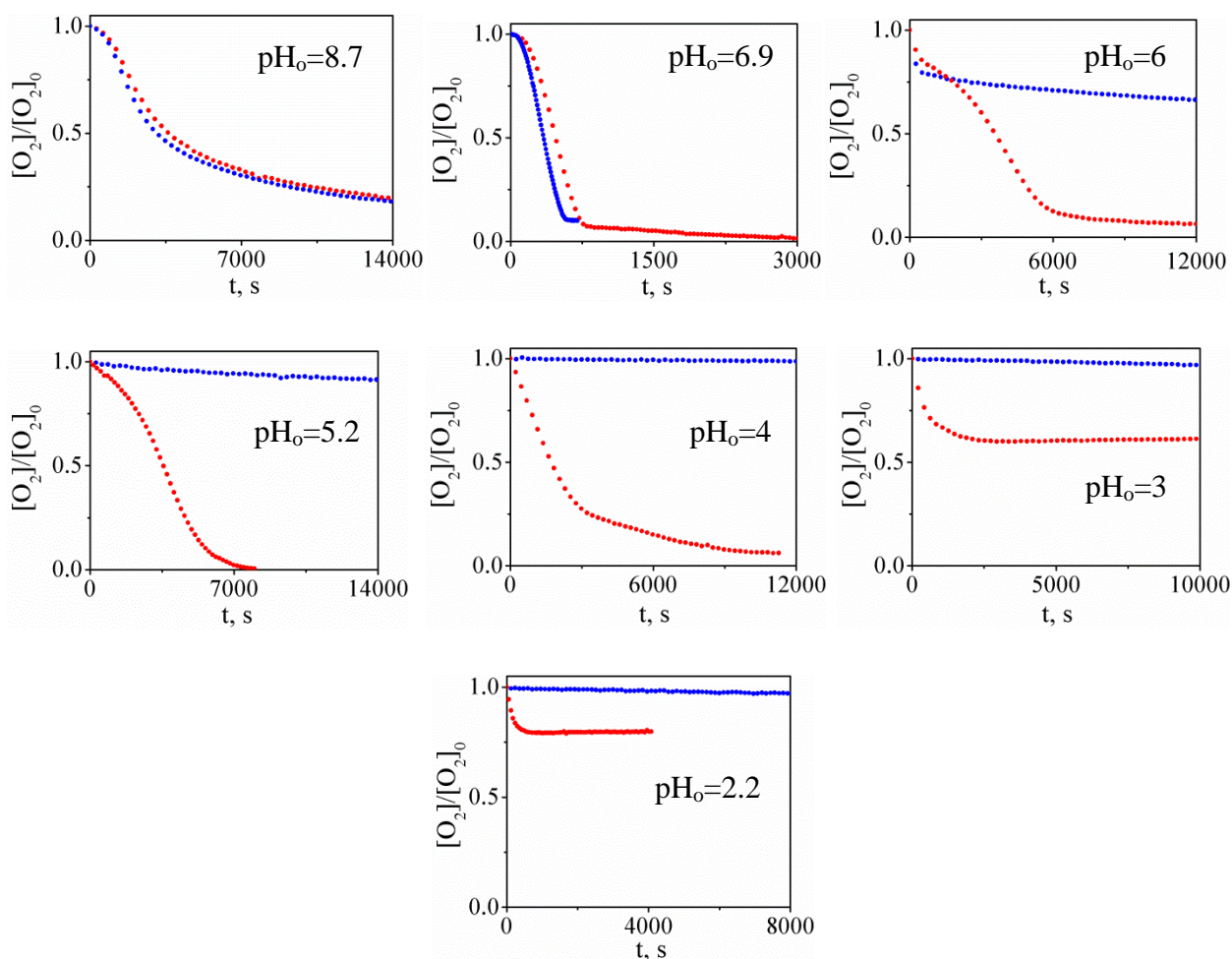
Fig. 4.12. *Decay of oxygen during the autoxidation of S(IV) at different initial acidities in the presence of: isoprene and nitrite ions (MOSCN expt) – red points and isoprene only (MOSC expt) – blue points.*

In alkaline solutions, nitrite ions did not stop the inhibiting action of isoprene on the S(IV) autoxidation. The rates of oxygen consumption were comparable, but conversion of isoprene was slightly smaller about 17%.

In neutral solutions, where both isoprene and nitrite ions accelerated the autoxidation of S(IV) (Fig. 4.8 and 4.4, respectively), their action added up so that the reaction was comparably fast (Fig. 4.12). The corresponding conversion of isoprene was slightly smaller than in MOSC experiments (Fig. 4.13).

In mild acidic solutions (pH = 6 − 4), nitrite/nitrous acid generally counteracted the inhibiting action of isoprene on the S(IV) autoxidation so that the reaction was faster than in the case of isoprene taken alone (Fig. 4.14).
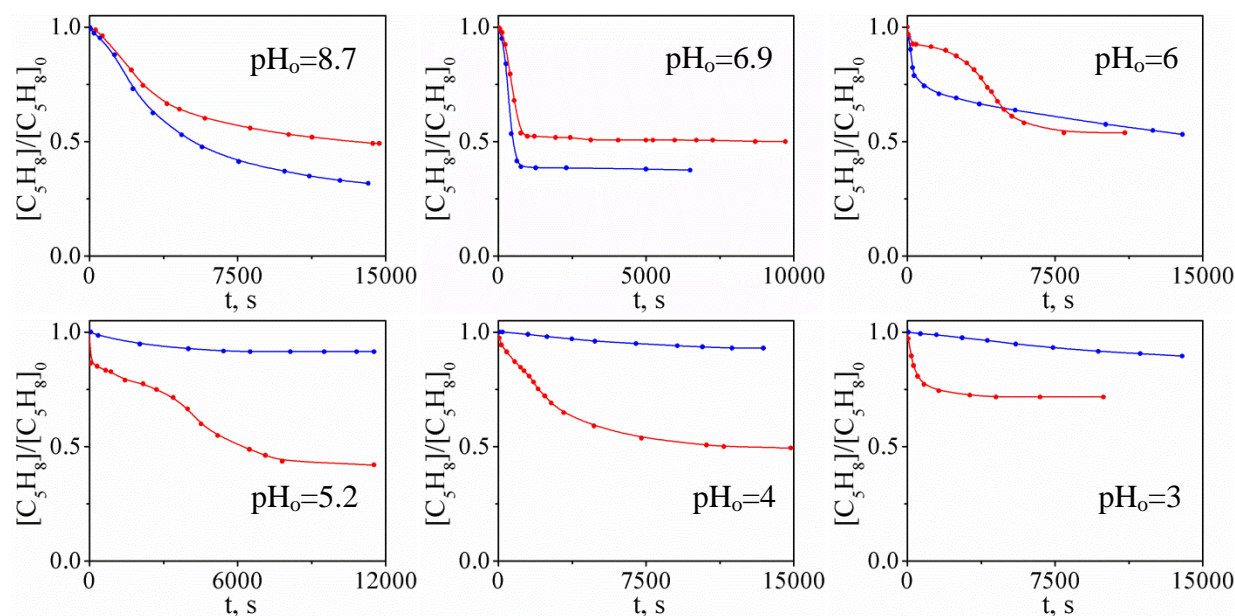
Fig. 4.13. *Decaying of isoprene during the autoxidation of S(IV): red dots correspond to experiments in the presence of nitrite ions (MOSCN expt); blue dots – in the absence of nitrite ions (MOSC expt).*
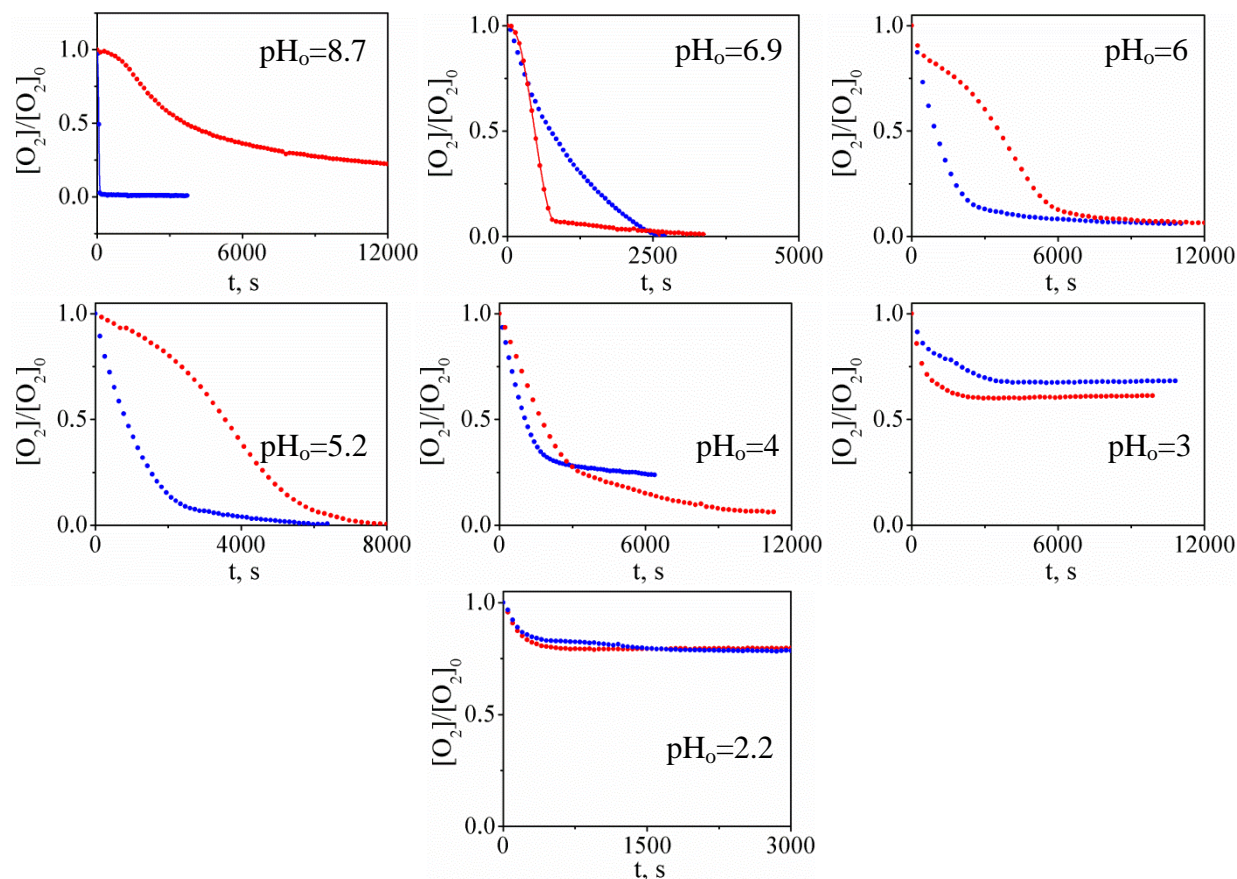
Fig. 4.14. *Influence of nitrous acid on the decay of oxygen during S(IV) autoxidation at different initial acidities in the presence and absence of isoprene. Blue points – experiments with nitrous acid and without isoprene (MOSN expt); red points – with nitrous acid and isoprene (MOSCN expt).*

It is interesting, however, that at pH = 4, isoprene made the reaction goes up to the complete consumption of oxygen, which was not the case of HONO acting alone. The conversion of isoprene in acidic experiments in the presence of nitrite/HONO was quite significant, ranging from 50.6% at $pH_o = 4$ to 58% at $pH_o = 5.2$. In solutions at $pH_o = 6$, there is no almost difference between isoprene conversion during MOSCN and MOSC experiments ($\sim 46\%$).

In most acidic solutions (pH = 2 and 3), the MOSCN and MOSN experiments were very similar, and both faster than MOSC experiments, albeit with incomplete consumption of oxygen halted at 40 and 20%, respectively.

Table 4.3 shows molar conversions and conversion ratios of oxygen, S(IV) and isoprene in MOSCN experiments. At $pH_o = 6.9 \div 4.0$, molar conversions of oxygen, S(IV) and isoprene in the MOSCN experiments vary only slightly with the acidity of reacting solutions – $\sim 95\%$, 54% and 96%, respectively. Conversion ratio $\Delta[C_5H_8]/\Delta[O_2]$ is about 0.32,while $\Delta[S(IV)]/\Delta[O_2]$ is 1.72 (with an exception at $pH_o = 4.0$). At $pH_o = 3.0 \div 2.2$, molar conversions of reagents drop with the increase of reacting solution acidities to $\sim 21\%$, 15% and 29% for O_2, S(IV) and C_5H_8, respectively. The conversion ratio $\Delta[C_5H_8]/\Delta[O_2]$ and $\Delta[S(IV)]/\Delta[O_2]$rise to 2.53 and 2.02, respectively.

Table 4.3. *Molar conversions and conversion ratios of oxygen, S(IV) and isoprene in MOSCN experiments at neutral and acidic conditions.*

pH_o	time h	$\Delta[O_2]$ mmol dm^{-3}	$\Delta[O_2]$ %	$\Delta[S(IV)]$ mmol dm^{-3}	$\Delta[S(IV)]$ %	$\Delta[C_5H_8]$ mmol dm^{-3}	$\Delta[C_5H_8]$ %	$\Delta[C_5H_8]/\Delta[O_2]$	$\Delta[S(IV)]/\Delta[O_2]$
6.9	2.2	0.247	99	0.420	54	0.0742	96	0.30	1.70
6.0	1.6	0.221	87	0.391	50	0.0818	100	0.37	1.77
5.2	2.2	0.247	99	0.420	54	0.0742	96	0.30	1.70
4.0	2.9	0.236	94	0.449	58	0.0684	90	0.29	1.90
3.0	0.9	0.100	40	0.199	28	0.0397	50	2.53	1.98
2.2	0.5	0.0538	21	0.111	15	0.0270	29	2.53	2.05

The general conclusion here is that MOSCN experiments – the most complicated in this work – most probably follow a chemical mechanism that includes the basic mechanism

developed for the MOSC system and modules developed here for the MOCN and MOSN systems. Further discussion is in the next chapter.

4.2 Chemical mechanism of the reaction

The chemical mechanism constructed to explain our experiments with transformation of isoprene coupled with autoxidation of S(IV) consisted of three groups of reactions – autoxidation of Mn(II) to Mn(III) in presence of sulfite or bisulfite ions (Fig. 4.15), autoxidation of S(IV) catalyzed by MnSO$_4$ (Fig. 4.16), and transformation of isoprene initiated by sulfate radical-anions (Fig. 4.17) or by sulfite radical-anions (not shown, since analogous to the scheme for sulfate radical-anions). The individual reactions in the schemes were identified by specific symbols of the rate constants rather than by consecutive numbers, to simplify the presentation and provide better mnemonic association. Values of the rate constants used in simulations were collected in Table 4.4, along with available references.

Table 4.4. *Rate constants used for simulation of chemical mechanism shown in Figs. 4.15 – 4.17.*

Constants in Fig. 4.15	Value $M^{-1}\,s^{-1}$	Constants in Fig.4.16	Value $M^{-1}\,s^{-1}$	Constants in Fig.4.17	Value $M^{-1}\,s^{-1}$
k_{ass}	1.0×10^{11}	k_{ass}	1.0×10^{11}	k_{s1}[k]	2.19×10^{9}
k_{dys}[a]	6.75×10^{3}	k_{dys}[a]	6.75×10^{3}	k_{s2}	1.0×10^{9}
k_{kfb}	6×10^{6}	k_{ib}	1.0×10^{3}	k_{s3b}	1.0×10^{9}
k_{kbb}	1	k_{ia}	3.0×10^{1}	k_{s3a}	1
k_{kfa}	6×10^{6}	k_{p1}[d]	1.5×10^{9}	k_{s3b}	1.0×10^{9}
k_{kba}	1	k_{p21b}[e]	3.25×10^{6}	k_{s4a}	1.0×10^{9}
k_{afb}	6	k_{p22b}[e]	9.75×10^{6}	k_{s5}	$(1\div5)\times10^{9}$
k_{abb}	1	k_{p21a}[e]	2.5×10^{4}	k_{s6}[l]	3.5×10^{9}
k_{afa}	$8\div10$	k_{p22a}[e]	7.5×10^{4}	Analogous constants for reactions of SO_3^{-} radicals (not shown in figures)	
k_{aba}	1	k_{p3b}[f]	1.4×10^{7}		
k_{dfb}	6	k_{p3a}[f]	1.4×10^{7}		
k_{dbb}	1	k_{ox11}	3.2×10^{6}	k_{2s1}	1.0×10^{9}
k_{dfa}	$8\div10$	k_{ox12}	1.2×10^{2}	k_{2s2}	1.0×10^{9}
k_{dba}	1	k_{ox2}	1.0×10^{6}	k_{2s3b}	5.0×10^{4}
k_{o2b}	6	k_{t22}[g]	1.0×10^{8}	k_{2s3a}	1.0×10^{6}
k_{o2a}	$8\div10$	k_{cas}	1.0×10^{10}	k_{2s4b}	$(1.2\div2.5)\times10^{4}$
k_{hpb}[b]	0.19	k_{cdy}[a]	3.98	k_{2s4a}	5.0×10^{4}
k_{hpa}[c]	3.4×10^{7}	k_{fb}	7.5×10^{3}	k_{2s5}	1
		k_{fa}	7.5×10^{3}		
		k_{t1}[h]	4.0×10^{8}		
		k_{t21}[i]	1.0×10^{7}		
		k_{t3}	1.0×10^{6}		
		k_{t4}[j]	5.0×10^{8}		

[a] s^{-1}. [b] (Drexler *et al.*, 1992). [c] $M^{-2}\,s^{-1}$, rate$=k_{hpa}[H^+][H_2O_2][HSO_3^-]$, (Drexler *et al.*, 1991). [d] (Huie and Neta, 1984). [e] (Huie and Neta, 1987). [f] Averaged in CAPRAM. [g] 5.5×10^{6} (Herrmann *et al.*, 1995), $\sim 2.2\times10^{8}$ (Buxton *et al.*, 1996). [h] (McElroy and Waygood, 1990). [i] 1.3×10^{8} (Herrmann *et al.*, 1995), 4.8×10^{7} (Buxton *et al.*, 1996). [j] (McElroy and Waygood, 1990). [k] (Rudziński, 2004). [l] 1.7×10^{9} (Buxton *et al.*, 1996).

4.2.1 Autoxidation of Mn(II) in presence of sulfite or bisulfite ions

For chemical-kinetic modeling of isoprene reactions coupled with autoxidation of S(IV), the initiation mechanism described by Rudziński and Pasiuk-Bronikowska (2000) was chosen (see also Chapter 1.2.3) (Fig. 4.15).
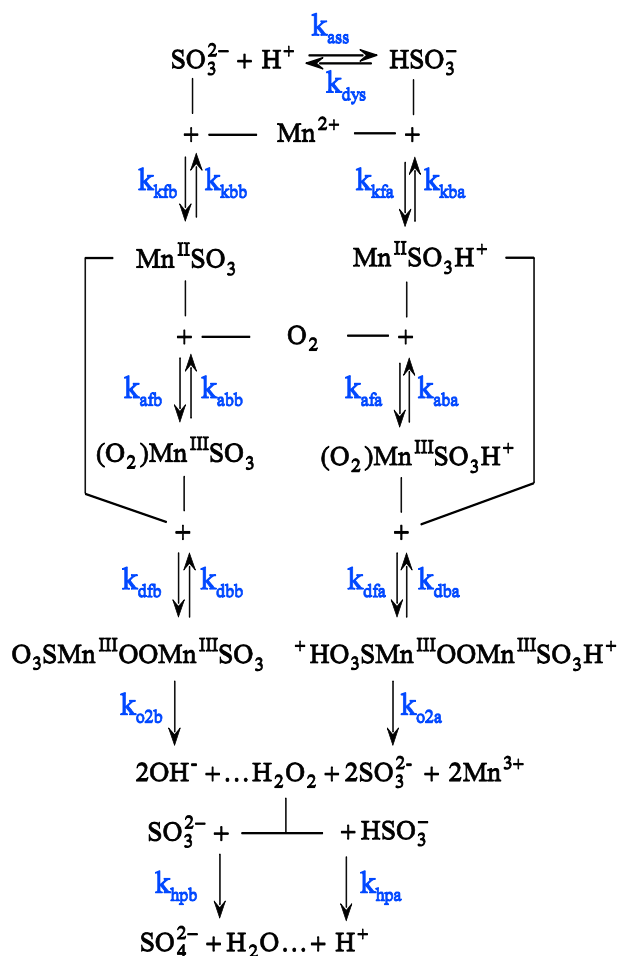
$$SO_3^{2-} + H^+ \underset{k_{dys}}{\overset{k_{ass}}{\rightleftharpoons}} HSO_3^-$$

$$+ \quad Mn^{2+} \quad +$$

$$k_{kfb} \downarrow\uparrow k_{kbb} \qquad k_{kfa} \downarrow\uparrow k_{kba}$$

$$Mn^{II}SO_3 \qquad Mn^{II}SO_3H^+$$

$$+ \quad O_2 \quad +$$

$$k_{afb} \downarrow\uparrow k_{abb} \qquad k_{afa} \downarrow\uparrow k_{aba}$$

$$(O_2)Mn^{III}SO_3 \qquad (O_2)Mn^{III}SO_3H^+$$

$$+ \qquad +$$

$$k_{dfb} \downarrow\uparrow k_{dbb} \qquad k_{dfa} \downarrow\uparrow k_{dba}$$

$$O_3SMn^{III}OOMn^{III}SO_3 \qquad {}^+HO_3SMn^{III}OOMn^{III}SO_3H^+$$

$$k_{o2b} \downarrow \qquad\qquad k_{o2a} \downarrow$$

$$2OH^- + \ldots H_2O_2 + 2SO_3^{2-} + 2Mn^{3+}$$

$$SO_3^{2-} + \qquad + HSO_3^-$$

$$k_{hpb} \downarrow \qquad\qquad k_{hpa} \downarrow$$

$$SO_4^{2-} + H_2O \ldots + H^+$$

Fig. 4.15. *Mechanism of autoxidation of Mn(II) in the presence of sulfite and bisulfite ions.*

The autoxidation is triggered by the oxidation of Mn(II) to Mn(III) in the presence of sulfite or bisulfite anions (Fig. 4.15) which linked together by a reversible association-dissociation reaction (k_{ass}/k_{dys}). Adding Mn^{2+} to these anions gives Mn(II)-sulfite complexes in two reversible reactions (k_{kfa}/k_{kba} and k_{kfb}/k_{kbb}). Metal oxidation in the complexes with molecular O_2 (k_{afa}/k_{aba} and k_{afb}/k_{abb}), and formation of dimers from adducts and the complexes (k_{dfa}/k_{dba} and k_{dfb}/k_{dbb}) are also reversible reactions. Subsequent stages are intramolecular oxidation of second Mn(III), and decomposition of the dimer to H_2O_2 and Mn^{3+} (k_{o2a}/k_{o2b}). H_2O_2 oxidized the sulfite ions that were released from the dimers directly to sulfate ions (k_{hpa} and k_{hpb}). Two hydroxyl ions

were also formed, which resulted in some alkalization of the reaction mixture. The extent of Mn(III) autoxidation was very minor, and its purpose was to start the autoxidation of S(IV) by supplying the very initial amount of Mn^{3+} in the absence of any other initiator. When the S(IV) autoxidation chain grew longer, Mn(II) was oxidized back to Mn(III) in several reactions with sulfoxy radicals and ions. This is exactly why manganese is also called a catalyst of S(IV) autoxidation.

4.2.2 Autoxidation of S(IV) catalyzed by manganese
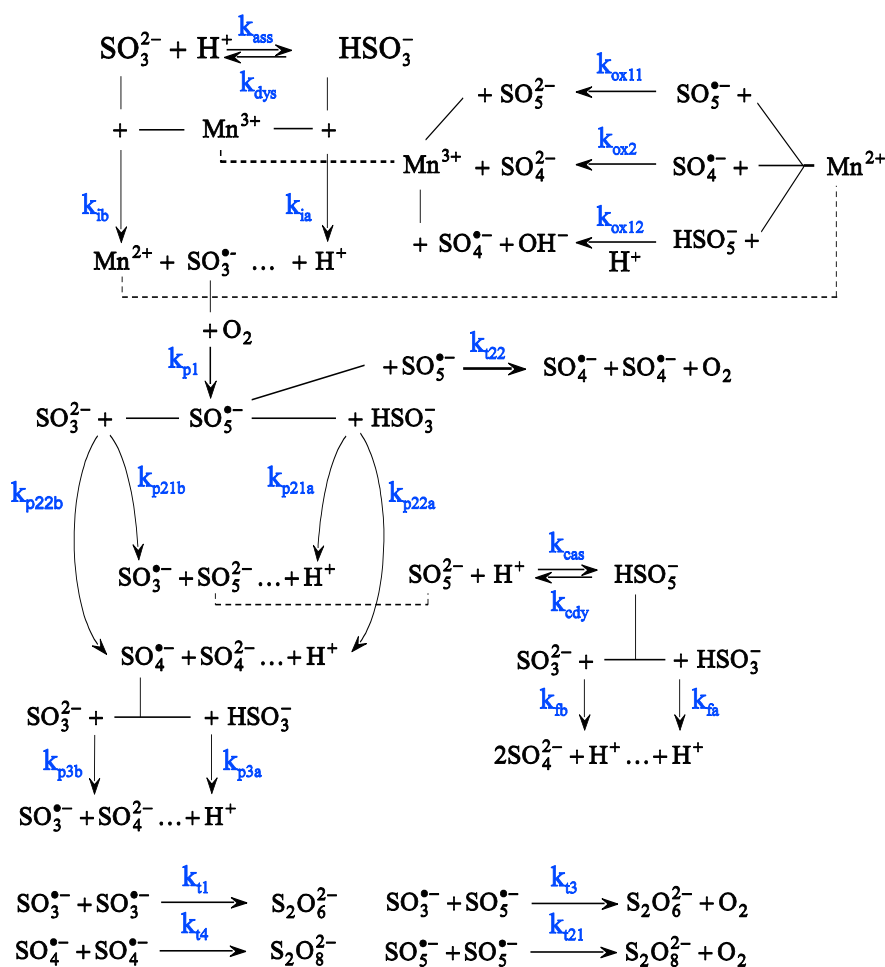

Fig. 4.16. *Mechanism of S(IV) autoxidation catalyzed by manganese.*

As it was mentioned before, autoxidation of S(IV) is a chain process initiated by sulfite radical-anions formed in the reaction of Mn^{3+} with sulfite or bisulfite ions (k_{ib} and k_{ia}) (Fig. 4.16). Propagation of the reaction chain has several steps – oxidation of sulfite radical-anions and

oxygen to peroxymonosulfate radical-anions (k_{p1}), split reactions of peroxymonosulfate radical-anions with sulfite or bisulfite ions that lead to formation of peroxymonosulfate ions and regeneration of sulfite radical-anions (k_{p21a} and k_{p21b}), or to production of sulfate radical-anions and sulfate ions (k_{p22a} and k_{p22b}), and reaction of sulfate radical-anions with sulfite or bisulfite ions, which regenerates sulfite radical-anions (k_{p3a} and k_{p3b}). Sulfate ions are formed during reaction of sulfite ions (k_{fa} and k_{fb}) with HSO_5^- ions which arise from reversible associate of peroxymonosulfate and H^+ ions (k_{cas} /k_{cdy}). Chain termination occurs via radical-radical reactions (k_{t1}, k_{t21}, k_{t3}, k_{t4}). Reaction of two peroxymonosulfate radical-anions can also regenerate sulfate radical-anions (k_{t22}). The chain initiator, Mn^{3+}, is regenerated in reactions of Mn^{2+} cations with sulfite radical-anions (k_{ox11}), sulfate radical-anions (k_{ox2}) and peroxymonosulfte ions (k_{ox12}).
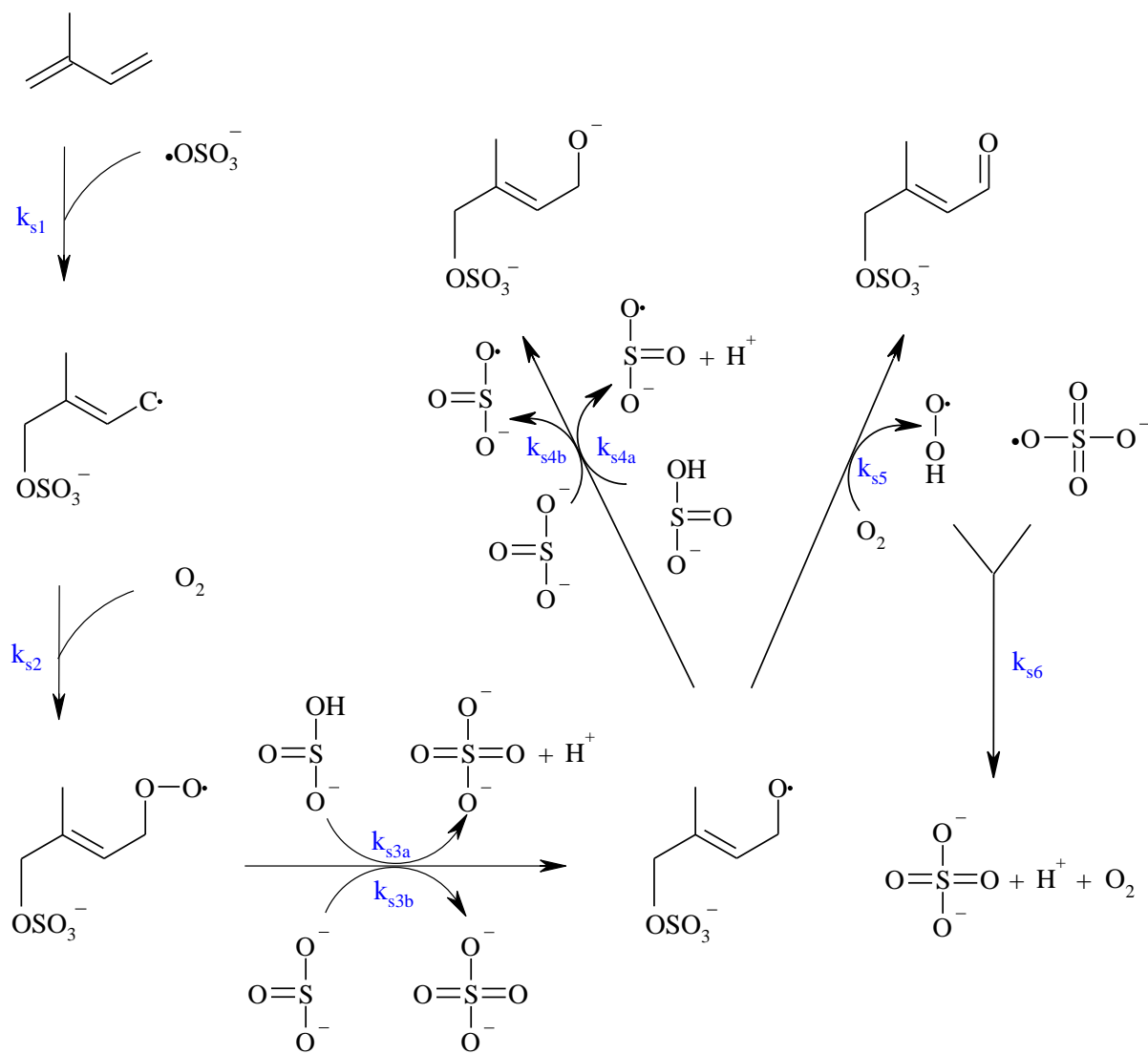
4.2.3 Transformation of isoprene initiated by sulfoxy radical-anions

The proposed mechanism is based on the isoprene could reaction with sulfite and sulfate radical-anions from autoxidation of S(IV). It was assumed that kinetics of the addition of each radical to either of two double bonds of isoprene at any of four positions (1, 2, 3, or 4) is equivalent. Therefore, these additions could be represented by a single reaction for each type of sulfoxy radicals.

The reaction chain of radical transformations of isoprene can be initiated either by sulfate radical-anions (k_{s1}) (Fig. 4.17) or by sulfite radical-anions (not shown on Fig. 4.13). Alkyl radicals react with molecular oxygen to give peroxyalkyl radicals (k_{s2}). The peroxyalkyl radicals oxidized the sulfite (k_{s3b}) or bisulfite ions (k_{s3a}) and form alkoxy radicals. These radicals can react either with sulfate radical anions or with oxygen molecules. The alkoxy radicals which react with sulfite (k_{s4b}) or bisulfite ions (k_{s4a}) form a hydroxy derivative of isoprene and regenerate sulfite radical-anions. In a parallel reaction with oxygen, the alkoxy radicals turn into an oxy derivative of isoprene and produce hydroperoxy radicals (k_{s5}). Hydroperoxy radicals reacted with sulfate radical-anions, producing sulfate ions (k_{s6}).

Similar mechanism can be written for sulfite radical anions reacting with a double bond in isoprene. The rate constants for the respective reactions were distinguished by adding "2" in the

subscript (k_{2s1}, k_{2s2}, k_{2s3a}, k_{2s3b}, k_{2s4a}, k_{2s4b}, k_{2s5}). The isoprene derivatives were similar to those obtained in the transformation initiated by sulfate radical-anions, but contained $-OSO_2$ substituent groups instead of $-OSO_3$.

Fig. 4.17. *Mechanism of transformation of isoprene initiated by sulfate radical-anions. Similar scheme (not shown) was used for transformation initiated by sulfite radicals, with reaction constants k_{2s1}, k_{2s2}, k_{2s3a}, k_{2s3b}, k_{2s4a}, k_{2s4b}, k_{2s5}.*

The unambiguous identification of products of isoprene transformation included in the mechanism was accomplished by interpretation of mass spectra of post-reaction solutions. A broad discussion on this topic is presented in the Chapter 4.4. Of novel products, two distinct chemical groups were identified:

- organic derivatives of sulfuric acid (organosulfate monoesters[*]): 4-*O*-sulfonyl-3-methylbut-2-enal (MW 180; *m/z* 179), and 1-*O*-sulfonyl-4-hydrox-2-methylbut-2-ene (MW 182; *m/z* 181);

- organic derivatives of sulfurous acid (organosulfite monoesters[*]): 4-*O*-sulfinyl-3-methylbut-2-enal (MW 164; *m/z* 163), 1-*O*-sulfinyl-4-hydrox-2-methylbut-2-ene (MW 166; *m/z* 165).

MW 180   *MW 182*   *MW 164*   *MW 166*
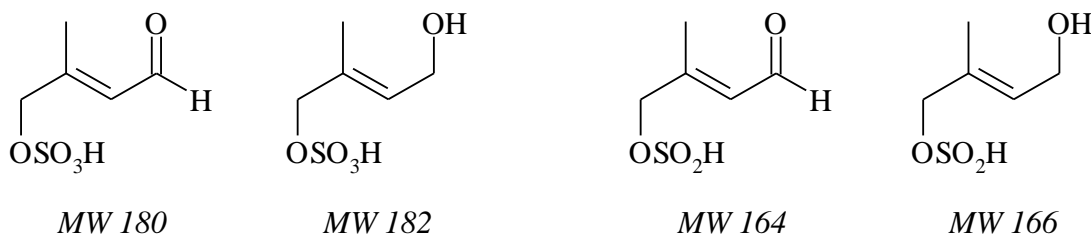
Scheme 4.1. *Molecular structures of identified products.*

As it is shown in Scheme 4.1 products formed in the reaction of aqueous-phase isoprene degradation are highly polar and possess a carbon-carbon double bond that is prone to react further, for instance with radical species. As a result of these reactions, a novel saturated organosulfate family is being produced with a molecular structure similar to the sulfate esters of methylglyceric acid and 2-methyltetrols that had been detected in field measurements (Surratt *et al.*, 2007b; 2008; Gómez-González *et al.*, 2007).

- **MOSCN** *(manganese, oxygen, sulfite and isoprene)*

The MOSCN mechanism that includes all considered reactants – sulfite, isoprene, nitrite, manganese, and oxygen – can be derived by extending the MOSC mechanism (Chapter 4.2.1 – 4.2.3) with MOSN module (Fig. 4.7) and the MOCN module containing the Reactions 4.15, 4.18 – 4.22, Figure 4.11, Chapter 4.1.2. The individual reactions in the added schemes were identified by consecutive numbers to simplify the presentation. The corresponding values of the rate constants used in MOSN module were collected in Table 4.5, along with available references.

---

[*]For convenience the terms "organosulfate/organosulfite" instead "organosulfate/organosulfite monoester" are used in this thesis

Table 4.5. *Rate constants used for simulation of chemical mechanism shown in Fig. 4.7.*

| Constants in Fig. 4.7	Value $M^{-1} s^{-1}$	Constants in Fig. 4.7	Value $M^{-1} s^{-1}$
k_{Nass}	unknown	k_6	[i] 1.6×10^7
k_{Ndys}	unknown		[b] 8.4×10^7
$K^{a} = k_{Ndys}/k_{Nass}$	7.08×10^{-4}	k_7^{h}	4.6×10^8
k_1^{b}	1.34×10^1	k_8^{i}	2.8×10^4
k_{-1}^{b}	1.6×10^8	k_{-8}^{i}	1.12×10^6
k_2^{c}	2.2×10^4	k_9^{j}	2×10^9
k_3^{d}	1.1×10^9	k_{10}^{k}	$3.6/5.5 \times 10^6$
k_4^{e}	8.8×10^8	k_{11}^{l}	1.5×10^7
k_5^{f}	[fa] $(0.15 \div 1) \times 10^8$ [fb] 4.6×10^8	k_{12}^{m}	1.5×10^6
		k_{13}^{n}	1.2×10^9

[a] (SC-Database, 1997, 2000); [b] (Park and Lee, 1988); [c] (Davies and Kustin, 1969); [d] (Grätzel *et al.*, 1970); [e] (Maruthamuthu and Neta, 1978); [fa] (Loegager and Sehested, 1993a; Grätzel *et al.*, 1969); [fb] (Coddington *et al.*, 1999); [h] (Broszkiewicz, 1976); [i] (Shen and Rochelle, 1998); [j] (Neta and Huie, 1986); [k] (Alder *et al.*, 1986; Krakjic, 1970); [l] (Clifton *et al.*, 1988); [m] (Gogolev *et al.*, 1986); [n] (Daniels, 1969).

4.3 Chemical-kinetic simulations

- **MOSC experiments** *(manganese, oxygen, sulfite and isoprene)*

Basing on the mechanism described above, a corresponding set of ordinary differential equations was constructed and solved using a Mathematica 2.3 package (Rudziński *et al.*, 2009). Reversible reactions were treated kinetically, each one as a pair of independent reactions. Rate constants used for simulations were collected in Table 4.4 (Section 4.2). Constants, for which no experimental estimates were available, were adjusted using trial and error guesses.

The results of chemical-kinetic simulations have been presented in Rudziński *et al.* (2009), and are included in the thesis directly.
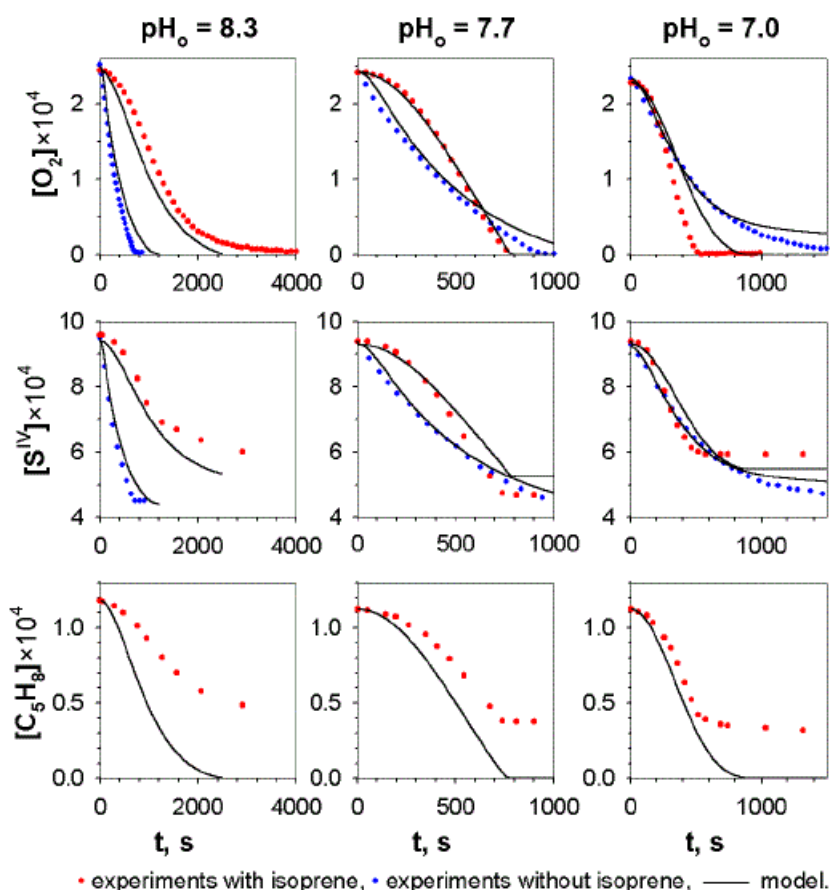
Fig. 4.18. *Chemical-kinetic simulation of temporal concentration profiles for experiments starting in basic and neutral solutions (pH_o ≥ 7).*
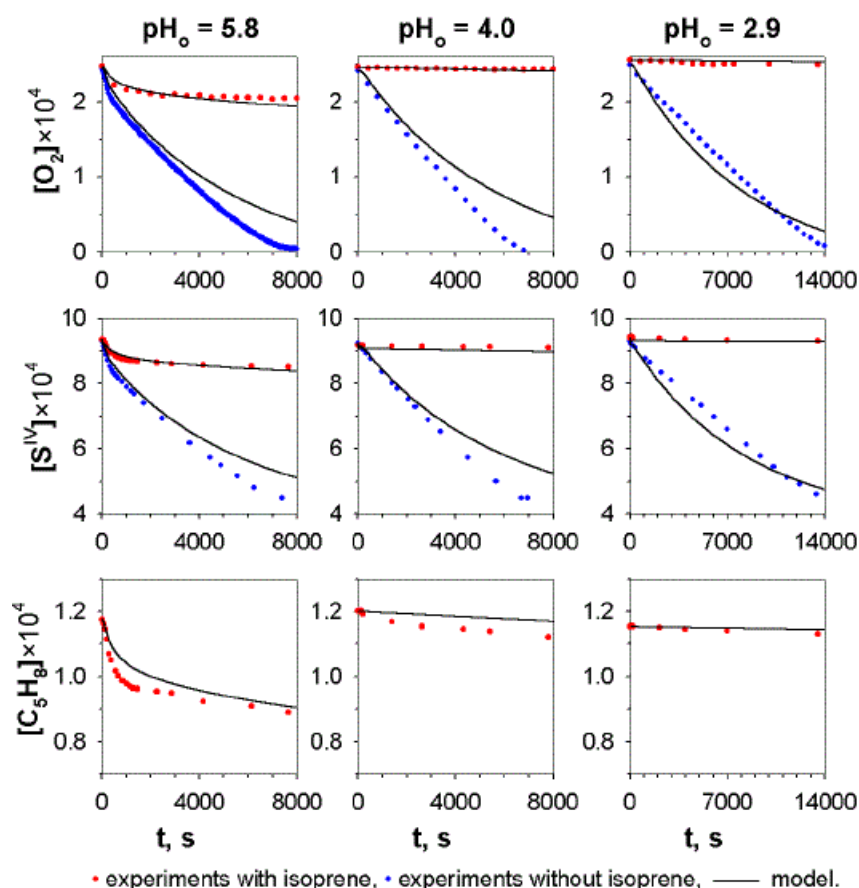
The results of simulation were compared to matching experiments in figures arranged according to the initial values pH of reacting mixtures. Time traces of reactant concentrations were shown in Figures 4.18 and 4.19, while changes of pH reacting solutions were shown in Figure 4.20. Generally, time traces of S(IV) and oxygen concentrations were reproduced with good accuracy at all acidities. Consumption of isoprene was simulated quite accurately in acidic solutions, but was overestimated in basic and neutral solutions. The simulation was still accurate qualitatively, reproducing the right shapes isoprene time traces from all experiments. The quantitative disagreement was explained by the deficiency of the mechanism used, which treated the primary nonradical products of isoprene degradation as nonreactive. Each of these products contained a double C–C bond, which could react with radicals in solutions to influence the overall inhibiting or accelerating action. In the present mechanism, "all the work" had to be done by isoprene, which consequently appeared to decay faster than in the experiments. The effect was more pronounced in basic and neutral solutions, because conversion of isoprene was higher than in acidic solutions. In addition, the mechanism would probably gain still more quantitative

flexibility, if included all primary nonradical products of isoprene transformation (see Chapter 4.4), not the four necessary representatives (Section 4.2.3). The ratio of simulated conversions of sulfite and oxygen was 2.0 in the absence of isoprene and 1.64 – 1.66 in the presence of isoprene, while the ratio of simulated conversions of isoprene and sulfite ranged from 0.28 to 0.31 (Table 4.6, right column). The calculated ratios agreed well with those determined experimentally (Table 4.6, left column). In the absence of isoprene all sulfite and bisulfite ions were converted into sulfate ions. Simulation showed that isoprene reduced this conversion by about 30%, as part of S(IV) species became the substituent groups in produced esters.

Table 4.6. *Experimental conversion ratios in transformation of isoprene coupled with S(IV) autoxidation.*

Initial pH	Experimental conversion ratios		Model conversion ratios	
	$\Delta[S(IV)]/\Delta[O_2]$	$\Delta[C_5H_8]/\Delta[S(IV)]$	$\Delta[S(IV)]/\Delta[O_2]$	$\Delta[C_5H_8]/\Delta[S(IV)]$
8.3	1.53	0.21	1.65	0.29
7.7	1.28	0.25	1.65	0.28
7.0	1.52	0.25	1.65	0.30
5.8	1.63	0.40	1.65	0.31
4.0	1.61[a]	1.21[a]	1.64	0.31

Fig. 4.19. *Chemical-kinetic simulation of temporal concentration profiles for experiments in acidic solutions (pH$_o$<7).*

The acidity of reacting mixtures was reproduced quite well, with the exception of experiments that started at pH$_o$ = 8.3 and included isoprene, in which the experimental acidity decreased, while the simulated acidity slightly increased. This disagreement could be explained by the ability of functional groups in isoprene derivatives to bind free protons from solutions, which had not been included the present mechanism. In acidic and basic solutions, the effect was masked by high yields of free protons released upon oxidation of HSO_3^- ions to SO_4^{2-}. It became visible in basic solutions, just because the initial reservoir of dissociable protons was smaller by orders of magnitude, while the extremely low initial concentration of free protons ($\sim 5\times10^{-9}$ M) was very sensitive to even small shifts in the protonation-deprotonation balance of species whose concentration was higher by three or four orders of magnitude. Thus, the prediction of hydrogen ion concentration in basic solutions should improve, if the protonation and deprotonation reactions of isoprene esters are added to the mechanism.
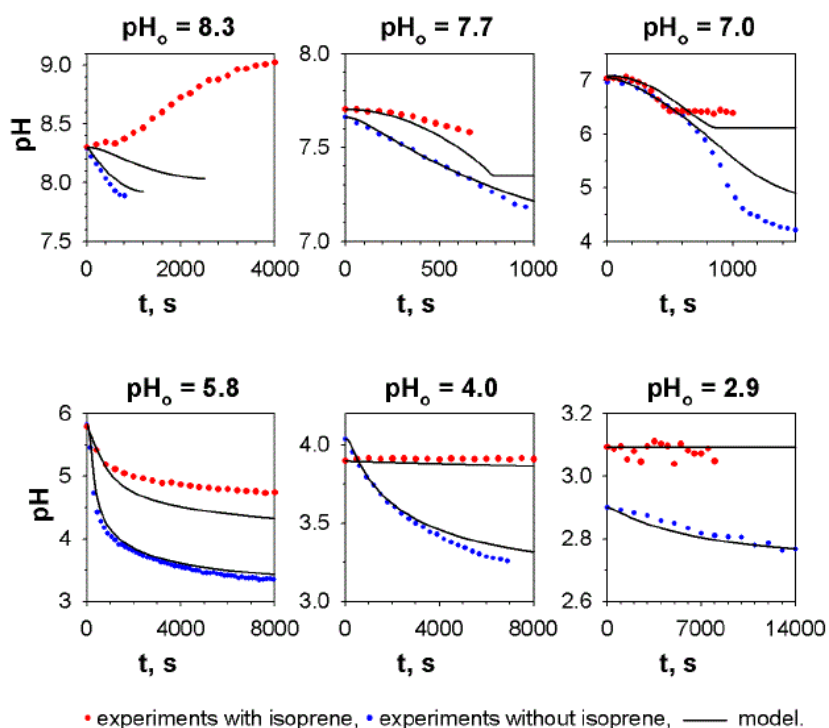
Fig. 4.20. *Chemical simulation of temporal pH profiles for experiments at all acidities.*

In summary, the results of simulation showed that the proposed mechanism of isoprene transformation during autoxidation of S(IV) was a reasonable approximation of the real-life chemistry in our experiments. The experimental and simulated data agreed very well qualitatively, and well quantitatively. The shapes of the concentration time traces, and the stoichiometry of transformation were reproduced accurately. The qualitative performance of the mechanism reflected its adequate structure. The quantitative performance can still improve within this structure, for instance if a better set of reaction rate constants is used. The working set of rate constants used for the presented simulation contained many constants, whose values were guessed by fitting, and should be replaced by values determined in future experiments. Further improvement is expected, if the mechanism is extended by adding the reactions indicated in this section. Despite the present limitations, the mechanism is ready for application in future studies.

- **MOSCN experiments** *(manganese, oxygen, sulfite, isoprene and nitrite)*

The simulation of MOSCN experiments using the proposed mechanism and the comparison of results thereof to experimental data presented in Section 4.1.2 are currently underway, so it has not been included in this work.

4.4 Molecular identification of products

As noted in the previous chapters, aqueous-phase transformations of isoprene coupled with autoxidation of S(IV) in the presence or absence of nitrite ions revealed the formation of chemical species of unknown structures. For all experiments, the concentration of S(IV) compound, i.e., sodium sulfite (Na_2SO_3) and sodium bisulfite ($Na_2S_2O_5$), manganese(II) sulfate ($MnSO_4$) and sodium nitrite ($NaNO_2$), as well as temperature remained unchanged. However, the amounts of dissolved oxygen in the aqueous phase were slightly different depending on the atmospheric pressure of the day when an experiment was started. Differences of the isoprene concentration could be explained by the fact that either not all isoprene was dissolved in the water solution or by it evaporation process that took place before the start of experiments. The only purposely altered parameter was acidity of reacting solution.

The analysis of UV spectra of reacting solutions showed that in all experiments isoprene decayed proportionally to the decay of sulfite. An interesting observation was made for the aqueous-phase isoprene transformation reaction coupled with the autoxidation of S(IV) in the absence of nitrite ions (NO_2^-) in neutral and slightly acidic solutions. A detailed interpretation of the UV spectra recorded on-line during the experiment run demonstrated interesting time profiles (Fig. 4.21a). It was noticed that during an experimental run a new absorption band at approximately 240 nm is growing in time (Fig. 4.21a, insert) at the expense of a decay of the reactant bands (Section 3.4.1.2) i.e., isoprene band ($\lambda_{max} = 235$ nm), bisulfite and sulfite ion bands ($\lambda_{max} < 210$ nm). For other experiments with isoprene, for instance at $pH_o = 5$, this phenomenon was practically unobserved (Fig. 4.21b).
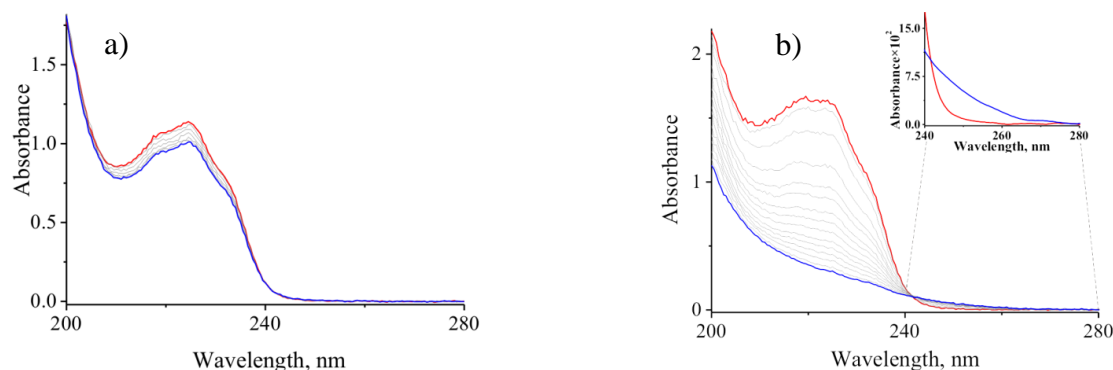
Fig. 4.21. *Raw UV spectra of a reacting solution at initial acidity: a)pH_o =5; b) pH_o =7. Red line is the first spectrum of the reaction solution, blue line is the last one.*

The difference between UV spectra of experiments at $pH_o = 5$ and 7 could be explained by the fact that the acidic pathway of isoprene transformation (involving HSO_3^-) is generally slower than the neutral one (involving SO_3^{2-}) (Chapter 4.1.1, MOS experiments). At $pH_o = 7$, the proportion of both ions is even, while at $pH_o = 5$, the HSO_3^- ions practically dominate, making the transformation of isoprene and formation of products extremely slow or practically hampered.
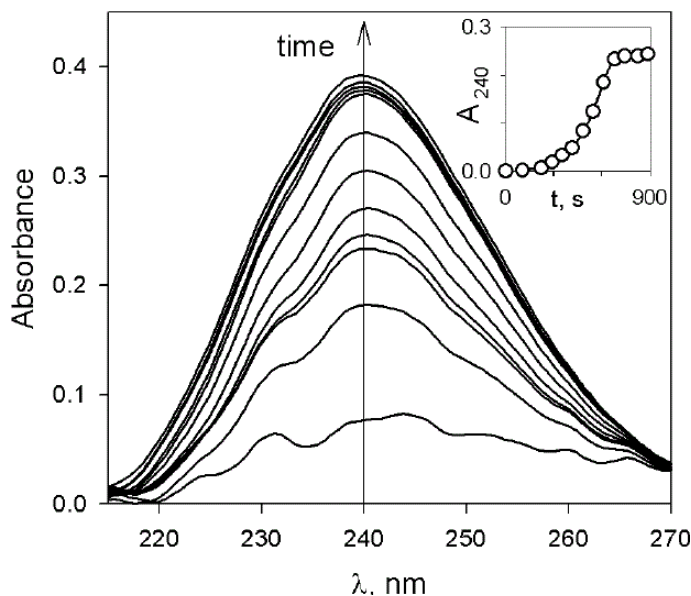
Fig. 4.22. *UV absorption spectra of products of isoprene transformation coupled with S(IV) autoxidation in an experiment starting at pH$_o$=7. Inset shows the time trace of absorbance at 240 nm.*

4.4.1 UV calculations

There is no a lot of structure information from UV-VIS spectra. Though, the Woodward-Fieser rules (Hesse *et al.*, 1997) permit to calculate approximate wavelength of absorption maximum of substances of known structure.

This method is described in Section 3.1.3.1. As basic structure it was taken unsaturated aldehyde with value 207 nm. Solvent correction for water has +8 nm. Methyl group in α position brings 10 nm, in β − 12 nm. The influence of sulfate or sulfite groups on UV absorption under 200 nm is negligible.
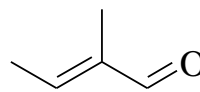
So, maximum of absorption of the unsaturated aldehydes 3-methylbut-2-enal (Scheme 4.2) is at 240 nm and 238 nm for 2-methylbut-2-enal, according to equation below:

$$\lambda_{max} = 207 + 2 \times 12 + 8 = 240 \text{ nm} \qquad \lambda_{max} = 207 + 12 + 10 + 8 = 238 \text{ nm}$$
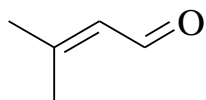
3-methylbut-2-enal   2-methylbut-2-enal

Scheme 4.2. *Structures of unsaturated aldehydes, which maximum of absorption were calculated utilizing increment method.*

The increment method gives a tentative hint that some of investigated products could have an unsaturated aldehyde carbon frame in their structure. It could be assumed that UV spectra (Fig. 4.22) indicate these compounds with sulfate or sulfite substituents, which influence on the UV absorption above 200 nm is likely negligible. Unfortunately, there is no option to calculate absorption maximum of compounds with hydroxyl group (other possible products (Section 4.2, MOSC experiments)) instead carbonyl using this method. These compounds would not absorb the UV light between 200 and 300 nm, and, if present, were invisible to our absorbance measurements.

## 4.4.2 Mass spectrometric characterization of post-reaction solution

In order to identify the molecular structure of unknown products, a representative experiment was performed under conditions showed in Table 4.7. During the experiment, the isoprene transformations at $pH_o = 7$ with sulfoxy radicals were carried out in the absence of nitrite ions. In order to gain insight into the chemical signature of the products, all post-reaction solutions were analyzed using triple quadruple mass spectrometry with electrospray ionization in the negative ion mode.

Table 4.7. *The conditions for the representative experiments.*

| [Mn]/ mol dm^{-3}	[O$_2$]/ mol dm^{-3}	[S(IV)]/ mol dm^{-3}	[C$_5$H$_8$]/ mol dm^{-3}	T/ °C	pH
1×10^{-5}	2.5×10^{-4}	7.8×10^{-4}	8×10^{-5}	25	7

The structural analyses were accomplished based on the careful examination of the time profiles of electrospray mass spectra as well as a series of Collision Induced Dissociation (CID) experiments.

It was observed that a profile of the electrospray mass spectrum before the addition of catalyst ions (Mn^{2+}) and upon its addition to the reaction solution reveals a striking deference.
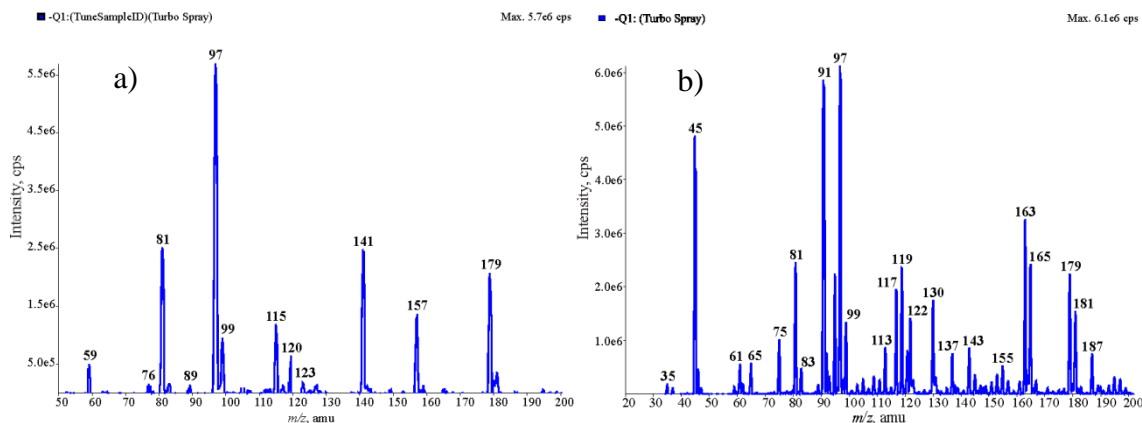
Fig. 4.23. *(−) Electrospray (ESI) first order mass spectra recorded for aqueous aliquots taken a) prior to the addition of manganese(II) ions; b) upon the completion of the reaction.*

In the upper *m/z* value range in the ESI mass spectrum of post-reaction solution (Fig.4.23b), a set of 4 peaks at *m/z* 163, 165, 179, and 181 are on display. These peaks are representative for the post reaction mixture as their presence was observed anytime when the reaction was repeated. It should be stressed that the appearance of these ions are not likely to be artifacts of the applied mass spectrometry technique (which is mostly the case of direct infusion mode) but are real signals corresponding to the presence of novel species formed during the reaction course. In order to clarify this hypothesis, the reaction mixture was subjected to mass spectrometry analysis with a prior liquid chromatography separation. The separation was performed on the T3 reversed phase HPLC column (Waters) using acetonitrile (B) – 0.1% acetic acid in water (A) solvent system based on the recent literature approaches (Gómez-González *et al.*, 2008). The following gradient system was applied: 5% B 3 min – 95% B 15 min – 95% B 3 min – 5% B 3 min. The HPLC/MS analysis revealed the presence of the discussed species with the MW 164, 166, 180, and 182 compounds that prevailed using the extracted current ion chromatogram method (Fig. 4.24).
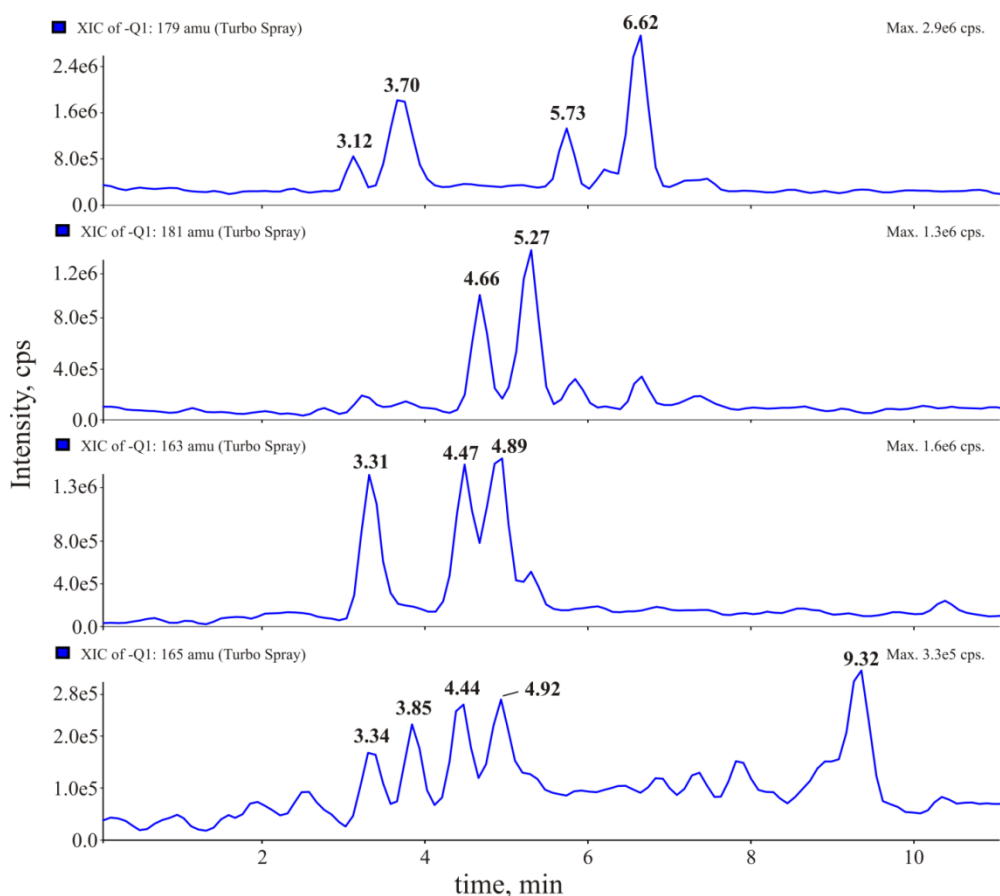
Fig. 4.24. *Extracted ion chromatogram obtained for m/z 179, 181, 163, 165 ions.*

The comparison of mass spectra prior to and upon reaction (Fig. 4.23a and b) shows also some similarities with a common peak at *m/z* 179 on display. In the first approach, it would suggest that the MW 180 compound is being formed at the beginning of the reaction or alternatively comes from the unidentified impurity of the starting material. The mass spectrometry of the initial species revealed no *m/z* 179 ion. In addition, a detailed molecular signature providing by a MS/MS analysis revealed that the molecular structures of the *m/z* 179 ions before and after reaction are completely different (Fig. 4.25a, b). In this context they are isobaric by mass-to-charge but distinct in terms of the structure.
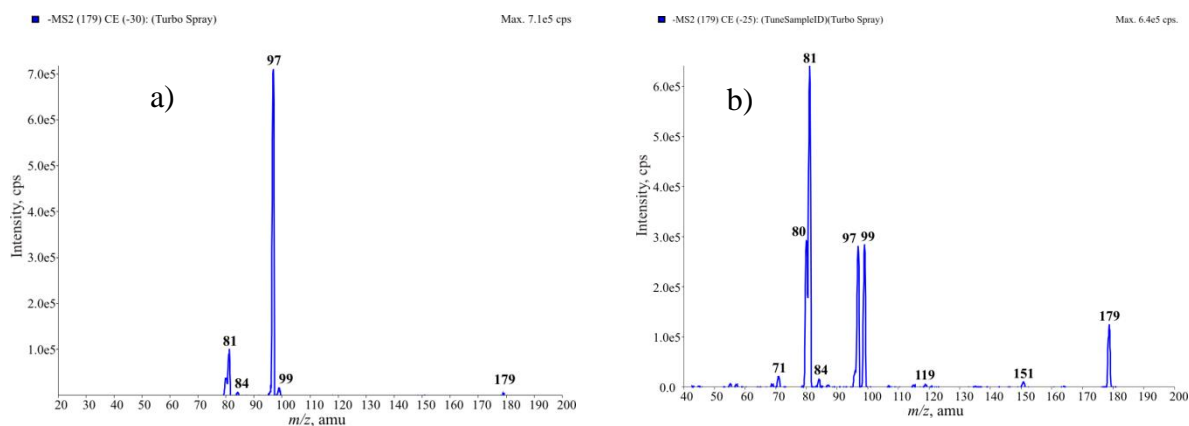
Fig. 4.25. *Collision induced dissociation electrospray mass spectra recorder for the m/z 179 ion observed in the first order ESI spectra a) prior to the addition of manganese(II) ions; b) upon the completion of the reaction.*

The rational explanation of the origin of the *m/z* 179 ion in the ESI spectrum of a prior reaction solution (Fig. 4.23a and Fig. 4.25a) is the formation of the $[HSO_4 + H_2SO_3]^-$ cluster in the ionization chamber during the electrospraying process. This cluster ion undergoes a characteristic fragmentation in the Q2 of a triple quadruple mass spectrometer at the collision energy of 30 eV giving rise to bisulfate anion (*m/z* 97) (Scheme 4.3).

$$[HSO_4 + H_2SO_3]^- \rightarrow HSO_4^- + H_2SO_3$$
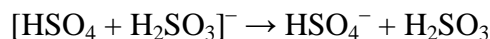
Scheme 4.3. *The plausible fragmentation pathway of the [HSO_4 + H_2SO_3]^- cluster (m/z 179).*

In contrast the *m/z* 179 ion follows a different fragmentation. A detailed discussion on the structural characterization for the MW 180 and other novel reaction products is provided in next chapters.

## 4.4.2.1 Structural identification for *m/z* 179

The first order ESI mass spectrum for the post-reaction solution displays the *m/z* 179 ion in the negative ion mode. Interestingly, there are no protonated, i.e., MH+ (*m/z* 181) or sodiated, i.e., MNa$^+$ (*m/z* 203) signals corresponding to the unknown compound in the ESI mass spectrum recorded in the positive ion mode. Thus, it can be inferred that the molecular weight (MW) of the unknown is 180 and the compound exhibits a highly polar acidic property. In order to provide more data regarding the most likely structure(s) for the *m/z* 179 ion, a series of CID experiments were conducted at optimized collision energy in the Q2 zone of a triple quadruple mass spectrometer. A broad collected data allows elucidating the most possible molecular structure for

the MW 180 compound along with its typical gas-phase fragmentation processes. This data are displayed in Scheme 4.4.
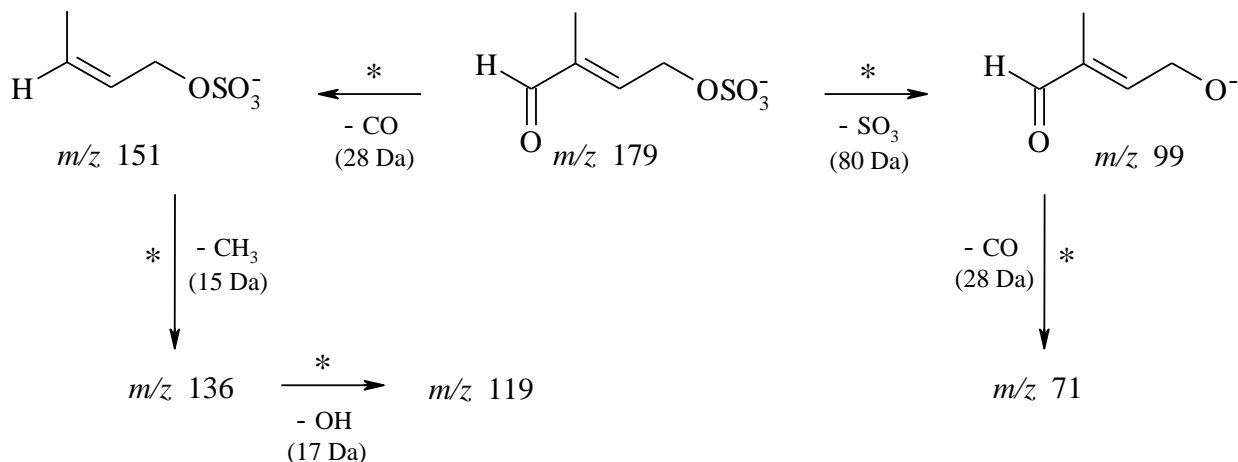
Scheme 4.4 *The representative fragmentation pathways for the MW 180 compound. Each fragmentation reaction confirmed by CID experiment was noted with asterisk.*

Induced dissociation mass spectrum at collision energy of 30 eV shows several daughter ion peaks with the most characteristic ones at the *m/z* 151 and 99 (Fig. 4.26).
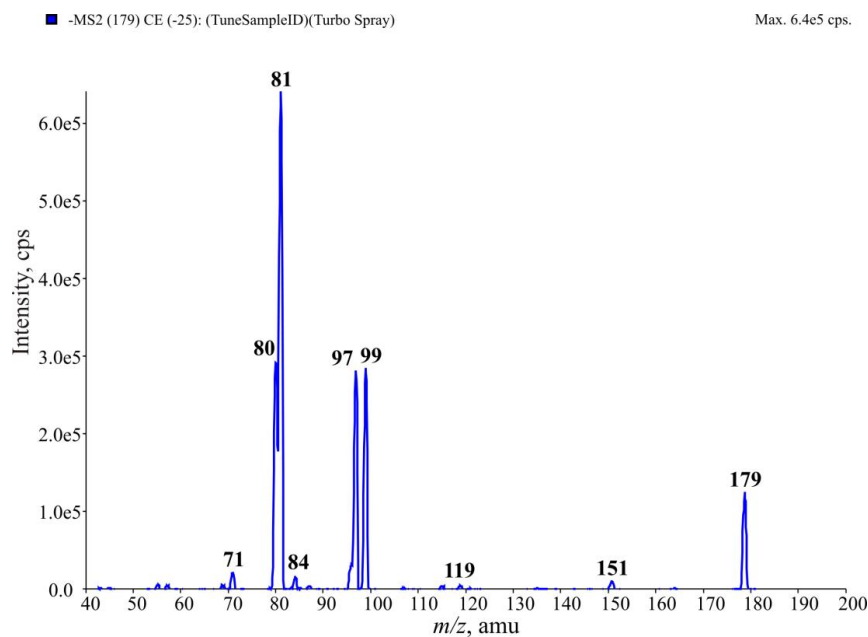
Fig. 4.26. *Collision induced dissociation ESI mass spectrum recorded for the parent m/z 179 ion at a collision level of 30 eV.*

The transition 179 → 151 points to the presence of a carbonyl moiety in the molecular skeleton. This is in agreement with a typical fragmentation for carbonyl compounds such as

aldehydes or ketones (Schurath *et al.*, 2003). Interestingly, the presence of an aldehyde residue was confirmed by the proton magnetic resonance spectrum recorded for the ether extract of the post-reaction solution. In the ^{1}H NMR spectrum recorded in CD$_3$CN (Fig. 4.27), one could observe a doublet situated in the higher delta scale region (CD$_3$CN; 300 MHz, d, 9.9768 ppm, [3]J = 7.94 Hz) with a coupling constant value typical of unsaturated aldehydes (Mazurkiewicz *et al.*, 1995; Attygalle *et al.*, 2001). The NMR spectrum displays in a close proximity an addition doublet signal. This observation could be rationalized taking into account the fact that aqueous-phase reaction of isoprene with sulfate radical-anions may result in the formation of a number of isomeric structures, some of which are presented in Scheme 4.5. It cannot be ruled out that the appearance of the additional doublets in the ^{1}H NMR spectrum of the ether extract solution arise from the presence of a chemically different family of the MW 164 products that are formed in the discussed experiments (Chapter 4.4.2.2).
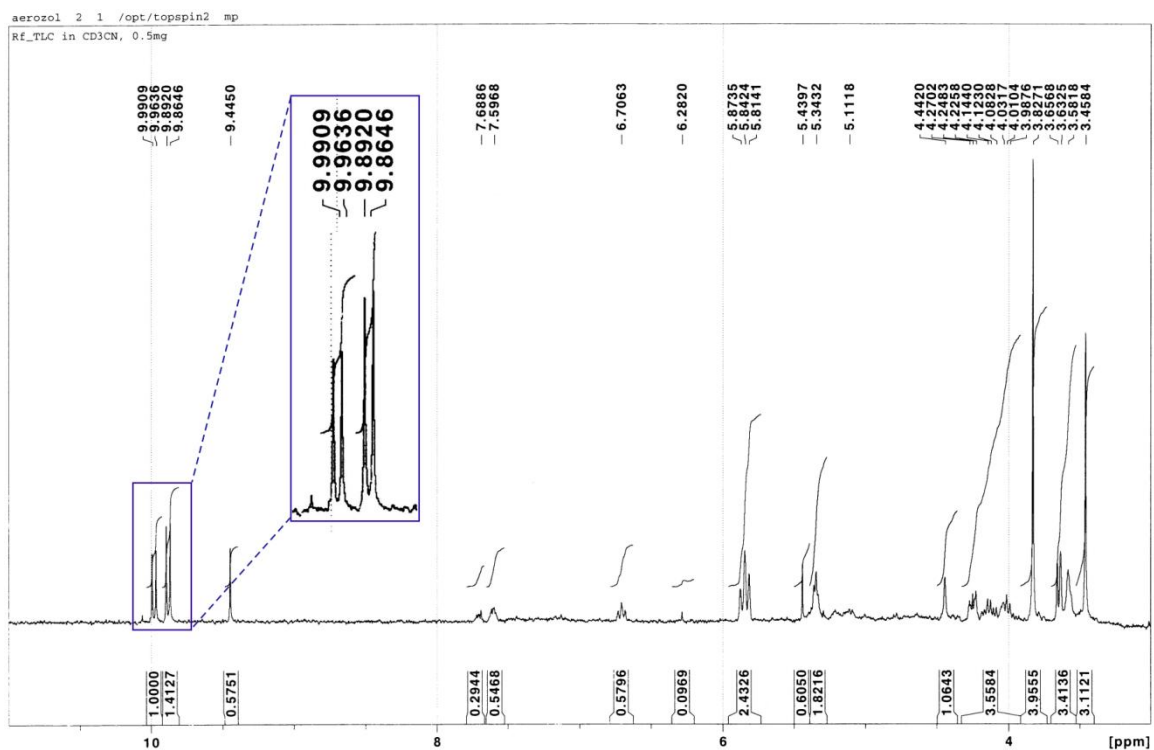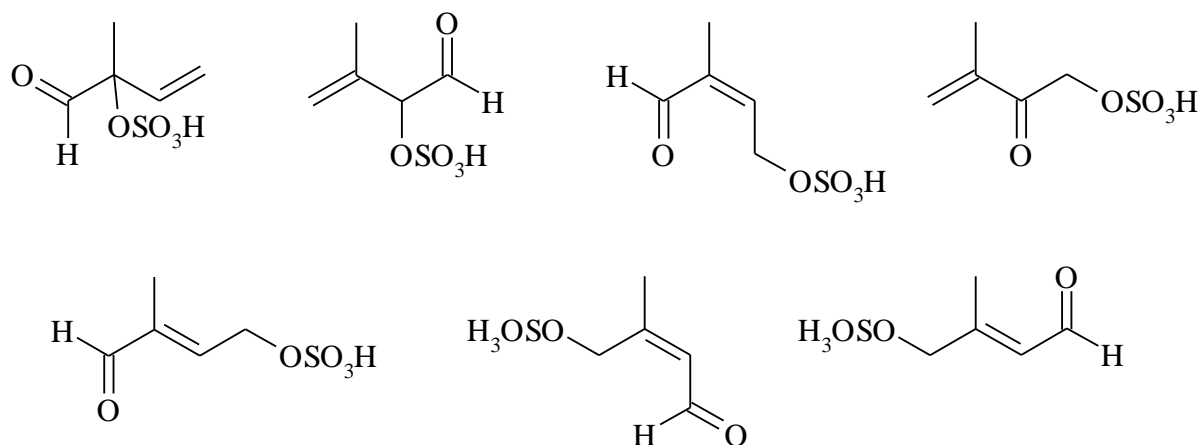

Fig. 4.27. *^{1}H NMR spectrum recorded for an ether extract of the post-reaction solution in deuterated acetonitrile.*

**Scheme 4.5.** *Possible positional isomers for the MW 180 compound.*

The 179 → 99 transition proved by the 30 eV CID mass spectrum (Fig. 4.26) provides a strong molecular signature for the presence of the C–O–SO$_3$H moiety. More specifically, the available literature documentation based on the organic mass spectrometry studies with deuterium labeling techniques (Attygalle *et al.*, 2001; Gómez-González *et al.*, 2008) shows that one of typical fragmentation channels for organosulfates is the 80 Da neutral loss, which corresponds to the SO$_3$ elimination. Taking this into consideration we can hypothesize that the MW 180 compound that forms in the course of studied reaction must bear a sulfate ester moiety. Thus, the formation of the *m/z* 99 daughter ion is likely to occur via a charge-directed heterolytic O–C bond cleavage (Scheme 4.6).
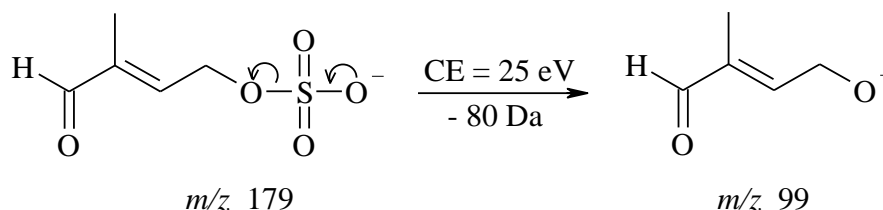
**Scheme 4.6** *The possible fragmentation pathway of the MW 180 compound.*

4.4.2.2 Structural identification for *m/z* 163

Another characteristic ion that is presented in the first order (−)ESI-MS spectrum for the post-reaction solution is the ion at *m/z* 163. Figure 4.28 shows its negative-ion CID spectrum acquired at the collision energy 25 eV with a prominent *m/z* 80 product ion.
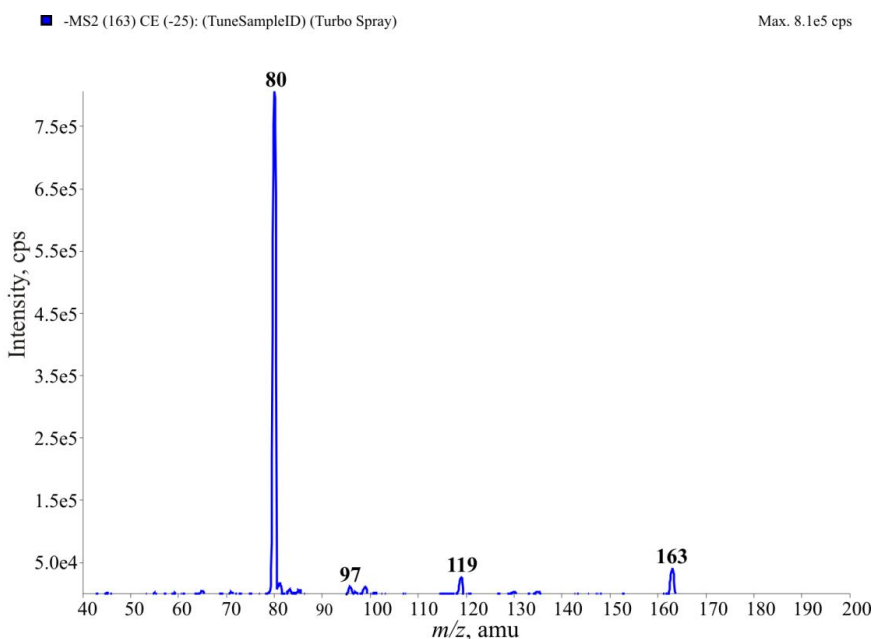
Fig. 4.28. *CID ESI mass spectrum recorded for the parent m/z 163 ion at a collision level of 25 eV.*

Accurate mass data recorded for the *m/z* 163 ion showed a formula of $C_5H_7O_4S$ with an error less than 9 ppm. These results points to the isoprene retained structure of the ion with a higher oxygenated state, in which it's likely to assume that two hydrogen atoms are formally replaced by SO_4H atom group. Taking into account the possible combination of these atoms, we hypothesize the presence of the $O–SO_2$ bond system in the isoprene derived molecular core. The most possible isomeric structures for the ion *m/z* 163 are displayed in Scheme 4.7.
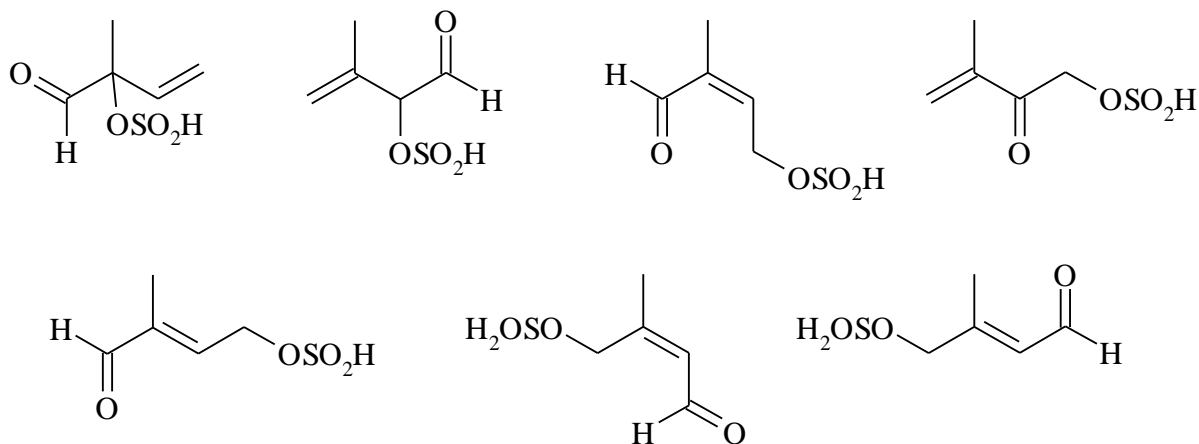
Scheme 4.7. *Possible positional isomers for the MW 164 compound.*

Regardless of the subtle differences in the molecular core of the isomers, the major fragmentation reaction for the *m/z* 163 ion, i.e. the transition 163 → 80, displayed in the CID mass spectrum (Fig. 4.28) could be rationalized by charge-induced homolytic C–O bond cleavage

as shown in Scheme 4.8. A driving force of this fragmentation reaction is the formation of a resonance-stabilized allyl radical intermediate.
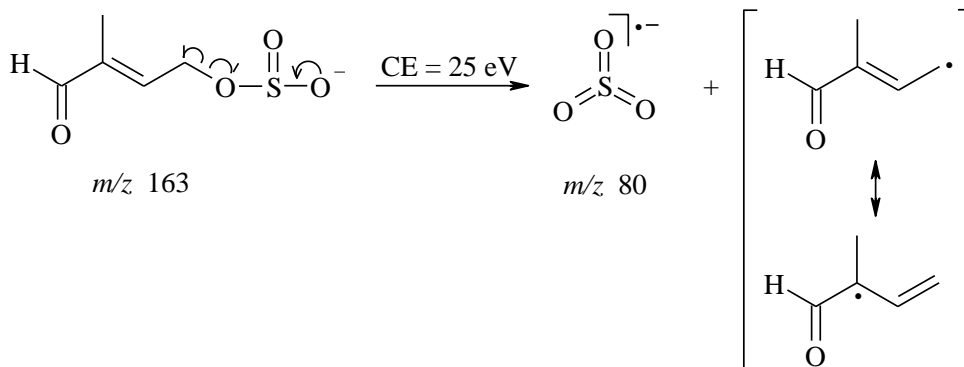
Scheme 4.8. *The possible fragmentation pathway of the MW 164 compound.*

A literature survey on the mass spectrometry behavior of organosulfite monoesters, in particular in reference to atmospheric ionization techniques, reveals a considerable lack of data. Following available literature data on the chemistry of organosulfite monoesters in the condense phase it should be stressed that in contrast to the organosulfate monoesters (March, 1992) or organosulfite diesters (Günther *et al.*, 1998), organosulfite monoesters are susceptible to spontaneous hydrolysis under acidic and alkaline conditions (van Woerden, 1963; Tillett, 1976). The very good leaving group ability of the $R–OSO_2–$ residue makes organosulfite diesters reactive species towards nucleophilic agents (Liebman *et al.*, 1999). These features would explain the absence of the corresponding signal in the total ion chromatogram obtained during LC/MS analysis for the post-reaction aliquots. It is evident that the MW 164 species undergoes a facile hydrolysis while traveling through a LC column in the eluent mixture containing 0.1% aqueous acetic acid as a buffer. However, a rapid mass spectrometry analysis using a direct infusion revealed the existence of the MW 164 compound in the aqueous reaction solution. This fact could be rationalized by a quick time analysis and the lack of contact between reaction solution and acidic column particles.

4.4.2.3 Structural identification for *m/z* 165

A wealth of structural information for the *m/z* 165 ion could be learned from the MS/MS as well as MS[3] mass spectra obtained for relevant MS/MS daughter ions. Figure 4.29 depicts the MS/MS fragmentation spectrum recorded at the collision energy of 25 eV.

Fig. 4.29. *ESI-MS/MS spectrum recorded for the parent m/z 165 ion at a collision level of 25 eV.*

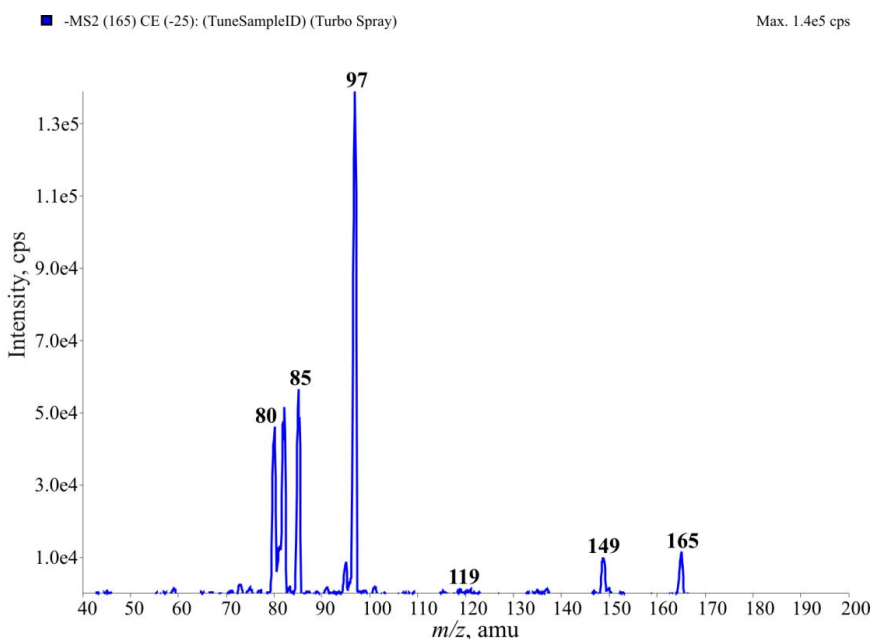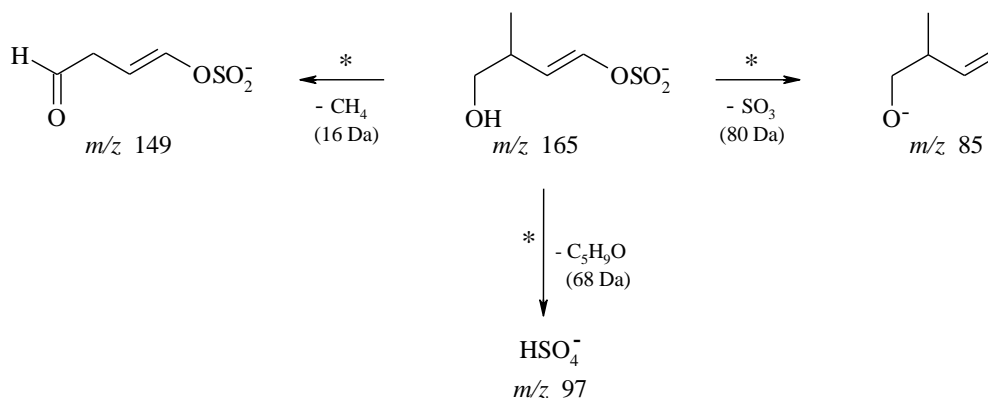As proved by MS/MS spectrum (Fig. 4.29), three fragmentation reactions for ion at m/z 165 at the collision energy of 25 eV are characteristic: a neutral loss of methane (16 Da), a neutral loss of SO_3 and the elimination of bisulfate ion (m/z 97). The proposed reaction channels are summarized in Scheme 4.9.

Scheme 4.9. *The representative fragmentation pathways for the MW 166 compound. Each fragmentation reaction confirmed by CID experiment was noted with asterisk.*

The transition 165 → 149 is highly interested as involves a cleavage of an even number of bonds and thus cannot be explained by a simple manner. Based on the theory of mass spectrometry fragmentations (McLafferty and Turecek, 1993; Longevialle, 1992) it can be proposed that the reaction may proceed via an anion-neutral complex (ANC) and involve the formation of the short-living CH_3 anion and six-membered disulfinic ester (Scheme 4.10). Once

formed, the CH_3 anion may abstract the acidic proton from the OH group within the ANC complex giving rise to the stable intermediate anion.
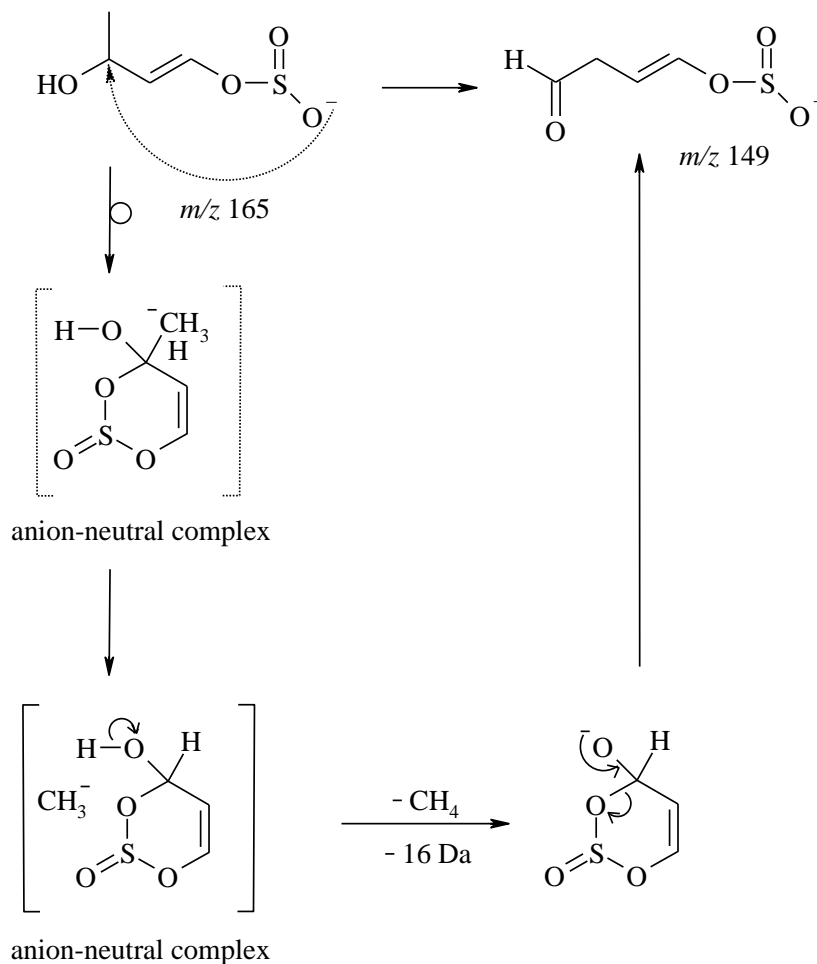
Scheme 4.10. *Plausible fragmentation pathways leading to the elimination of methane from the quasi-molecular ion of the MW 166 product.*

As mentioned above, the MW 166 product can also be formed in a "cocktail" of several isomers owing to a number of possible additions of SO_3 radical ions to a conjugated isoprene backbone. The relevant structural isomers are shown in Scheme 4.11.
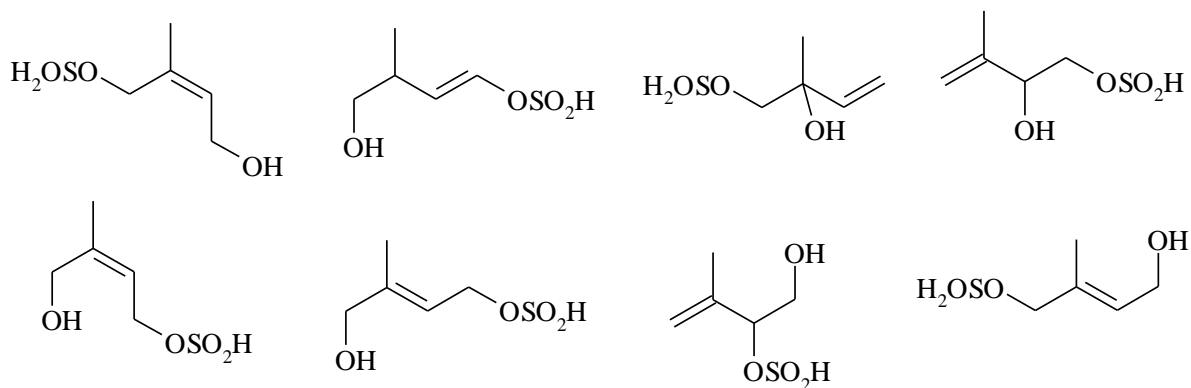
Scheme 4.11. *Possible positional isomers for the MW 166 compound.*

Taking into account the diversity of isobaric structures, the formation of *m/z* 85 can be easy explained by a homolytic C–O bond rupture through a charge remote fragmentation pathway (Scheme 4.12).

$$m/z \ 165 \qquad\qquad m/z \ 85$$
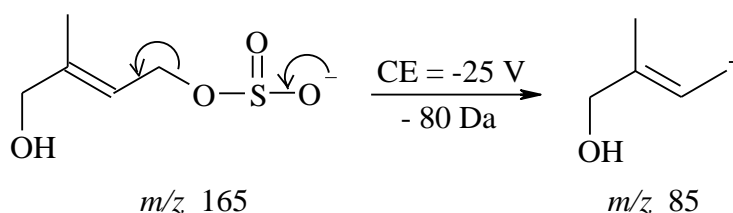
Scheme 4.12. *Elimination of the neutral SO₃ fragment from the quasi-molecular ion of the MW 166 product leading to the resonance-stabilized carbanion at m/z 85.*

4.4.2.4 Structural identification for *m/z* 181

The last one ion that was revealed at first-order ESI mass spectrum of post-reaction solution in negative mode is *m/z* 181. As all other product molecules, this ion has acidity property with absence of peaks corresponding to protonated, i.e., MH^+ (*m/z* 183) or sodiated, i.e., MNa^+ (*m/z* 205) signals in positive mode of ESI mass spectrometer. The typical fragmentation channels of ion at *m/z* 181(Scheme 4.13) are include SO_3 and HSO_4^- elimination.
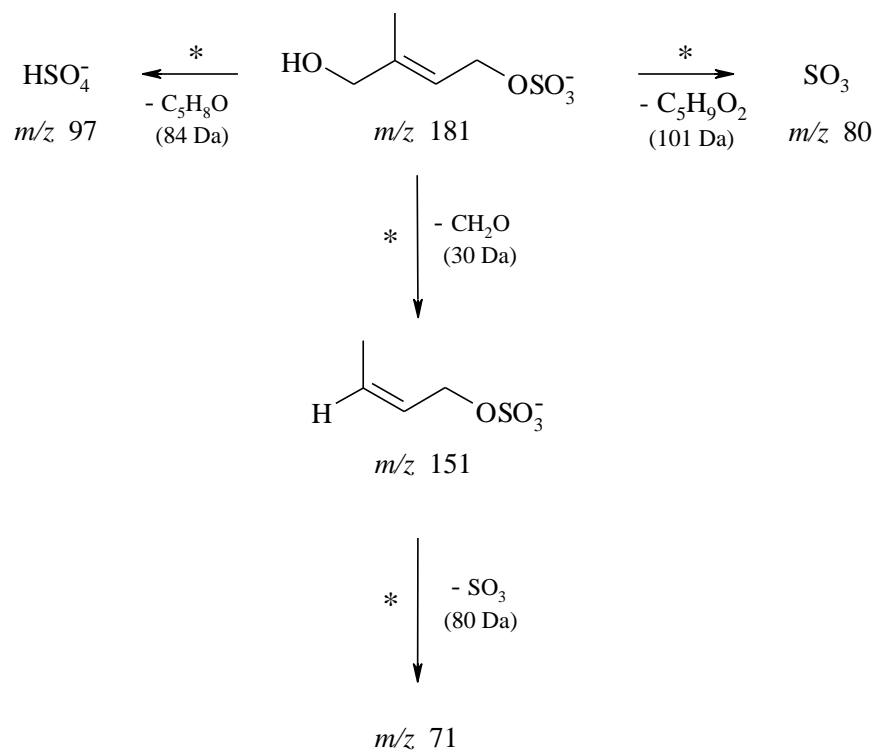
Scheme 4.13. *The representative fragmentation pathways for the MW 182 compound. Each fragmentation reaction confirmed by CID experiment was noted with asterisk.*
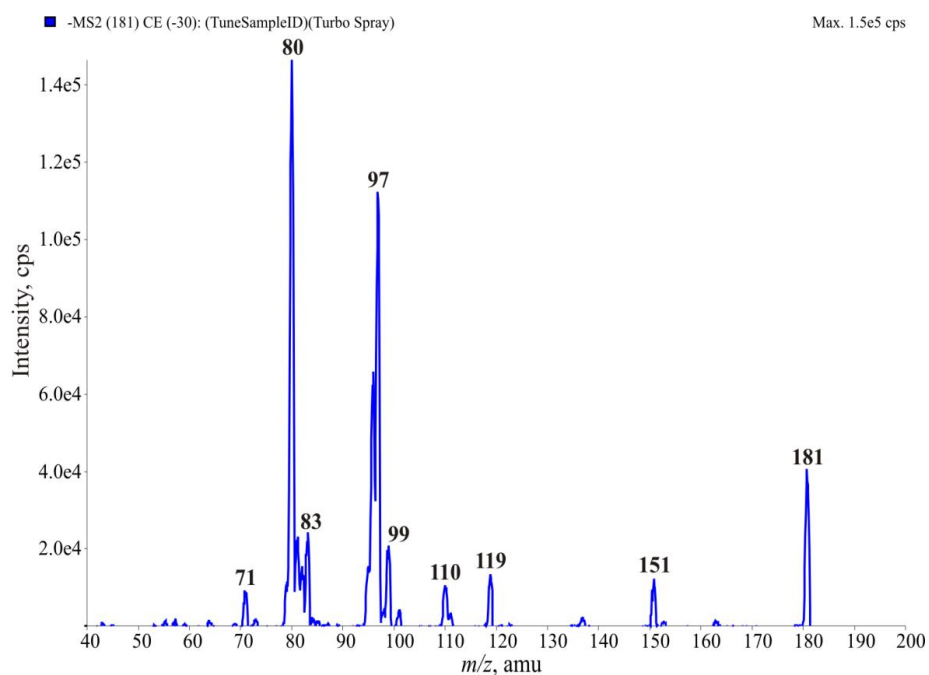
Fig. 4.30. *ESI-MS/MS spectrum recorded for the parent m/z 181 ion at a collision level of 25 eV.*

The 181 → 151 transition provides (Fig. 4.30) a strong molecular signature for the presence of the hydroxyl groups in structure of molecule. This consideration is in a good agreement with the general fragmentation mechanism for even electron ions (Ham, 2008).

The 181 → 97 transition points (Fig. 4.30) to the presence of the sulfate moiety in the structure of molecule. This consideration is in a good agreement with fragmentation behavior data of organosulfate showed by Attygalle *et al.*, (2001) where one of the commonly observed fragmentation reaction is a formation of bisulfate anion (HSO_4^-). Moreover, there are requirements of the proton presence in the β position and ability of formation double bound between C-1 and C-2. Thus, only some of possible positional isomers (Scheme 4.14) are undergone this type of fragmentation. For isomers of MW 166 compound, which form non-resonance-stabilized radicals during bisulfate (HSO_4^-) elimination, loss of SO_3 is a most frequent fragmentation channel.

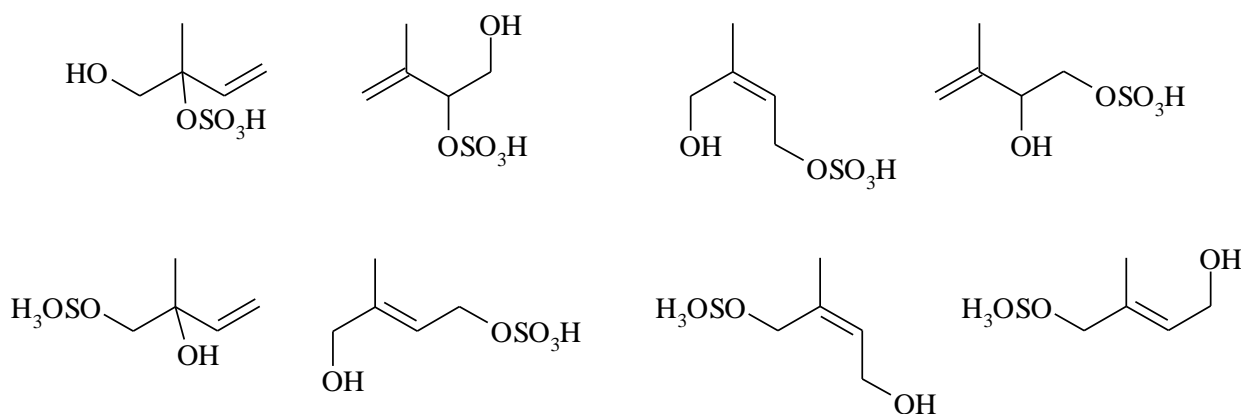**Scheme 4.14.** *Possible positional isomers for the MW 182 compound.*

In order to support the proposed structure of products of the isoprene reaction with sulfoxy radical-anions, the reference compounds should be synthesized. Literature review on synthesis of compounds with structures that are similar to structures of the products showed lack of data.

The synthesis of compound with structure similar to MW 182 (*m/z* 181) was worked out (Section 3.4.5). It comprised two stages: reduction of dimethyl citraconate to appropriative 2-methylbut-2-ene-1,4-diol and its further sulfation (Scheme 4.15). The ratio of sulfate agent to diol was taken 1:1 for the purpose to obtain monoesters and eliminate diesters as probable. Because of asymmetric structure of the diol, there are two possible isomers of the organosulfate with the same molecular weight but different position of the ester group in the post-synthesis mixture.
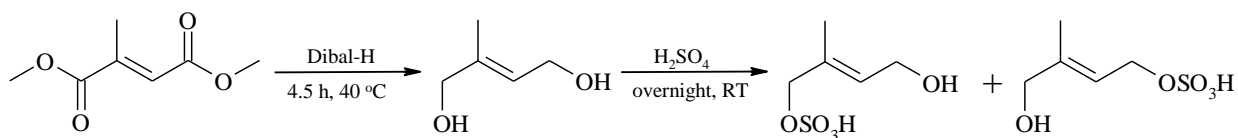
Scheme 4.15. *Formation of the reference mixture containing of isobaric molecular core of MW 182 compound*.

Confirmation of the structure of MW 182 arises from comparison of fragmentation behavior of reference and investigated compounds during CID experiments in the same conditions (Fig. 4.31.).
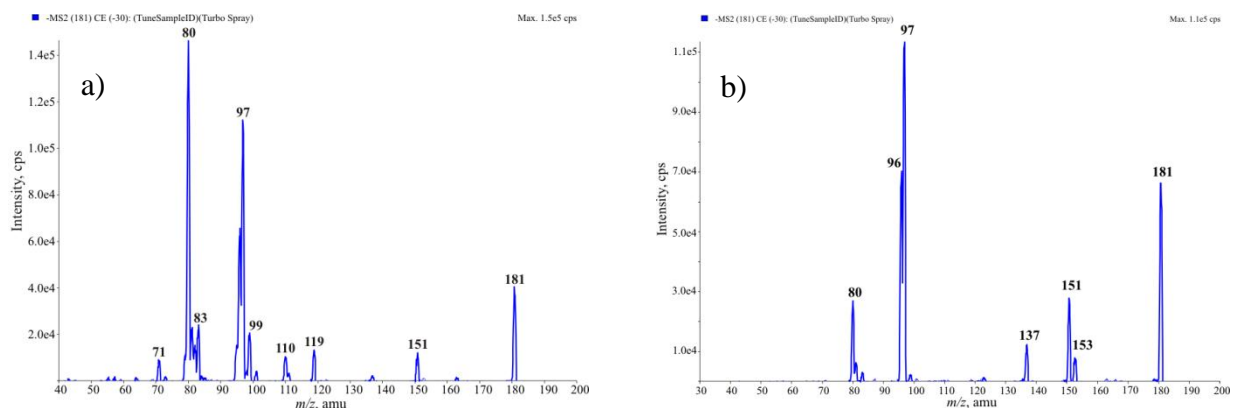
Fig. 4.31. *(−)ESI MS/MS spectra of m/z 181 ion: a) from the post-reaction solution; b) of the synthesized compound.*

The fragmentation behavior of both *m/z* 181 ions is practically similar regard to the formation of *m/z* 151, 97, 96, and 80 ions − products of the main fragmentation reactions of MW 182 compound. The insignificant differences on these CID spectra are resulted from the fact that organosulfate formed during the investigation reaction and synthesis of the reference compound could be positional isomers with distinguishing fragmentation behaviors.

Organosulfite were impossible synthesized because of lack of sulfite agent. While, there is no information about synthesis of organoesters with aldehyde groups at all.

4.4.3 Sulfonates and organosulfates – mechanistic insights

Sulfite trioxide radical-anion has a radical center situated either on oxygen atom or on sulfur atom.
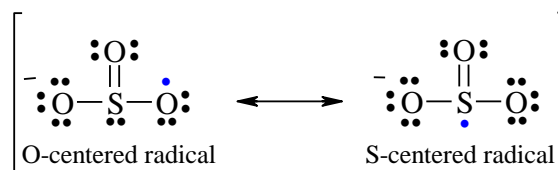
Scheme 4.16. *Mezomeric forms of SO₃ radical-anion.*

Therefore, the addition of $SO_3^{\bullet-}$ radicals to double bonds in organic compounds can result in two types of products – organosulfite or sulfonates (Scheme 4.16).
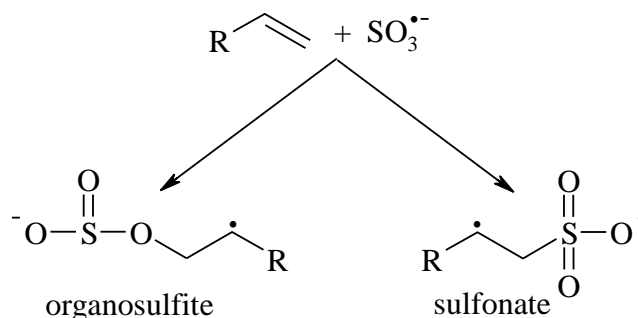
Scheme 4.16. *Addition via O and S atom.*

To verify whether the investigated products MW 164 (4-*O*-sulfinyl-3-methylbut-2-enal) and MW 166 (1-*O*-sulfinyl-4-hydrox-2-methylbut-2-ene) were organoesters (C–O–S bond) or sulfonates (C–S bond), the simplest reference compounds were synthesized by methods described in Chapter 3.4.5 that contained double bonds in β positions (Scheme 4.17).

Mono-prop-2-ene-1-yl sulfate (3) and mono(phenylmethyl) sulfate (4) are organosulfate monoesters assumed to undergo similar fragmentation as organosulfite monoesters which were not synthesized because of their instability in aqueous solution.

Electrospray mass spectra of sodium prop-2-ene sulfonate (1), sodium phenyl-methanesulfonate (2), mono-prop-2-ene-1-yl sulfate (3) and mono(phenylmethyl) sulfate (4) were obtained in the negative mode. The ESI fragmentation mechanisms were studied in details based on product ion mass spectra of selected ions at different collision energy levels. The structures of these compounds are shown in Scheme 4.17.
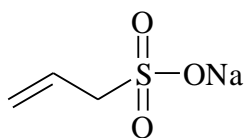
Sodium prop-2-ene sulfonate (1)

MW 144; *m/z* 121
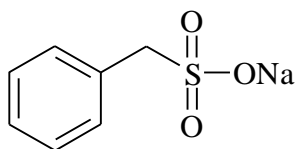
Sodium phenyl-methane sulfonate (2)

MW 194; *m/z* 171
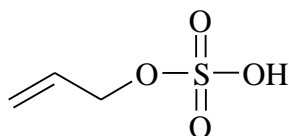
Mono-prop-2-ene-1-yl sulfate (3)

MW 138; *m/z* 137
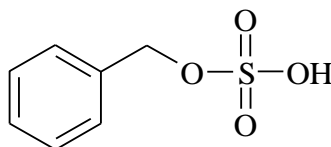
Mono(phenylmethyl) sulfate (4)

MW 188; *m/z* 187

Scheme 4.17. *Structures of synthesized reference compounds.*

MS/MS spectra (Fig.4.23) for sulfonates 1, 2 are similar; however, visible differences appear when compared to analogues spectra recorded for sulfates 3, 4.
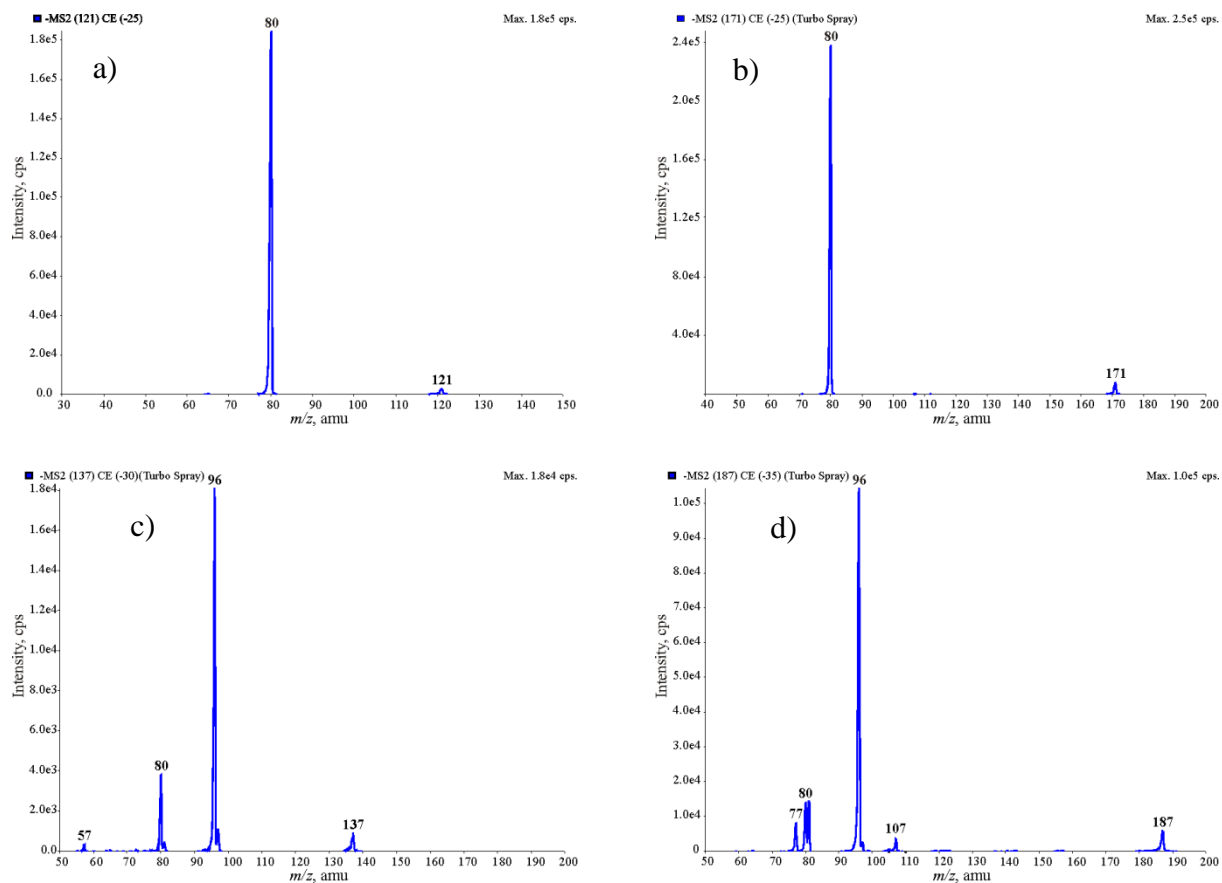
Fig. 4.32. *(−)ESI-MS/MS spectra of: a) allyl sulfonate (m/z 121); b) benzyl sulfonate (m/z 171); allyl sulfate (m/z 137); d) benzyl sulfate (m/z 187).*

The common fragmentation reactions at the collision energy 25 eV observed for *pseudo*-molecular ions of sodium prop-2-ene sulfonate (1), sodium phenyl-methanesulfonate (2) are losses of allyl and benzyl radical, respectively (Scheme 4.18). It can be accounted for a charge remote fragmentation induced homolytic C–S bond cleavage.
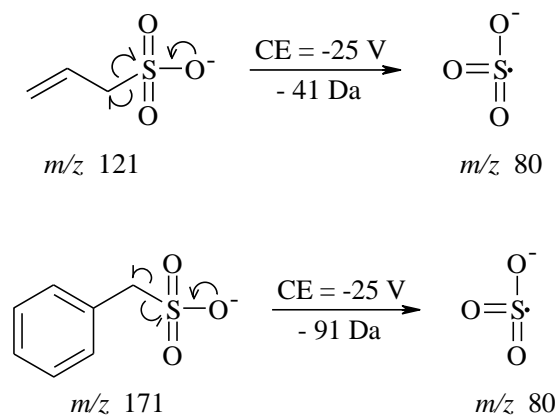
Scheme 4.18. *Elimination of the SO_3 radical-anion from the m/z 121 and 171 ion which correspond to sulfonates.*

In both cases the formation of highly stable radical ion corresponding to sulfur trioxide is observed.

In contrast, gas-phase reactions of *pseudo*-molecular anions of mono-prop-2-ene-1-yl sulfate (3) and mono(phenylmethyl) sulfate (4) proceed via homolytic C–O bond cleavage that lead to the formation of the stable *m/z* 96 radical anion. Its plausible structures and the way of its formation are depicted in Scheme 4.19.
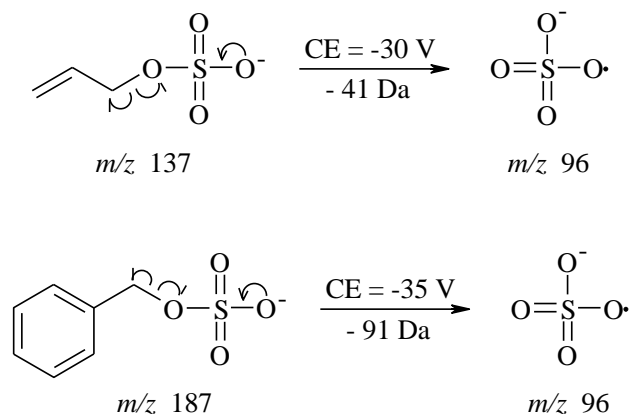
Scheme 4.19. *Elimination of SO_4 radical-anion from m/z 187 and 137 ions which indicate organosulfate.*

It should be noted that other competitive fragmentation channels for 3 and 4 are observed (Scheme 4.20). Their common feature is a rapture of the O–S bond. Provided that this bond is

cleavage homogeneously, the stable *m/z* 80 radical anion of sulfur trioxide is formed. However, when the bond breaks heterogeneously, the *m/z* 57 anion is formed and its structure corresponds to the anion of allyl alcohol.
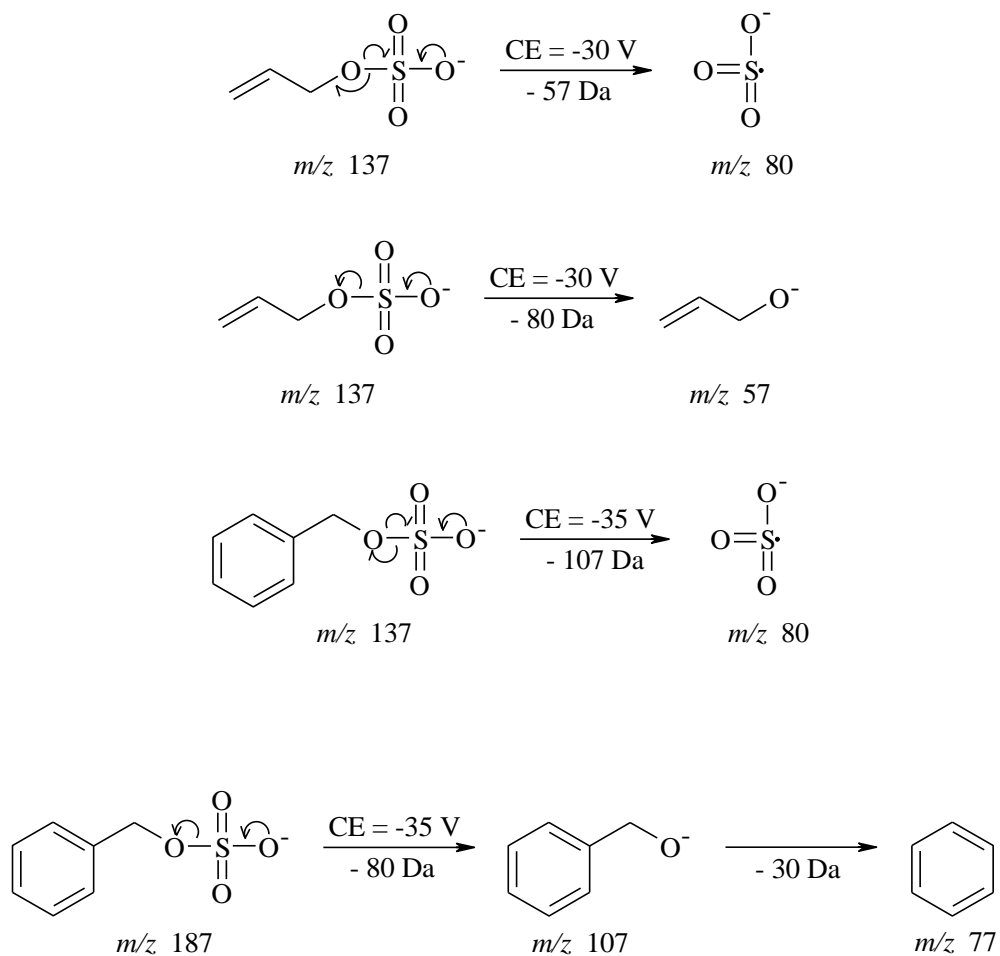
Scheme 4.20. *Plausible paths of fragmentation of m/z 137 and 187 ions.*

A detailed analysis of fragmentation spectra of organic sulfonates and organosulfates discussed above showed characteristic features. Therefore, it can serve as a useful probe for a firm structural elucidation of unknown compounds that formed in the cause of aqueous-phase isoprene degradation reactions.

In the light of the finals from collision induced discussion experiments for model compounds 1 – 4 it can be hypothesized that the liked structures for unknown compounds that form in the aqueous phase from isoprene are organosulfates rather than organic sulfonates.
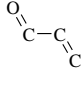
4.5 Quantum mechanical calculations

In order to estimate the relative stability of possible structure of the products of the reaction of isoprene with sulfoxy-radical anions theoretical calculation were performed. For each compound, dominant species is a structure of minimum Gibbs energy. The higher ΔG of conformer, the smaller it's abundant in the thermodynamically stable mixture.

4.5.1 MW 180 compound

Possible conformers of the product MW 180 depending on the relative energies were presented in Figure 4.21.
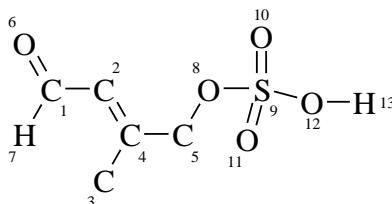
The most abundant species in the solution at the thermodynamic equilibrium is stereoisomer I, for which the relative Gibbs free energy is assumed 0 kJ mol⁻¹. This conformer has an assembly where atoms 1, 2, 3, 4, 5, 6, 7, 8, 9, and 10 (see structure above) are situated on one plane. Moreover, the conjugated double bonds O=C–C=C have a "chair" shape which is known as a very stable construction (March, 1992).
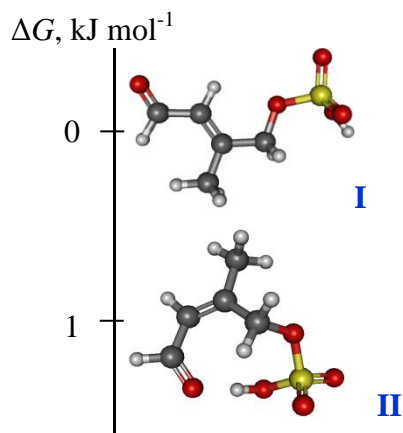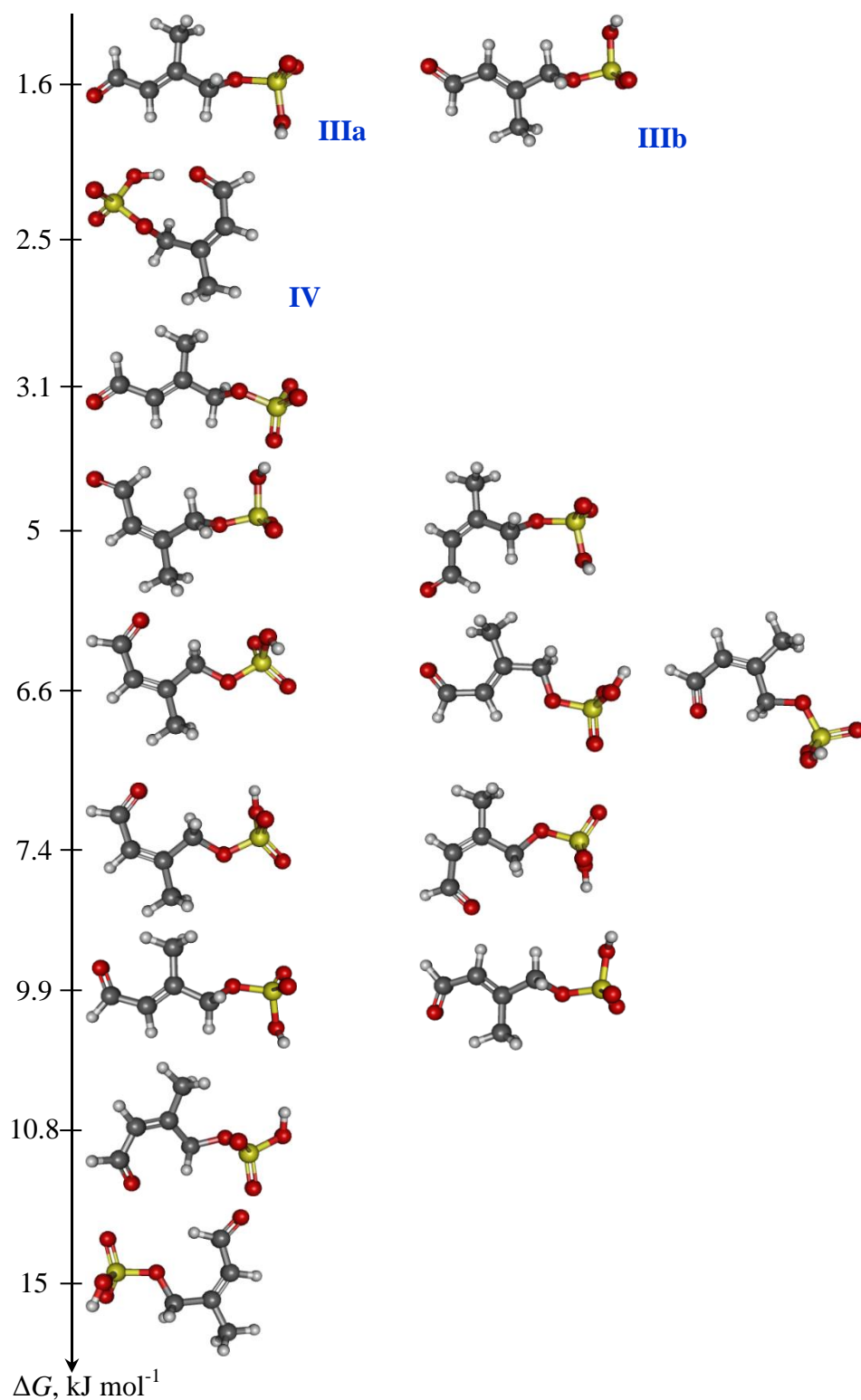
Fig. 4.21. *Schematic representation of relative energies of possible conformers of MW 180.*

Conformer II is less lavish than conformer I. Additionally, it structure is similar to that of isomer IV. Hydrogen 13 of the sulfate group in both configurations forms a hydrogen bond with oxygen 6 of the carbonyl group. Quantum calculations showed that distance between oxygen 6

and 8 in isomer I is longer than in isomer IV. It makes isomer I more stabilized. Since the case considered deals with aqueous-phase reaction of isoprene, a molecule of water brakes this hydrogen bond making the conformers II and IV unstable in this continuum. Disagreement between quantum calculations and theoretical data result from performing computations with the PCM. In this model, the studied molecule is considered an entire electron density while the solvent continuum is not treated as an individual molecule of water which can break internal hydrogen bonding.

In stereoisomers III(a, b), with ΔG = 1.6 kJ mol^{-1}, atoms 8, 9 and 10 are not situated on the same plane as the carbon frame (1, 2, 3, 4, 5, 6 and 7 atoms), unlike as in isomer I. It makes the conformer II less energetically favorable than I.

Conformers with relative energy higher 4 J mol^{-1} are not described in this thesis because their abundance in the thermodynamically stable solution is less than 20% relative to the most stable conformer, according to Boltzmann distribution:

$$\frac{N_i}{N_j} = e^{\frac{-\Delta E_{ij}}{kT}} \tag{4.23}$$

where, N is the total number of particles; E – difference between the energy levels; k – the Boltzmann constant; T – temperature.

The more unstable conformer, the amount of which is less than 0.3%, has ΔG = 15 kJ mol^{-1}. In this structure, oxygen 8 is in close vicinity to hydrogen 7; however a hydrogen bond between them does not stabilize this isomer because H7 is not labile, i.e. has low acidity.

4.5.2 MW 164 compound

Figure 4.22 shows relative energies of possible isomers of the MW 164 compound. Quantum calculation showed that, the dominant species (conformers I) in the thermodynamically stable mixture has the same atoms arrangement as I isomers of MW 180 compound – atoms 1, 2, 3, 4, 5, 6, 7, 8, 9 and 10 are located on one plane with "chair" shape of O=C–C=C bond (see structure below).
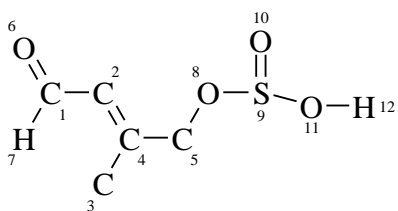
Smaller concentration of conformers II(a,b) is explained by the localization of sulfite groups' atoms (8, 9, and 10) out the plane of carbon frame that makes isomers II less energetically favorable then isomer I.

Stereoisomer of the lowest stability, as in case of MW 180 compound, possesses hydrogen bond between H7 and O8 – energetically unfavorable conformers.

ΔG, kJ mol^{-1}

11.2

12.3

15.1

ΔG, kJ mol^{-1}
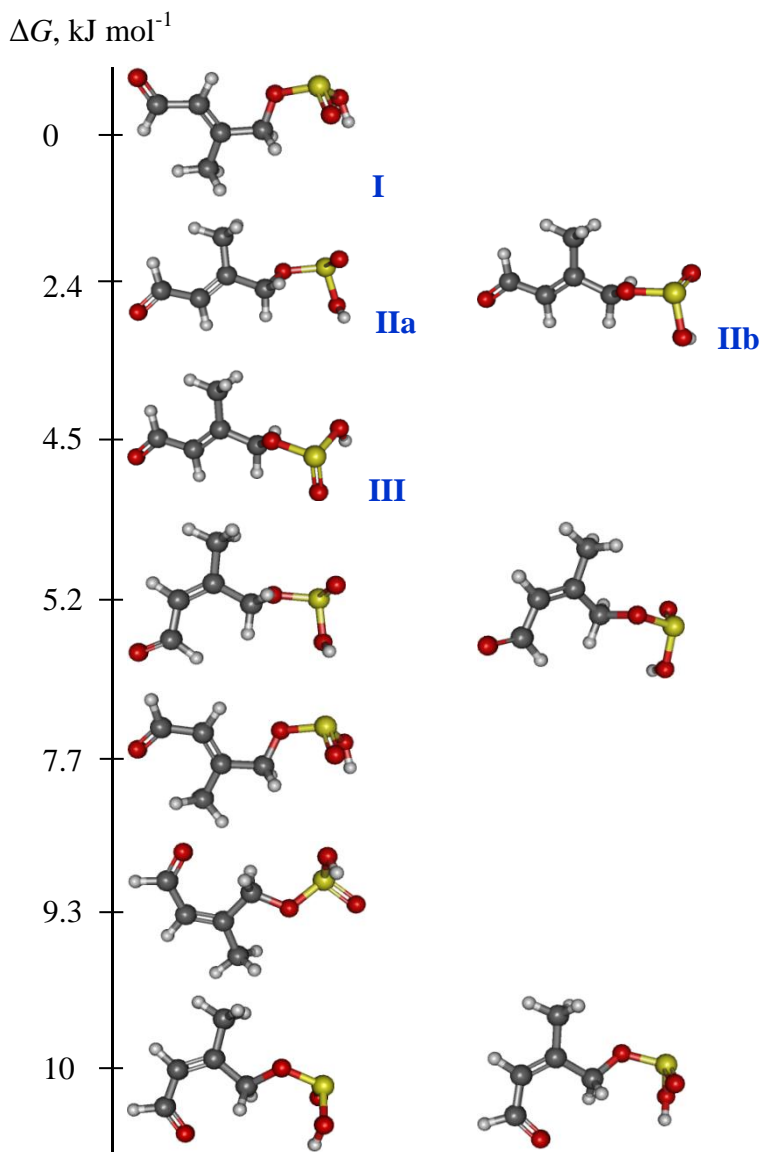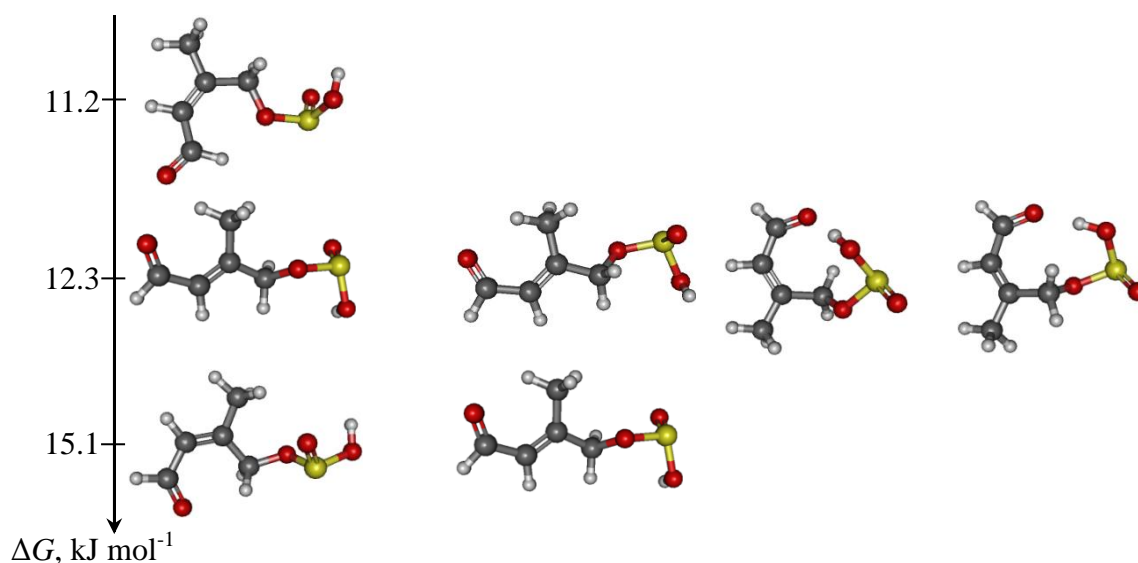
Fig. 4.22. *Schematic representation of relative energies of possible conformers of the MW 164 compound.*

4.5.3 MW 166 compound

Relative energies of conformers of MW 166 compound also were estimated by quantum chemical calculations and its results are presented in Figure 4.23.

In conformers with minimum energy, carbon frame (1, 2, 3, 4, and 5(see structure below)) are localized on one plane. Additionally, there is hydrogen bond between oxygen 8 and hydrogen 7 which are situated on one side of that plane.
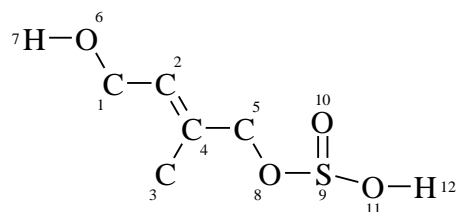
Stereoisomers II of $\Delta G = 1.1$ kJ mol^{-1} has similar atoms location to isomers I – carbon frame on one plane, sulfite and hydroxyl group on the one side of that plane – however, hydrogen 7 is "turned" from oxygen 8 what makes formation of hydrogen bonding difficult, and structure is less energetically favorable.

The distinguish situation is in conformer III where sulfite and hydroxyl group are on the other side of the carbon frame plane causes less abundance of this structure in thermodynamically stable mixture of MW 166 compound.

The more unstable conformer has $\Delta G = 17.5$ kJ mol^{-1} with structure where two hydroxyl groups, on both side of molecule, are in close vicinity and repulse each other.

ΔG, kJ mol^{-1}
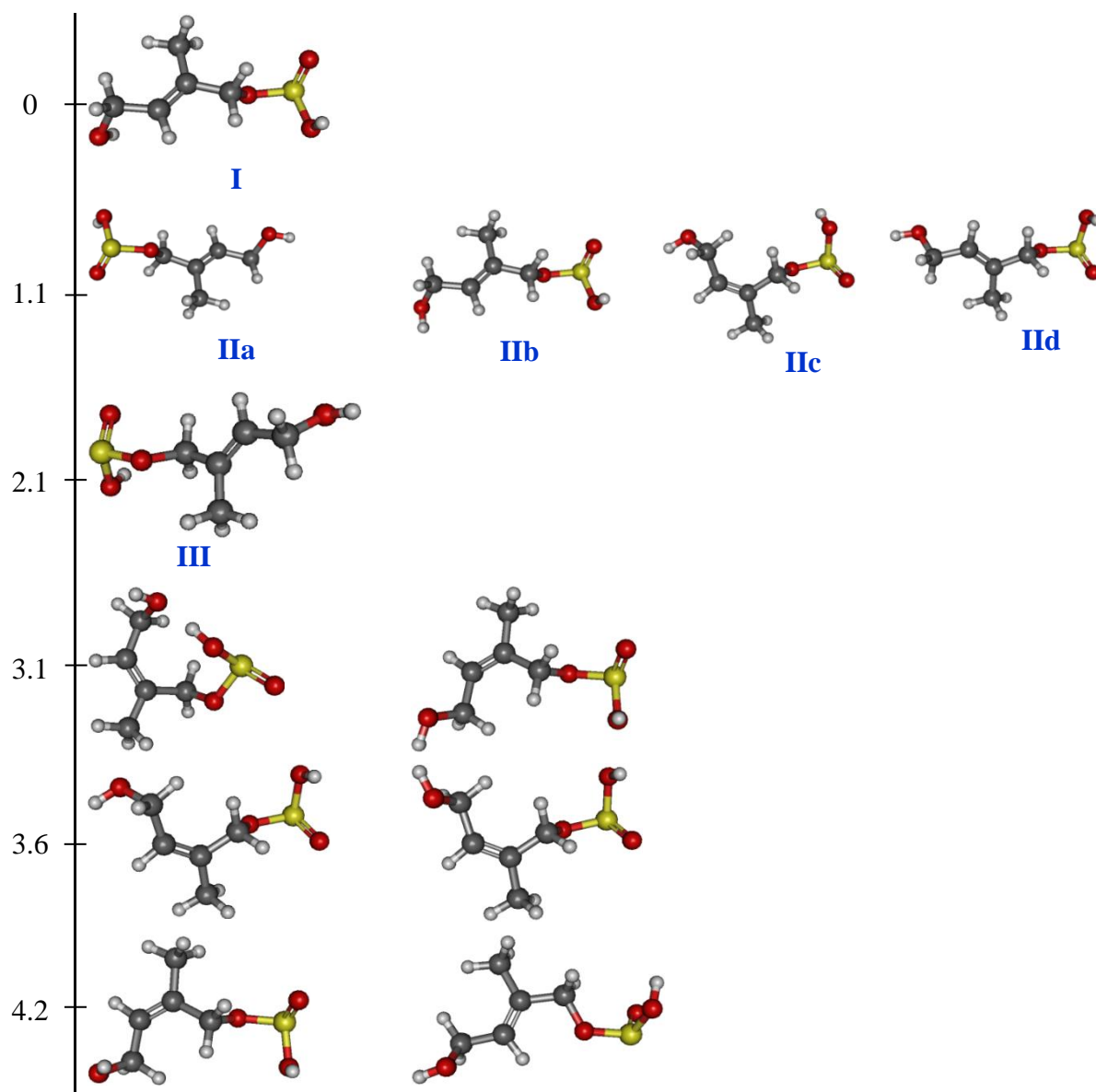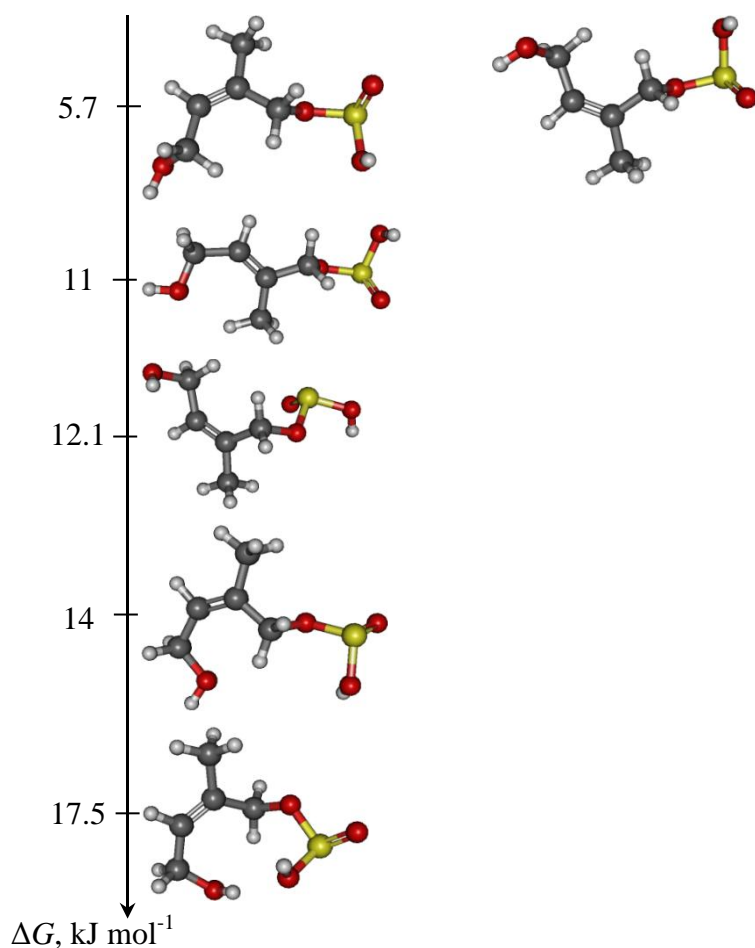
Fig. 4.23. *Schematic representation of relative energies of possible conformers of the MW 166 compound.*

4.5.4 MW 182 compound

Schematic representation of relative energies of possible conformers of the MW 182 compound (Fig. 4.24) shows that the dominant species (I) possess atoms of carbon frame (1, 2, 3, 4, and 5(see structure below)) situated on the same plane and sulfate group is out the plane. There is hydrogen bonding between hydrogen 13 and oxygen 6, meanwhile, hydrogen 7 is turned form the 13 one – no repulse – that additionally stabilize conformer.
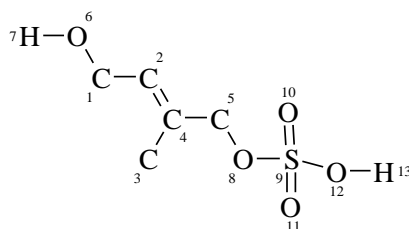
Conformer II, like conformer I, has atoms of carbon frame located on the same plane, and a hydrogen bond between H13 and O6. However, its C5–O8 bond is located on the carbon-frame plane, which causes intramolecular tension, according to the calculations.

Conformer III, which amounts to 0.0014%, is the least stable stereoisomer. A high relative energy of this molecule ($\Delta G = 27.8$ kJ mol^{-1}) results from two antagonistic effects:

1. formation of the hydrogen bond between H7 and O11;
2. untypical, energetically unfavorable conformation necessary to form a hydrogen bond between H7 and O11 – a dominant effect.

ΔG, kJ mol^{-1}
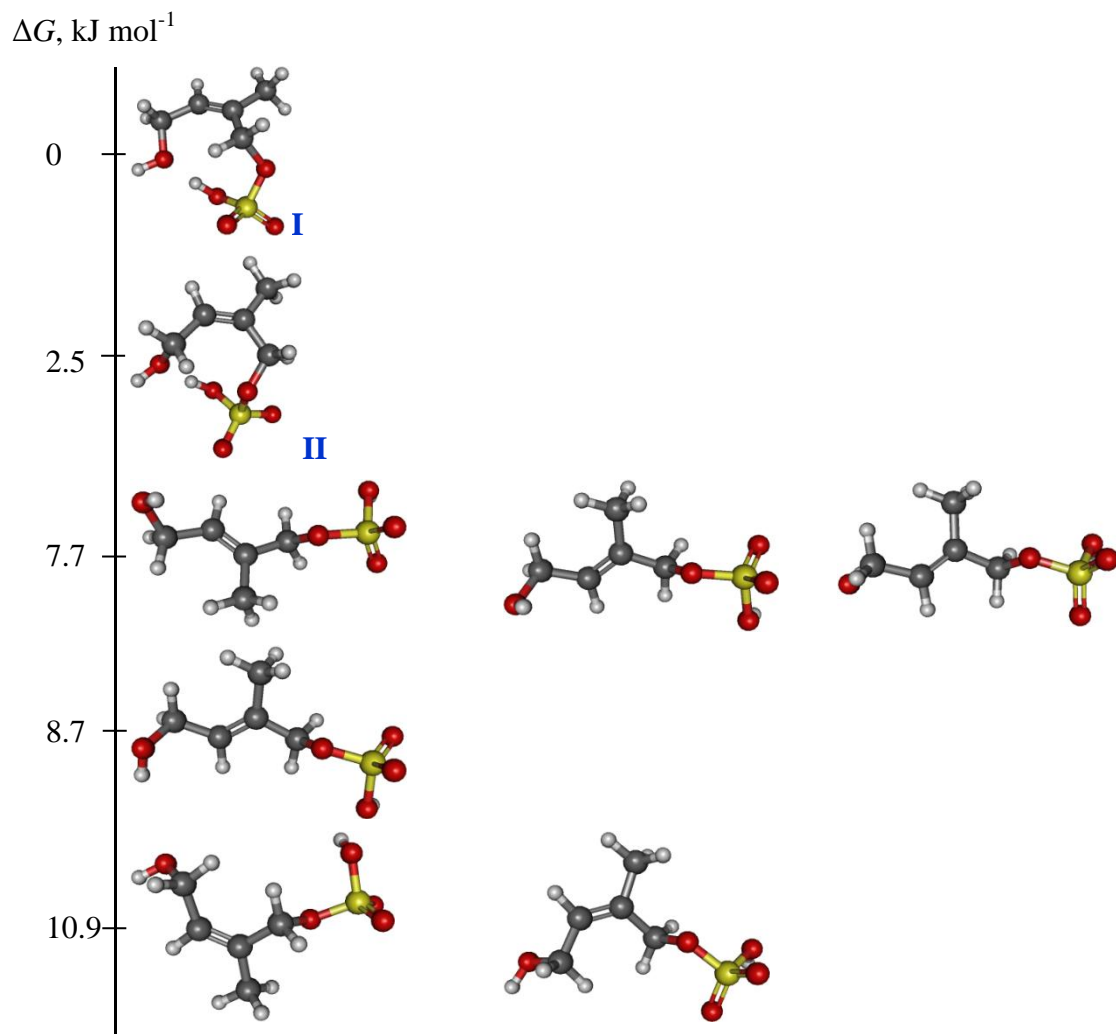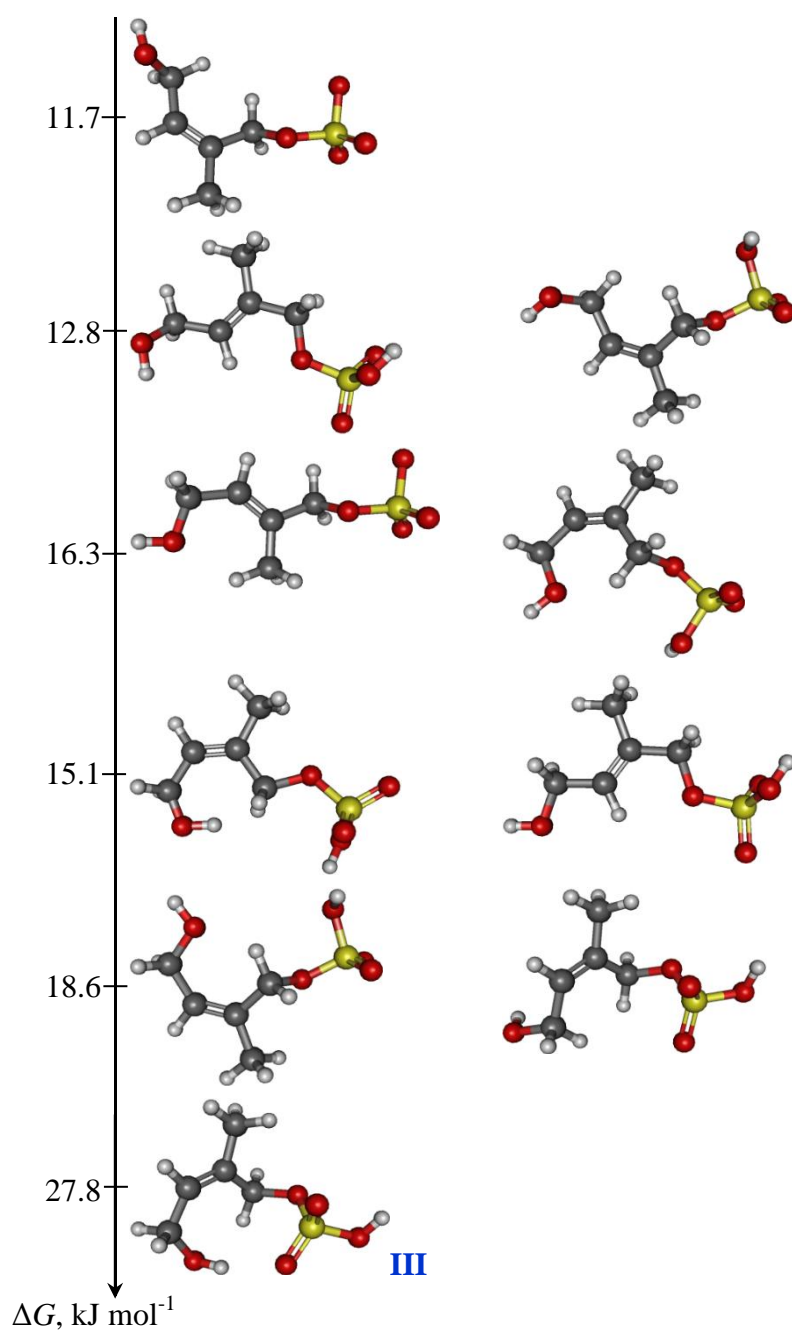
Fig. 4.24. *Schematic representation of relative energies of possible conformers of the MW 182 compound.*

5 Conclusions

The chemical kinetics, mechanisms and products of aqueous-phase reactions of isoprene in the presence of dissolved forms of SO_2 and HONO, oxygen and manganese(II) sulfate have been studied. The complex investigations, started from the studies of S(IV) autoxidation catalyzed by $MnSO_4$ at different initial acidities of the reacting solutions, followed by determination of the impact of isoprene and nitrous acid added separately and together on this process.

The rate of S(IV) autoxidation (MOS experiments) depended on the initial acidity of the reacting solutions. Generally, the higher acidity, the slower was the rates of the process.

The addition of sodium nitrite (MOSN experiments) increased the rate of the autoxidation of S(IV) in slightly alkaline and neutral solutions. Fast beginning of the reaction was also observed in neutral and acidic solutions where the end of the autoxidation was slowed down or even stopped. Moreover, the consumption of oxygen depended on the acidity of the reacting solutions. Total oxygen consumption was observed in slightly alkaline, neutral and slightly acidic solutions. At $pH_o \geq 4.0$, the oxygen decay was only $20 \div 80\%$.

Isoprene alone (MOSC experiments) slowed down or even stopped the S(IV) autoxidation in slightly alkaline and acidic solutions, but accelerated it in neutral solutions.

Isoprene and sodium nitrite taken together (MOSCN experiments) had a negligible influence on the autoxidation of S(IV) in slightly alkaline and neutral solutions. However, their impact in slightly acidic media was significant. Nitrite ions/nitrous acid deactivated the inhibitive behavior of isoprene. The addition of isoprene in acidic solution did not change the S(IV) autoxidation in the presence of nitrous acid.

The influence of isoprene and nitrite ions has been explained by a chemical mechanism derived from experimental observations, which included:

- isoprene oxidations initiated by sulfate and sulfite radical-anions;
- isoprene oxidation initiated by nitrite ions and nitrous acid.

These mechanisms were used to extend the well-known mechanism of S(IV) autoxidation catalyzed by transition metal ions to the overall mechanism describing the transformation of isoprene coupled with autoxidation of S(IV) in the presence of nitrite ions/nitrous acid.

Chemical-kinetic simulations based on the proposed mechanism of isoprene reaction with sulfoxy radical-anions showed a good agreement of experimental and modeling data.

To prove the suggested mechanism of the transformation of isoprene coupled with autoxidation of S(IV) in the presence of nitrite ions/HONO, kinetic simulations should be done in the future.

A detailed characterization of the observed products of isoprene transformation with a triple-quadruple negative electrospray mass spectrometry (−)ESI-MS/MS along with additional analytical techniques such as nuclear magnetic resonance and UV spectroscopy showed their key structural features. A thorough interpretation of analytical data revealed all products contained isoprene the with C-5 skeleton possessing modified carbonyl or hydroxyl moieties in the molecular core. Specially, the molecules were proved to bear the O–SO$_3$H or the O–SO$_2$H moieties. Evidence for the sulfoxy ester function was given by the *m/z* 97 and 80 diagnostic ions formed by a charge-directed heterolytic O–C bond cleavage. The sulfite ester group was also confirmed by the comparison of the mass spectrometric behavior of the product molecules with that of a model compounds specially synthesized for this purpose. Products containing C–S bonds (sulfonic and sulfinic acid) were proved not to form. Namely, the following organosulfate and organosulfite compounds were identified: 1-O-sulfonyl-4-hydroxy-2-methylbut-2-ene, 4-O-sulfonyl-3-methylbut-2-enal, 4-O-sulfinyl-3-methylbut-2-enal, and 1-O-sulfinyl-4-hydroxy-2-methylbut-2-ene.

Quantum chemical calculations showed that the most stable structural conformers of 4-O-sulfonyl-3-methylbut-2-enal and 4-O-sulfinyl-3-methylbut-2-enal had carbon frame, oxygen from carbonyl group and one from sulfate/sulfite groups located on the same plane. Moreover, the O=C–C=C sequence has a "chair" shape. The most stable structural conformers of 1-O-sulfonyl-4-hydrox-2-methylbut-2-ene and 1-O-sulfinyl-4-hydroxy-2-methylbut-2-ene had carbon frame located on one plane and sulfate/sulfite stretching out of that plane.

Aqueous-phase reactions of isoprene, in the presence of oxygen, dissolved forms of sulfur dioxide, and manganese(II) sulfate presented in this thesis are possible sources of atmospheric organosulfates and organosulfites. Products of these reactions can react further and form higher molecular weight organoesters with molecular structures similar to the saturated sulfate esters identified in the secondary organic aerosols collected in field measurements (Romero and Oehme, 2005; Surratt *et al.*, 2007b), or even oligomers. These reactions and their products deserve further experimental study to reveal more possible

constituents of secondary organic aerosols and atmospheric waters (e.g. rains) which can be formed during the aqueous-phase transformations of atmospheric isoprene.

Organosulfates and organosulfites are considered as a substantial fraction of humic-like substances (HULIS) contained in ambient aerosol. Their highly acidic polarities lead to suggestion that they may enhance the capacity of ambient aerosol to act as cloud condensation nuclei impacting the air quality. However, true effect of organosulfates and organosulfites, including the aforementioned substances identified, on the properties of SOA, and condition of biota and human health and life are not known yet and should be one of the priority topics of further studies in the field of atmospheric chemistry.

6 Bibliography

Acker K., Febo A., Trick S., Perrino C., Bruno P., Wiesen P., Moller D., Wieprecht W., Auel R., Giusto M., Geyer A., Platt U., Allegrini I. (2006) Nitrous acid in the urban area of Rome. Atmosph. Environ. 40:3123-3133

Acuna-Alvarez L., Exton D.A., Timmis K.N., Suggett D.J., McGenity T.J. (2009) Characterization of marine isoprene-degrading communities. Environ. Microbiol. 11:3280–3291

Affek H.P., Yakir D. (2002) Protection by isoprene against singlet oxygen in leaves. Plant Physiol. 129:269-277

Aiken A.C., DeCarlo P.F., Kroll J.H., Worsnop D.R., Huffman J.A., Docherty K.S., Ulbrich I.M., Mohr C., Kimmel J.R., Sueper D., Sun Y., Zhang Q., Trimborn A., Northway M., Ziemann P.J., Canagaratna M.R., Onasch T.B., Alfarra M.R., Prevot A.S.H., Dommen J., Duplissy J., Metzger A., Baltensperger U., Jimenez J.L. (2008) O/C and OM/OC ratios of primary, secondary, and ambient organic aerosols with highresolution time-of-flight aerosol mass spectrometry. Environ. Sci. Technol. 42:4478-4485

Alder R.W., Bonifacic M., Asmus K.D. (1986) Reaction of a stable N-N bonded radical cation with free radicals generated by puls radiolysis: Exceedingly rapid hydrogen abstraction from C-H bonds. J. Chem. Soc. Perkin Trans. 2:277-284

Ammann M., Kalbere M., Jost D.T., Tobler L., Rossler E., Piguet D., Gaggeler H.W., Baltensperger U. (1998) Heterogeneous production of nitrous acid on soot in polluted air masses. Nature 395:157-160

Ammann M., Rossler E., Strekowski R., George C. (2005) Nitrogen dioxide multiphase chemistry: uptake kinetics on aqueous solutions containing phenolic compounds. Phys. Chem. Chem. Phys. 7:2513-2518

Andreae M.O., Crutzen P.J. (1997) Atmospheric aerosols: biogeochemical sources and role in atmospheric chemistry. Science 276:1052-1058

Arnold F., Scheid J., Stilp T., Schalger H., Reinhardt M.E. (1992) Measurements of jet aircraft emissions at cruise altitude I: the odd-nitrogen gases NO, NO_2, HNO_2 and HNO_3 Geophys. Res. Lett. 19:2421-2424

Atkins P.W. (2007) Chemia Fizyczna. PWN, Warszawa

Attygalle A.B., García-Rubio S., Ta J., J. M. (2001) Collisionally-induced dissociation mass spectra of organic sulfate anions. J. Chem. Soc., Perkin Trans. 2 2:498-506

Aumont B., Chervier F., Laval S. (2003) Contribution of HONO sources to the NO_x/HO_x/O_3 chemistry in the polluted boundary layer. Atmos. Environ. 37:487-498

Baek S.O., Jenkins R.A. (2004) Characterization of trace organic compounds associated with aged and diluted sidestream tobacco smoke in a controlled atmosphere-volatile organic compounds and polycyclic aromatic hydrocarbons. Atmos. Environ. 38:6583-6599

Baes C.F.J., Mesmer R.E. (1976) The hydrolysis of cations. Joh Wiley & Sons, New York

Baker A.R., Turner S.M., Broadgate W.J., Thompson A., McFiggans G.B., Vesperini O., Nightingale P.D., Liss P.S., Jickells T.D. (2000) Distribution and sea– air fluxes of biogenic trace gases in the eastern Atlantic Ocean. Global Biochem. Cy. 14:871-886

Bates T.S., Lamb B.K., Guenther A., Dignon J., Stoiber R.E. (1992) Sulfur emissions to the atmosphere from natural sources. J. Atmos. Chem. 14:315-337

Becke A.D. (1988) Density-functional exchange-energy approximation with correct asymptotic behavior. Phys. Rev. A 38

Becke A.D. (1993) Density-functional tehrmochemistry. III. The role of exact exchange. J. Chem. Phys. 98:5648

Beckett W.S., Russi M.B., Haber A.D., Rivkin R.M., Sullivan J.R., Tameroglu Z., Mohsenin V., Leaderer B.P. (1995) Effect of nitrous acid on lung function in asthmatics: a chamber study. Environ. Health Perspect. 103:372-375

Bejan I., Aal Y.A.E., Barnes I., Benter T., Bohn B., Wiesen P., Kleffmann J. (2006) The photolysis of ortho-nitrophenols: a new gas phase source of HONO. Phys. Chem. Chem. Phys. 8:2028-2035

Berenguer J.A., Calderon V., Herce M.D., Sanchez J.J. (1991) Spoilage of a bakery product by isoprene producing molds. Rev. Agroquim. Technol. Aliment 31:580-583

Berglund J., Elding L.I. (1995) Manganese-catalysed autoxidation of dissolved sulfur dioxide in the atmospheric aqueous phase. Atmos. Environ. 29:1379-1391

Berresheim H., Jaeschke W. (1983) The contribution of volcanoes to the global atmospheric sulfur budget. J. Geophys. Res. 88:3732-3740

Blando J.D., Turpin B.J. (2000) Secondary organic aerosol formation in cloud and fog droplets: a literature evaluation of plausibility. Atmos. Environ. 34:1623-1632

Böge O., Miao Y., Plewka A., Herrmann H. (2006) Formation of secondary organic particle phase compounds from isoprene gas-phase oxidation products:an aerosol chamber and field study. Atmos. Environ. 40:2501-2509

Borbon A., Fontaine H., Locoge N., Veillerot M., Galloo J.C. (2003b) Developing receptor-oriented methods for non-methane hydrocarbon characterisation in urban air - part II: source apportionment. Atmos. Environ. 37:4065-4076

Borbon A., Fontaine, H., Locoge, N., Veillerot, M., Galloo, J. C. (2003a) Developing receptor-oriented methods for non-methane hydrocarbon characterisation in urban air –part I: source identification. Atmos. Environ. 37:4051-4064

Brandt C., van Eldik R. (1995) Transition metal-catalyzed oxidation of sulfur(IV) oxides. Atmospheric-relevant processe and mechanisms. Chem. Rev. 95:119-190

Broszkiewicz R.K. (1976) The pulse radiolysis study of $NaNO_2$ and $NaNO_3$ solutions. Bull. Acad. Pol. Sci, Ser. Sci. Chim. 24:221-229

Burgess R.A., Penkett S.A. (1993) Ground-based non-methane hydrocarbon measurements in England. In: Borrell P (ed) Proceedings of the EUROTRAC '92. Academic Publishing, The Hague, The Nederlands, pp 165-169

Buxton G.V., McGowan S., Salmon G.A., Williams J.E., Wood N.D. (1996) A study of the spectra and reactivity of oxysulphurradical anions involved in the chain oxidation of S(IV): A pulse and gamma – radiolysis study. Atmos. Environ. 30:2483–2493

Calvert J.G., Yarwood G., Dunker A.M. (1994) An evaluation of the mechanism of nitrous acid formation in the urban atmosphere. Res. Chem. Intermed. 20:463-502

Carlton A.G., Turpin B.J., Lim H.J., Altieri K.E., Seitzinger S. (2006) Link between isoprene and secondary organic aerosol (SOA): pyruvic acid oxidation yields low volatility organic acids in clouds. Geophys. Res. Lett. 33:L06822

Carlton A.G., Wiedinmyer C., Kroll J.H. (2009) A review of Secondary Organic Aerosol (SOA) formation from isoprene. Atmos. Chem. Phys. 9:4987-5005. doi:10.5194/acp-9-4987-2009

Chen L., Lin J.W., Yang C.L. (2002) Absorption of NO_2 in a packed tower with Na_2SO_3 aqueous solution. Environ. Prog. 21:225-230

Claeys M., Graham B., Vas G., Wang W., Vermeylen R., Pashynska V., Cafmeyer J., Guyon P., Andreae M.O., Araxo P., Maenhaut W. (2004a) Formation of secondary organic aerosols through photooxidation of isoprene. Science 303:1173-1176

Claeys M., Kourtchev I., Pashynska V., Vas G., Vermeylen R., Wang W., Cafmeyer J., Chi X., Artaxo P., Andreae M.O., Maenhaut W. (2010) Polar organic marker compounds in atmospheric aerosols during the LBA-SMOCC 2002 biomass burning experiment in Rondônia, Brazil: sources and source processes, time series, diel variations and size distributions. Atmos. Chem. Phys. 10:9319-9331. doi:10.5194/acp-10-9319-2010

Claeys M., Wang W., Ion A.C., Kourtchev I., Gelencser A., Maenhaut W. (2004b) Formation of secondary organic aerosols from isoprene and its gas-phase oxidation products through reaction with hydrogen peroxide. Atmos. Environ. 38:4093-4098

Clifton C.L., Altstein N., Huie R.E. (1988) Rate constant for the reaction of nitrogen dioxide with sulfur(IV) over the pH range 5.3-13. Environ. Sci. Technol. 22:586-589

Coddington J.W., Hurst J.K., Lymar S.V. (1999) Hydroxyl radical formation during peroxynitrous acid decomposition. J. Am. Chem. Soc. 121:2438-2443

Couvidat F., Seigneur C. (2011) Modeling secondary organic aerosol formation from isoprene oxidation under dry and humid conditions. Atmos. Chem. Phys. 11:893-909

Czoschke N.M., Jang M., Kamens R.M. (2003) Effect of acidic seed on biogenic secondary organic aerosol growth. Atmos. Environ. 37:4287-4299

Daniels M. (1969) Radiation chemistry of the aqueous nitrate system. III. Pulse electron radiolysis of concentrated sodium nitrate solutions. J. Phys. Chem. 73:3710-3717

Davies G., Kustin K. (1969) Stoichiometry and kinetics of manganese(III) reactions with hydroxylamine, O-methylhydroxylamine, and nitrous acid in acid perchlorate solution. Inorganic Chemistry 8:484-490

Delwiche C.F., Sharkey T.D. (1993) Rapid appearance of ^{13}C in biogenic isoprene when $^{13}CO_2$ is fed into intact leaves. Plant Cell Environ. 16:587-591

Deneris E.S., Stein R.A., Mead J.F. (1984) In vitro biosynthesis of isoprene from mevalonate utilizing a rat liver cytosolic fraction. Biochem.Biophys.Res.Comm. 123:691-696

Deneris E.S., Stein R.A., Mead J.F. (1985) Acid-catalyzed formation of isoprene from a mevalonate-derived product using a rat liver cytosolic fraction. J. Biol. Chem. 260:1382-1385

Derwent R.G., Middleton D.R., Field R.A., Goldstone M.E., Lester J.N., Perry R. (1995) Analysis and interpretation of air quality data from an urban roadside location in central London over the period from July 1991 to July 1992. Atmos. Environ. 29:923-946

Dibb J.E., Huey L.G., Slusher D.L., Tanner D.J. (2004) Soluble reactive nitrogen oxides at South Pole during ISCAT 2000. Atmos. Environ. 38:5399 - 5409

Dignon J., Hameed S. (1989) Global emission of nitrogen and sulfur oxides from 1860 and 1980. J. Air Pollut. Control Assoc. 39:180-186

Diskin A.M., Spanel P., Smith D. (2003) Time variation of ammonia, acetone, isoprene and ethanol in breath: a quantitative SIFT-MS study over 30 days. Physiol. Meas. 24:107-119

Djehiche M., Tomas A., Fittschen C., Coddeville P. (2011) First direct detection of HONO in the reaction of methylnitrite (CH_3ONO) with OH radicals. Environ. Sci. Technol. 45:608-614

Drexler C., Elias H., Fecher B., Wannowius K.J. (1991) Kinetic investigation of sulfur(IV) oxidation by peroxo compounds R-OOH in aqueous solution, Fresen J. Anal. Chem. 340:605-616

Drexler C., Elias H., Fecher B., Wannowius K.J. (1992) Kinetics and mechanism of sulfur(IV) oxidation by hydrogen peroxide in aqueous phase: the non-linear parts of the pH-profile Ber. Bunsen Gesell. 96:481-485

Eatough D.J., Benner C.L., Bayona J.M., Richards G., Lamb J.D., Lee M.L., Lewis E.A., Hansen L.D. (1989) Chemical compositlon of environmental tobacco smoke. 1a gas-phase acids and bases. Environ. Sci. Technol. 23:679-687

Edney E.O., Kleindienst T.E., Jaoui M., Lewandowski M., Offenberg J.H., Wang W., Claeys M. (2005) Formation of 2-methyl tetrols and 2-methylglyceric acid in secondary organic aerosol from laboratory irradiated isoprene/NO_x/SO_2/air mixtures and their detection in ambient $PM_{2.5}$ samples collected in the eastern United States. Atmos. Environ. 39:5281-5289

Ekberg A., Arneth A., Hakola H., Hayward S., Holst T. (2009) Isoprene emission from wetland sedges. Biogeosciences 6:601-613

Ellison T.K., Eckert C.A. (1984) The oxidation of aqueous sulfur dioxide. 4. The influence of nitrogen dioxide at low pH. J. Phys. Chem. 88:2335-2339

Ervens B., Carlton A.G., Turpin B.J., Altieri K.E., Kreidenweis S.M., Feingold G. (2008) Secondary organic aerosol yields from cloud-processing of isoprene oxidation products. Geophys. Res. Lett. 35:L02816. doi:10.1029/2007GL031828

Ervens B., Kreidenweis S.M. (2007) SOA formation by biogenic and carbonyl compounds: data evaluation and application. Environ. Sci. Technol. 41:3904-3910

Facchini M.C., Fuzzi S., Zappoli S., Andracchio A., Gelencsér A., Kiss G., Krivácsy Z., Mészáros E., Hansson H.-C., Alsberg T., Zebühr Y. (1999) Partitioning of the organic aerosol component between fog droplets and interstitial air. J. Geophys. Res. 104:26821-26832

Fall R., Copley S.D. (2000) Bacterial sources and sinks of isoprene, a reactive atmospheric hydrocarbon. Environ. Microbiol. 2:123-130

Fan J., Zhang R. (2004) Atmospheric oxidation mechanism of isoprene. Environ. Chem. 1:140-149

Febo A., Perrino C. (1995) Measurement of high concentration of nitrous acid inside automobiles. Atmos. Environ. 29:345-351

Fenske J.D., Paulson S.E. (1999) Human breath emissions of VOCs. J. Air Waste Manage. Assoc. 49:594-598

Fiocco G., Fua D. (1996) The Mount Pinatubo eruption, vol 42. NATO ASI Series I. Springer, Berlin

Foresman J.B., Frish A. (1996) Exploring chemistry with electronic structure methods. Second ed. edn. Gaussian Incm, Pittsburgh PA

Frisch M.J., Trucks G.W., Schlegel H.B., Scuseria G.E., Robb M.A., Cheeseman J.R., Montgomery J.J.A., Vreven T., Kudin K.N., Burant J.C., Millam J.M., Iyengar S.S., Tomasi J., Barone V., Mennucci B., Cossi M., Scalmani G., Rega N., Petersson G.A., Nakatsuji H., Hada M., Ehara M., Toyota K., Fukuda R., Hasegawa J., Ishida M., T. N., Honda Y., Kitao O., Nakai H., Klene M., Li X., Knox J.E., Hratchian H.P., Cross J.B., Adamo C., Jaramillo J., Gomperts R., Stratmann R.E., Yazyev O., Austin A.J., Cammi R., Pomelli C., Ochterski J.W., Ayala P.Y., Morokuma K., Voth G.A., Salvador P., Dannenberg J.J., Zakrzewski V.G., Dapprich S., Daniels A.D., Strain M.C., Farkas O., Malick D.K., Rabuck A.D., Raghavachari K., Foresman J.B., Ortiz J.V., Cui Q., Baboul A.G., Clifford S., Cioslowski J., Stefanov B.B., Liu G., Liashenko A., Piskorz P., Komaromi I., Martin R.L., Fox D.J., Keith T., Al-Laham M.A., Peng C.Y., Nanayakkara A., Challacombe M., Gill P.M.W., Johnson B.G., Chen W., Wong M.W., Gonzalez C., Pople J.A. (2003) Gaussian 03, vol vol. Revision B.03. Gaussia, Inc., Pittsburgh PA

Fronaeus S., Berglund J., Elding L.I. (1998) Iron-manganese redox processes and synergism in the mechanism for manganese-catalyzed autoxidation of hydrogen sulfite. Inorganic Chemistry 37:4939-4944

Fu T.M., Jacob D.J., Heald C.L. (2009) Aqueous-phase reactive uptake of dicarbonyls as a source of organic aerosol over eastern North America. Atmos. Environ. 43:1814-1822

Gaeggeler K., Prevot A.S.H., Dommen J., Legreid G., Reimann S., Baltensperger U. (2008) Residential wood burning in an Alpine valley as a source for oxygenated volatile organic compounds, hydrocarbons and organic acids. Atmos. Environ. 42:8278-8287

Gelencsér A., Hoffer A., Krivacsy Z., Kiss G., Molnar A., Meszaros E. (2002) On the possible origin of humic matter in fine continental aerosol. J. Geophys. Res. 107:4137

George C., Srekowski R.S., Kleffman J., Stemmler K., Ammann M. (2005) Photoenhanced uptake of gaseous NO_2 on solid organic compounds: a photochemical source of HONO. Faraday Discuss 130:195-210

Gist N., Lewis A.C. (2006) Seasonal variations of dissolved alkenes in costoal waters. Mar. Chem. 100:1-10

Gogolev A.V., Makarov I.E., Fedeneev A.M., Pikaev A.K. (1986) Reactivity of NO_3 and HSO_4 radicals toward multivalent metal ions in aqueous solutions. High Energy 20:229-233

Gómez-González Y., Surratt J.D., Cuyckens F., Szmigielski R., Vermeylen R., Jaoui M., Lewandowski M., Offenberg J.H., Kleindienst T.E., Edney E.O., Blockhuys F., Van Alsenoy C., Maenhaut W., Claeys M. (2008) Characterization of organosulfates from the photooxidation of isoprene and unsaturated fatty acids in ambient aerosol using liquid chromatography/(-) electrospray ionization mass spectrometry. J. Mass Spectrom. 43:371-382

Gómez-González Y., Vermeylen R., Szmigielski R., Surratt J.D., Kleindienst T.E., Jaoui M., Lewandowski M., Offenberg J.H., Edney E.O., Maenhaut W., Claeys M. (eds) (2007) Characterisation of organosulphates from the photo-oxidation of isoprene in ambient $PM_{2.5}$ aerosol by LC/(-)ESI-linear ion trap mass spectrometry. European Aerosol Conference, Salzburg, Austria 9-14 September 2007, T01A018

Graedel T.E., Mandich M.L., Weschler C.J. (1986) Kinetic model studies of atmospheric droplet chemistry. 2. Homogeneous transition metal chemistry in raindrops. J. Geophys. Res. 91:5205

Grätzel M., Henglein A., Lilie J., Beck G. (1969) Pulsradiolytische untersuchung einiger elementarprozesse der oxydation und reduktion des nitritions. Ber. Bunsen. Phys.Chem. 73:646-653

Grätzel M., Taniguchi S., Henglein A. (1970) Pulsradiolytische untersuchung der NO-oxydation und des gleichgewichts $N_2O_3 \rightarrow NO + NO_2$ in waessriger loesung. Ber. Bunsenges. Phys. Chem. 74:488-492

Grgič I., Losno R., Pasiuk-Bronikowska W. (2003) in *EUROTRAC-2 CMD Final Report 2003, part III-1*. In: (Eds. Schurath U, Naumann, K. H.) (ed). pp Available at http://imk-aida.fzk.de/CMD/final_report/index.html [Verified 5 April 2007]

Günther A., Karl T., Harley P., Wiedinmyer C., Palmer P.I., Geron C. (2006) Estimates of global terrestrial isoprene emissions using MEGAN (Model of Emissions of Gases and Aerosols from Nature). Atmos. Chem. Phys. 6:3181-3210. doi:10.5194/acp-6-3181-2006

Günther A., König T., Habicher W.D., Schewetlick K. (1998) Antioxidant action of organic sulfites-II. Esters of sulfurous acid as primary antioxidants. Polim. Degrad. Stab. 60:385-391

Gustafsson R.J., Kyriakou G., Lambert R.M. (2008) The molecular mechanism of troposopheric nitrous acid production on mineral dust surfaces. Chem. Phys.Chem. 9:1390-1393

Gustafsson R.J., Orlov A., Griffiths P.T., Cox A., Lambert R.M. (2006) Reduction of NO_2 to nitrous acid on illuminated titanium dioxide aerosol surfaces: implications for photocatalysis and atmospheric chemistry. Chem. Commun.:3936-3938

Haapanala S., Rinne J., Pystynen K.H., Hellén H., Hakola H., Riutta T. (2006) Measurements of hydrocarbon emissions from a boreal fen using the REA technique. Biogeosciences 3:103-112. doi:10.5194/bg-3-103-2006

Hallquist M., Wenger J.C., Baltensperger U., Rudich Y., Simpson D., Claeys M., Dommen J., Donahue N.M., George C., Goldstein A.H., Hamilton J.F., Herrmann H., Hoffmann T., Iinuma Y., Jang M., Jenkin M.E., Jimenez J.L., Kiendler-Scharr A., Maenhaut W., McFiggans G., Mentel T.F., Monod A., Prevot A.S.H., Seinfeld J.H., Surratt J.D., Szmigielski R., Wildt J. (2009) The formation, properties and impact of secondary organic aerosols:current and emerging issues. Atmos. Chem. Phys. 9:5155-5236

Ham B.M. (2008) Even electron mass spectrometry with biomolecule applications. John Wiley & Sons New Jersey

Harley P.C., Guenther A.B., Zimmerman P.R. (1996) Effects of light, temperature and canopy position on net photosynthesis and isoprene emission from sweetgum (*Liquidamber styraciflua*) leaves. Tree Physiol. 16:25-32

Harris D.C., Laboratory M., China Lake C. (2010) Quantitative chemical analysis. Eight edn. W. H. Freeman and C^{o}, New York

Harris G.W., Carter W.P.L., Winer A.M., Pitts J.N.J. (1982) Observations of nitrous acid in the Los Angeles atmosphere and implications for predictions of ozone-precursor relationships. Environ. Sci. Technol. 16:414-419

Healy R.M., Wenger J.C., Metzger A., Duplissy J., Kalberer M., Dommen J. (2008) Gas/particle partitioning of carbonyls in the photooxidation of isoprene and 1,3,5-trimethylbenzene. Atmos. Chem. Phys. 8:3215-3230. doi:10.5194/acp-8-3215-2008

Hellén H., Hakola H., Pystynen K.H., Rinne J., Haapanala S. (2006) C2-C10 hydrocarbon emissions from a boreal wetland and forest floor. Biogeosciences 3:167-174. doi:10.5194/bg-3-167-2006

Herrmann H., Reese A., Zellner R. (1995) Time-resolved UV/VIS diode array absorption spectroscopy of SO_x^- (x=3,4,5) radical anions in aqueous solution. J. Mol. Struct. 348:183–186

Hesse M., Meier H., Zeeh B. (1997) Spectroscopic methods in organic chemistry. Georg Thieme Verlag Stuttgart, New York

Huie R.E., Neta P. (1984) Chemical behavior of SO_3^- and SO_5^- radicals in aqueous solutions. J. Phys. Chem. 88: 5665–5669

Huie R.E., Neta P. (1987) Rate constants for some oxidations of S(IV) by radicals in aqueous solutions. Atmos. Environ. 21:1743-1747

Jang M., Czoschke N.M., Lee S., Kamens R.M. (2002) Heterogeneous atmospheric aerosol production by acid- catalyzed particle-phase reactions. Science 298:814-817

Jiang L.S., Chan W.H., Lee W.M. (1999) Synthesis and diels-alder reactions of prop-1-ene-1,3-sultone, and chemical. transformations of the diels-aIder adducts. Tetrahedron 55:2245-2262

Josipovic M., Annegarn H.J., Kneen M.A., Pienaar J.J., Piketh S.J. (2010) Concentrations, distributions and critical level exceedance assessment of SO_2, NO_2 and O_3 in South Africa. Environ. Monit. Assess. 171:181-196

Kanakidou M., Seinfeld J.H., Pandis S.N., Farnes I., Dentener F.J., Facchini M.C., Van Dingenen R., Ervens B., Nenes A., Nielsen C.J., Swietlicki E., Putaud J.P., Balkanski Y., Fuzzi S., Horth J., Moortgat G.T., Wnterhalter R., Myhre C.E.L., Tsigaridis K., Vignati E., Stephanou E.G., Wilson J. (2005) Organic aerosols and global climate modelling:a review. Atmos. Chem. Phys. 5:1053-1123

Kesselmeier J., Staudt M. (1999) Biogenic volatile organic compounds (VOC): an overview on emission, physiology and ecology. J. Atmos. Chem. 33:23-88

Kirchner J.J., Hopkins P.B. (1991) Nitrous acid cross-links duplex DNA fragments through deoxyguanosine residues at the sequence 5'-CC. J. Am. Chem. Soc. 113 (12):4681-4682

Kiss G., Tombacz E., Varga B., Alsberg T., Persson L. (2003) Estimation of the average molecular weight of humic-like substances isolated from fine atmospheric aerosol. Atmos. Environ. 37:3783-3794

Kleffmann J. (2007) Daytime sources of nitrous acid (HONO) in the atmospheric boundary layer Chem. Phys.Chem. 8:1137-1144

Kleffmann J., Becker K.H., Wiesen P. (1998) Heterogonous NO_2 conversion processes on acid surfaces. Atmos. Environ. 32:2721-2729

Kleindienst T.E., Jaoui M., Lewandowski M., Offenberg J.H., Lewis C.W., Bhave P.V., Edney E.O. (2007) Estimates of the contributions of biogenic and anthropogenic hydrocarbons to secondary organic aerosol at a southeastern US location. Atmos. Environ. 41:8288-8300

Kleindienst T.E., O. E.E., Lewandowski M., Offenberg J.H., Jaoui M. (2006) Secondary organic carbon and aerosol yields from the Irradiations of isoprene and α-pinene in the presence of NO$_x$ and SO$_2$. Environ. Sci. Technol. 40 (3807-3812)

Klinger L.F., Greenberg J., Guenther A., Tyndall G., Zimmerman P., M'Bangui M., Moutsamboté J.-M., Kenfack D. (1998) Patterns in volatile organic compound emissions along a savanna-rainforest gradient in central Africa. J. Geophys. Res. 103:1443-1454

Krakjic I. (1970) Photolytic determination of SO$_4^-$ rate constants. Int. J. Radiat. Phys. Chem. 2:59-68

Kroll J.H., Ng N.L., Murphy S.M., Flagan R.C., Seinfeld J.H. (2006) Secondary organic aerosol formation from isoprene photooxidation. Environ. Sci. Technol. 40:1869-1877

Kuzma J., Nemecek-Marshall M., Pollock W.H., Fall R. (1995) Bacteria produce the volatile hydrocarbon isoprene. Curr. Microbiol. 30:97-103

Lammel G., Cape J.N. (1996) Nitrous acid and nitrite in the atmosphere. Chem. Soc. Rev. 25:361-369

Laothawornkitkul J., Paul N.D., Vickers C.E., Possell M., Taylor J.E., Mullineaux P.M., Hewitt C.N. (2008) Isoprene emissions influence herbivore feeding decisions. Plant Cell Environ. 31:1410-1415

Le Bras G., LACTOZ, gropu: S., isoprene O.m.o. (1997) in: Chemical process in atmospheric oxidation: laboratory studies of chemistry related to tropospheric ozone, vol 3. Spinger, Berlin

Leber A.P. (2001) Overview of isoprene monomer and polyisoprene production processes. New Phytol. 157:199-211

Lee C., Yang W., Parr R.G. (1988) Development of the Colle-Salvetti correlation-energy formula into a functional of the electron density. Phys. Rev. B 37

Li S., Mattews J., Sihna A. (2008a) Atmospheric hydroxyl radicalproduction from electronically excited NO$_2$ and H$_2$O. Science 319:1657

Liebman J.F., Petersen K.N., Skacke P.N. (1999) Computational study of ring strain in 1,3,2-dioxathiolane, its 2-oxide and its 2,2-dioxide. Acta Chem. Scand. 53:1003-1008

Liggio J., Li S.M., Brook J.R., Mihele C. (2007) Direct polymerization of isoprene and α-pinene on acidic aerosols. Geophys. Res. Lett. 34:L05814

Lim H.J., Carltopn A.G., Turpin B.J. (2005) Isoprene forms Secondary Organic Aerosol through cloud processing: model simulations. Environ. Sci. Technol. 39:4441-4446

Limbeck A., Kulmala M., Puxbaum H. (2003) Secondary organic aerosol formation in the atmosphere via heterogenous reaction of gaseous isoprene on acidic particles. Geophys. Res. Lett. 30 (1996)

Loeffler K.W., Koehler C.A., Paul N.M., DeHann D.O. (2006) Oligomer formation in evaporating aqueous glyoxal and methyl glyoxal solutions. Environ. Sci. Technol. 40:6318-6323

Loegager T., Sehested K. (1993a) Formation and decay of peroxynitrous acid: a pulse radiolysis study. J. Phys. Chem. 97:6664-6669

Logan B.A., Monson R.K., Potosnak M.J. (2000) Biochemistry and physiology of foliar isoprene production. Trends Plant Sci. 5:477-481

Loivamäki M., Mumm R., Dicke M., Schnitzler J.-P. (2008) Isoprene interferes with the attraction of bodyguards by herbaceous plants. P. Natl. Acad. Sci. USA 105 (45):17430-17435

Longevialle P. (1992) Ion-neutral complexes in the unimolecular reactivity of organic cations in the gas phase. Mass Spectrometry Reviews 11:157-192

Loreto F., Mannozzi M., Maris C., Nascetti P., Ferranti F., S. P. (2001) Ozone quenching properties of isoprene and its antioxidant role in leaves. Plant Physiol. 126:993-1000

Loreto F., Velikova V. (2001) Isoprene produced by leaves protects the photosynthetic apparatus against ozone damage, quenches ozone products, and reduces lipid peroxidation of cellular membranes. Plant Physiol. 127:1781-1787

Lukács H., Gelencsér A., Hoffer A., Kiss G., Horváth K., Hartyáni Z. (2009) Quantitative assessment of organosulfates in size-segregated rural fine aerosol. Atmos. Chem. Phys. 9:231-238. doi:10.5194/acp-9-231-2009

Manahan S.E. (2010) Environmental Chemistry. Ninth edn. CRC Press Talor& Francis Group, Boca Raton

March J. (1992) Advanced organic chemistry. IV edn. John Wiley & Sons, New York, Chichester, Brisbane, Singapore

Maruthamuthu P., Neta P. (1978) Phosphate radicals. Spectra, acid-base equilibriums, and reactions with inorganic compounds. J. Phys. Chem. 82:710-713

Matsunaga S., Mochida M., Saito T., Kwamura K. (2002) In situ measurements of isoprene in the marine air and surface seawater from the western North Pacific. Atmos. Environ. 36:6051-6057

Mazurkiewicz R., Rajca A., E. S., Skibiński A., Suwiński J., Zieliński W. (1995) Metody spektroskopowe i ich zastosowanie do identyfikacji zwiaziązków organicznych. Wydawnictwo Naukowo-Techniczne, Warszawa

McElroy W.J., Waygood S. (1990) Kinetics of the reactions of the SO_4^- radical with SO_4^-, $S_2O_8^{2-}$, H_2O and Fe^{2+}. J. Chem. Soc., Faraday T. 86:2557-2564

McLafferty F.W., Turecek F. (1993) Interpretation of mass spectra. Forth edn. University science books, Sausalito, California

McLaren R., Singleton D.L., Lai J.Y.K., Khouw B., Singer E., Wu Z., Niki H. (1995) Analysis of motor vehicle sources and their contribution to ambient hydrocarbon distributions at urban sites in Toronto during the southern oxidants study. Atmos. Environ. 30:2219-2232

Merrick J.P., Moran D., Radom L. (2007) An evaluation of harmonic vibrational frequency Scale Factors. J. Phys. Chem. A 111:11683-11700

Monson R.K., Trahan N., Rosenstiel T.N., Veres P., Moore D., Wilkinson M., Norby R.J., Volder A., Tjoelker M.G., Briske D.D., Karnosky D.F., Fall R. (2007) Isoprene emission from terrestrial ecosystems in response to global change: minding the gap between models and observations. Philos. T. Roy. Soc. A 365:1677-1695

Müller J.F., Stavrakou T., Wallens S., De Smedt I., van Roozendael M., Potosnak M.J., Rinne J., Munger B., Goldstein A., Guenther A.B. (2008) Global isoprene emissions estimated using MEGAN, ECMWF analyses and a detailed canopy environment model. Atmos. Chem. Phys. 8:1329-1341. doi:10.5194/acp-8-1329-2008

Neftel A., Blatter A., Hesterberg R., Staffelbach T. (1996) Measurements of concentration gradients of HNO2 and HNO3 over a semi-natural ecosystem. Atmos. Environ. 30:3017-3025

Nellemann C., Thomsen M.G. (2001) Long-term changes in forest growth: Potential effects of nitrogen deposition and acidification. Water Air Soil Poll. 128:197-205

Neta P., Huie R.E. (1986) Rate constants for reactions of nitrogen oxide (NO_3) radicals in aqueous solutions. J. Phys. Chem. 90:4644-4648

Ng N.L., Kwan A.J., Surratt J.D., Chan A.W.H., Chabra P.S., Sorooshian A., Pye H.O.T., Crounse J.D., Wennberg P.O., Flagan R.C., Seinfeld J.H. (2008) Secondary organic aerosol (SOA) formation from reaction of isoprene with nitrate radicals (NO_3). Atmos. Chem. Phys. 8:4117-4140

Oden S. (1968) The acidification of air and precipitation and its consequences in the natural environment. Ecology Committee Bulletin No. 1. Swedish National Sciences Research Council, Stockholm

Pacifico F., Harrison S.P., Jones C.D., Sitch S. (2009) Isoprene emissions and climate. Atmos. Environ. 43:6121-6135

Pandis S.N., Paulson S.E., Seinfeld J.H., Flagan R.C. (1991) Aerosol formation in the photooxidation of isoprene and β-pinene. Atmos. Environ. 25:997-1008

Park J.-Y., Lee Y.-N. (1988) Solubility and decomposition kinetics of nitrous acid in aqueous solution. J. Phys. Chem. 92:6294-6302

Pasiuk-Bronikowska W., Rudzinski K.J. (1982) Complex sulphite-nitrite reaction.Part I. Synthetic review of chemical-kinetic data. Chem. Eng. Commun. 18:287-309

Pasiuk-Bronikowska W., Ziajka J., Bronikowski T. (1992) Autoxidtation of sulphur compounds. PWN-Polish Scientific Publisher, Ellis Horwood, Warszawa, New York London Toronto Sydney Tokyo Singapore

Paulot F., Crounse J.D., Kjaergaard H.G., Kroll J.H., Seinfeld J.H., Wennberg P.O. (2009) Isoprene photooxidation: new insights into the production of acids and organic nitrates. Atmos. Chem. Phys. 9:1479-1501. doi:10.5194/acp-9-1479-2009

Pedersen T., Sehested K. (2001) Rate constants and activation energies for ozonolysis of isoprene, methacrolein and methyl-vinyl-ketone in aqueous solution: significance to the in-cloud ozonation of isoprene. Int. J. Chem. Kin. 33:182-190

Peñuelas J., Llusià J., Munné-Bosch S. (2005) Linking isoprene with plant thermotolerance, antioxidants and monoterpene emissions. Plant Cell Environ. 28:278-286

Pitts J.N., Grosjean D., van Cauwenberghe K., Schmid J.P., Fitz D.R. (1978) Photooxidation of aliphatic amines under simulated atmospheric conditions: Formation of nitrosamines, nitramines, amides and photochemical oxidant. Environ. Sci. Technol. 12:946-953

Pitts J.N.J., Biermann H.W., Tuazon E.C., Green M., Long W.D., Winer A.M. (1989) Time-resolved identification and measurement of indoor air pollutants by spectroscopic techniques: Gaseous nitrous acid, methanol, formaldehyde and formic acid. J. Air Waste Manage. Assoc. 39:1344-1347

Platt U., Alicke B., Dubois R., Geyer A., Hofzumahaus A., Holland F., Martinez M., Mihelcic D., Klupfel T., Lohrmann B., Patz W., Perner D., Rohrer F., Schafer J., Stutz J. (2002) Free radicals and fast photochemistry during BERLIOZ. J. Atmos. Chem. 42:359-394

Pope C.A., Dockery D.W. (2006) Health effects of fine particulate air pollution: Lines that connect. J. Air Waste Manage. Assoc. 54:709-724

Poschl U. (2005) Atmospheric aerosols: Composition, transformation, climate and health effects. Angew. Chem. Int. Edit. 44 (46):7520-7540

Pouli A.E., Hatzinikolaou D.G., Piperi C., Stavridou A., Psallidopoulos M.C., Stavrides J.C. (2003) The cytotoxic effect of volatile organic compounds of the gas phase of cigarette smoke on lung epithelial cells. Free Radical Bio. Med. 34:345-355

Pun B.K., Seigneur C. (2007) Investigative modeling of new pathways for secondary organic aerosol formation. Atmos. Chem. Phys. 7:2199-2216

Rasmussen T.R., Brauer M., Kjaergaard S. (1995) Effects of nitrous acid exposure on human mucous membranes. Am. J. Respir. Crit. Care Med. 151:1504-1511

Rayson M.S., Mackie J.C., Kennedy E.M., Dlugogorski B.Z. (2012) Accurate rate constants for decomposition of aqueous nitrous acid. Inorganic Chemistry 51:2178-2185

Reimann S., Calanca P., Hofer P. (2000) The anthropogenic contribution to isoprene concentrations in a rural atmosphere. Atmos. Environ. 34

Reinning M.C., Muller L., Warnke J., Hoffmann T. (2008) Characterization of selected organic compound classes i secondary organic aerosols from biogenic VOCs by HPLC/MS^n. Anal. Bioanal. Chem. 391:171-182

Roberts G.C., Andreae M.O., Zhou J., Artaxo P. (2001) Cloud condensation nuclei in the Amazon Basin: "Marine" conditions over a continent? Geophys. Res. Lett. 28:2807-2810

Rodriguez-Concepcion M., Boronat A. (2002) Elucidation of the methylerythritol phosphate pathway for isoprenoid biosynthesis in bacteria and plastids. A metabolic milestone achieved through genomics. Plant Physiol. 130:1079-1089

Romero F., Oehme M. (2005) Organosulfates-a new component of humic-like substances in atmosheric aeroslos? J. Atmos. Chem. 52:283-294 doi:210.1007/s10874-10005-10594-y

Rudziński K.J. (2004) Degradation of isoprene in the presents of sulphoxy radical-anions. J. Atmos. Chem. 48:191-216

Rudziński K.J., Gmachowski L., Kuznietsova I. (2009) Reaction of isoprene and sulphoxy radical-anions - a possible source of atmospheric organosulphite and organosulphates. Atmos. Chem. Phys. 9:2129-2140

Rudziński K.J., Pasiuk-Bronikowska W. (2000) Inhibition of SO_2 oxidation in aqueous phase. Works Stud. Inst. Environ. Eng P.A.S. 54:175-191

Saliba N.A., Mochida M., Finlayson-Pitts B.J. (2000) Laboratory studies of sources of HONO in polluted urban atmosphere. Geophys. Res. Lett. 27:3229-3232

Sanderson M.G., Jones C.D., Collins W.J., Johnson C.E., Derwent R.G. (2003) Effect of climate change on isoprene emissions and surface ozone levels. Geophys. Res. Lett. 30:1936

Sato K. (2008) Detection of nitrooxypolyols in secondary organic aerosol formed from the photooxidation of conjugated dienes under high-NO_x conditions. Atmos. Environ. 42:6851-6861

Saxena P., Hildemann L.M. (1996) Water-soluble organics in atmospheric particles: A critical review of the literature and application of thermodynamics to identify candidate compounds. J. Atmos. Chem. 24:57-109

SC-Database (1997, 2000) IUPAC Stability Constance Database. IUPAC and Academic Software, UK

Schöpp W., Posch M., Mylona S., Johansson M. (2003) Long-term development of acid deposition (1880–2030) in sensitive freshwater regions in Europe. Hydrol. Earth Syst. Sc. 7:436-446

Schurath U., Peeters J., Wayne R.P., Moortagat G.K., Grgic I., George, C., Herrmann H., Poppe D. (2003) in *Towards cleaner air for Europe- science, tools and applications Part 2. Overviews from the final reports of the EUROTRAC-2 subprojects*. In: (Eds. Midgley PM, Reuther, M.) (ed) pp.73-79. (Margraf Verlag: Weikersheim), p Available at http://www.gsf.de/eurotrac/index_publ_fin_rep.html [Verified 5 April 2007]

Seinfeld J.H., Pandis S.N. (1998) Atmospheric chemistry and physics: from air pollution to climate change. J. Wiley, New York

Seinfeld J.H., Pankow J.F. (2003) ORGANIC ATMOSPHERIC PARTICULATE MATERIAL. Annu. Rev. Phys. Chem. 54:121-140

Sharkey T.D., L. S.E., Vanderveer P.J., Geron C.D. (1996) Field measurements of isoprene emission from trees in response to temperature and light. Tree Physiol. 16:649-654

Sharkey T.D., Wiberley A.E., Donohue A.R. (2007) Isoprene emission from plants: why and how. Ann. Bot-London:1-14

Shaw S.L., Chisholm S.W., Prinn R.G. (2003) Isoprene production by Prochlorococcus, a marine cyanobacterium, and other phytoplankton. Mar. Chem. 88:61-73

Shen C.H., Rochelle G.T. (1998) Nitrogen dioxide absorption and sulfite oxidation in aqueous sulfite. Environ. Sci Tech. 32:1994-2003

Shirley T.R., Brune W.H., Ren X., Mao J., Lesher R., Cardenas B., Volkamer R., Molina L.T., Molina M.J., Lamb B., Velasco E., Jobson T., Alexander M. (2006) Atmospheric oxidation in the Mexico City Metropolitan Area (MCMA) during April 2003. Atmos. Chem. Phys. 6:2753–2765

Simpson D., Winiwarter W., Börjesson G., Cinderby S., Ferreiro A., Guenther A., Hewitt C.N., Janson R., Khalil M.A.K., Owen S., Pierce T.E., Puxbaum H., Shearer M., Skiba U., Steinbrecher R., Tarrason L., Öquist M.G. (1999) Inventorying emissions from nature in Europe. J. Geophys. Res. 104:8113-8152

Sleiman M., Gundel L.A., Pankow J.F., J. P., Singer B.C., Destaillats H. (2010) Formation of carcinogens indoors by surface-mediated reactions of nicotine with nitrous acid, leading to potential thirdhand smoke hazards. P. Natl. Acad. Sci. USA 107:6576-6581

Spengler J.D., Brauer M., Samet J.M., Lambert W.E. (1993) Nitrous acid in Albuquerque, New Mexico, homes. Environ. Sci. Technol. 27:841-845

Stemmler K., Ndour M., Elshorbany Y., Kleffmann J., D'Anna B., George C., Bohn B., Ammann M. (2007) Light induced conversion of nitrogen dioxide into nitrous acid on submicron humic acid aerosols. Atmos. Chem. Phys. 7:4237-4248

Stockwell B., Calvert J.G. (1983) The mechanism of NO_3 and HONO formation of nighttime chemistry of the urban atmosphere. J. Geophys. Res. 88:6673-6682

Stutz J., Oh H.-J., Whitlow S.I., Anderson C., Dibb J.E., Flynn J.H., Rappengluck B., Lefer B. (2010) Simultaneous DOAS and mist-chamber IC measurements of HONO in Houston, TX. Atmos. Environ. 44:4090-4098

Surratt J.D., Gomez-Gonzalez Y., Chan A.W.H., Vermeylen R., Shahgholi M., Kleindienst T.E., Edney E.O., Offenberg J.H., Lewandowski M., Jaoui M., Maenhaut W., Claeys M., Flagan R.C., Seinfeld J.H. (2008) Organosulfate formation in biogenic secondary organic aerosol. J. Phys. Chem. 112:8345-8378

Surratt J.D., Kroll J.H., Kleindienst T.E., Edney E.O., Claeys M., Sorooshian A., Ng N.L., Offenberg J.H., Lewandowski M., Jaoui M., Flagan R.C., Seinfeld J.H. (2007b) Evidence for organosulfates in secondary organic aerosol. Environ. Sci. Technol. 41:517-527

Surratt J.D., Lewandowski M., Offenberg J.H., Jaoui M., Kleindienst T.E., Edney E.O., Seinfeld J.H. (2007a) Effect of acidity on secondary organic aerosols formation from isoprene. Environ. Sci Tech. 41:5363-5369

Surratt J.D., Murphy S.M., Kroll J.H., Ng N.L., Hildebrandt L., Sorooshian A., Szmigielski R., Vermeylen R., Maenhaut W., Claeys M., Flagan R.C., Seinfeld J.H. (2006) Chemical composition of secondary organic aerosol formed from the photooxidation of isoprene. J. Phys. Chem. 110:9665-9690

Susianto, Petrissans M., Zoulalian A. (2001) Influence of the pH on the Interactions between nitrite and sulfite Ions. Kinetic of the reaction at pH 4 and 5. Ind. Eng. Chem. Res. 40:6068-6072

Taraborelli D., Lawrence M.G., Butler T.M., Sander R., Lelieveld J. (2009) Mainz Isoprene Mechanism 2 (MIM2): an isoprene oxidation mechanism for regional and global atmospheric modelling. Atmos. Chem. Phys. 9:2751-2777

Terry G.M., Stokes N.J., Hewitt C.N., Mansfield T.A. (1995) Exposure to isoprene promotes flowering in plants. J. Exp. Bot. 46 (10):1629-1631

Tiiva P., Rinnan R., Holopainen T., Mörsky S.K., Holopainen J.K. (2007) Isoprene emissions from boreal peatland microcosms; effects of elevated ozone concentration in an open field experiment. Atmos. Environ. 41:3819-3828

Tillett J.G. (1976) Nucleophilic substitution at tricoordinate sulfur. Chem. Rev. 76:747-772

Tolocka M.P., Jang M., Ginter J.M., Cox F.J., Kamens R.M., Johnston M.V. (2004) Formation of oligomers in secondary organic aerosol. Environ. Sci. Technol. 38:1428-1434

van Wijk A.A.C., Lugtenburg J. (2002) Synthetic scheme for the preparation of ^{13}C-Labeled 2,7-Dimethylocta2,4,6-triene-1,8-dial, the central part of carotenoids. Eur. J. Org. Chem:4217-4221

van Woerden H.F. (1963) Organic Sulfites. Chem. Rev. 63:557-571

Vestreng V., Myhre G., Fagerli H., Reis S., Tarrason L. (2007) Twenty-five years of continuous sulphur dioxide emission reduction in Europe. Atmos. Chem. Phys. 7:3663-3681. doi:10.5194/acp-7-3663-2007

Vivanco M.G., Santiago M., Martínez-Tarifa A., Borrás E., Ródenas M., García-Diego C., Sánchez M. (2011) SOA formation in a photoreactor from a mixture of organic gases and HONO for different experimental conditions. Atmos. Environ. 45:708-715

Vogel B., Vogel H., Kleffmann J., Kurtenbach R. (2003) Measured and simulated vertical profiles of nitrous acid-Part II. Model simulations and indications for a photolytic source. Atmos. Environ. 37:2957-2966

Wagner W.P., Nemecek-Marshall M., Fall R. (1999) Three distinct phases of isoprene formation during growth and sporulation of Bacillus subtilis. J. Bacteriol. 181:4700-4703

Wilkins K., Larsen K. (1996) Volatile organic compounds from garden waste. Chemosphere 32:2049-2055

Zappoli S., Andracchio A., Fuzzi S., Facchini M.C., Gelencser A., Kiss G., Krivacsy Z., Molnar A., Meszaros E., Hansson H.-C., Rosman K., Zebuhr Y. (1998) Inorganic, organic and macromolecular components of Þne aerosol in different areas of Europe in relation to their water solubility. Atmos. Environ. 33:2733-2743

Zellner R. (1999) Global aspects of atmospheric chemistry, vol Topics in physical chemistry; Vol 6. Springer, New York

Zhang R., Leu M.T., Keyser L.F. (1996) Heterogeneous chemistry of HONO on liquid sulfuric acid: a new mechanism of chlorine activation on stratospheric sulfate aerosols. J. Phys. Chem. 100:339-345

Zhou X., Beine H.J., Honrath R.E., Fuentes J.D., Simpson W., Shepson P.B., Bottenheim J.W. (2001) Snowpack photochemical production of HONO: A major source of OH in the Arctic boundary layer in springtime. Geophys. Res. Lett. 28:4087-4090

Zhou X., Civerolo K., Dai H., Huang G., Schwab J., Demerjian K. (2002a) Summertime nitrous acid chemistry in the atmospheric boundary layer at a rural site in New York State J. Geophys. Res. 107:4590

Zhou X., He Y., Huang G., Thomberry T.D., Carroll M.A., Bertman S.B. (2002b) Photochemical production of nitrous acid on glass sample manifold surface. Geophys. Res. Lett. 29:1681